

# TI Designs

## Interface to Sin/Cos Encoders With High-Resolution Position Interpolation

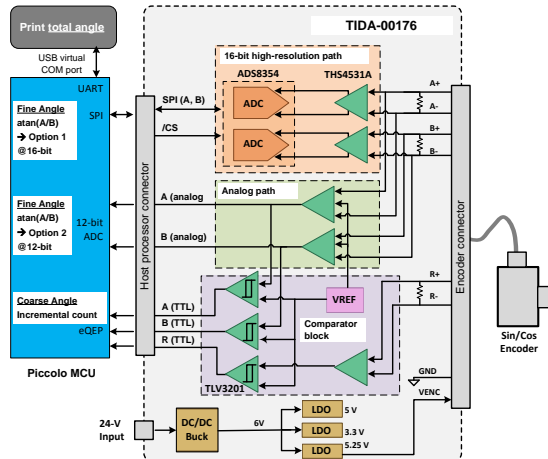


### TI Designs

This reference design is an EMC compliant industrial interface to Sin/Cos position encoders. Applications include industrial drives, which require accurate speed and position control. The design uses a 16-bit dual sample ADC with drop-in compatible 14- or 12-bit versions available, allowing for optimization of performance and cost. TIDA-00176 is also provides a simple to connection to external processors using SPI and QEP interfaces and allows for the use of optional, embedded ADCs. For quick evaluation an example firmware for Piccolo™ F28069M MCU LaunchPad™ is provided, which outputs the measured angle from the Sin/Cos encoder with up to 28-bit resolution through the MCU's USB virtual COM port.

### Design Resources

<a href="#">TIDA-00176</a>	Design Folder
<a href="#">ADS8354</a>	Product Folder
<a href="#">THS4531A</a>	Product Folder
<a href="#">TLV3202</a>	Product Folder
<a href="#">OPA2365</a>	Product Folder
<a href="#">REF2033</a>	Product Folder
<a href="#">TPS54040A</a>	Product Folder
<a href="#">TIPD117</a>	Tool Folder
<a href="#">Piccolo F28069M MCU LaunchPad</a>	Tool Folder



### Design Features

- EMC-Compliant Industrial Interface Design for Sin/Cos Encoders With  $1-V_{PP}$  Differential Output at 2.5-V Offset, Input Frequencies up to 500 kHz
- High-Resolution Interpolated Position, up to 28-bit Resolution, Cable Length Tested up to 70 m
- Dual Analog Signal Chain for Simultaneous Use of 16-bit Dual SAR ADC and MCU Embedded ADCs Allows for Evaluation of Both Paths and Optimization of One Path for Increased Noise Immunity With Reduced Bandwidth
- Easy to Connect to MCU With SPI and QEP Interface and Option for Cost Optimization Pending Resolution Requirements, Thanks to Drop-in Compatible 14- or 12-bit ADC
- Example Firmware for C2000™ MCU With High-Resolution Angle Calculated at 16-kHz and Angle Data Send Through USB Virtual COM Port for Easy Performance Evaluation
- Tested for IEC61000-4-2, 4-4, and 4-5 (ESD, EFT, and Surge EMC Immunity Requirements)

### Featured Applications

- AC Drives
- Precision Speed-Variable Drives
- Servo Drives



An IMPORTANT NOTICE at the end of this TI reference design addresses authorized use, intellectual property matters and other important disclaimers and information.

## 1 System Description

### 1.1 TI Design Overview

This TI design implements an industrial temperature, EMC-compliant interface to Sin/Cos incremental position encoders with  $1-V_{PP}$  differential analog output signals, frequencies up to 500 kHz, and a 5-V supply voltage. The major building blocks of this TI design are the dual path analog signal chain, the highspeed comparator block, the power management block, and the interfaces to the Sin/Cos encoder as well as the interface to a host microcontroller for digital signal processing and high-resolution position calculation. A simplified system block diagram is shown in [Figure 1](#), with the TI hardware design represented by the box in light green.

To allow for an easy evaluation of this TI design, an example firmware is provided for the TMS320F28069M InstaSPIN™-MOTION LaunchPad. The TMS320F28069M calculates the high-resolution angle position for both analog signal paths. One path is leveraging the external 16-bit dual ADC through SPI. The other path is using the F28069M embedded dual S/H 12-bit ADC. The angle is calculated with up to 28-bit resolution and output for evaluation through USB virtual COM port.

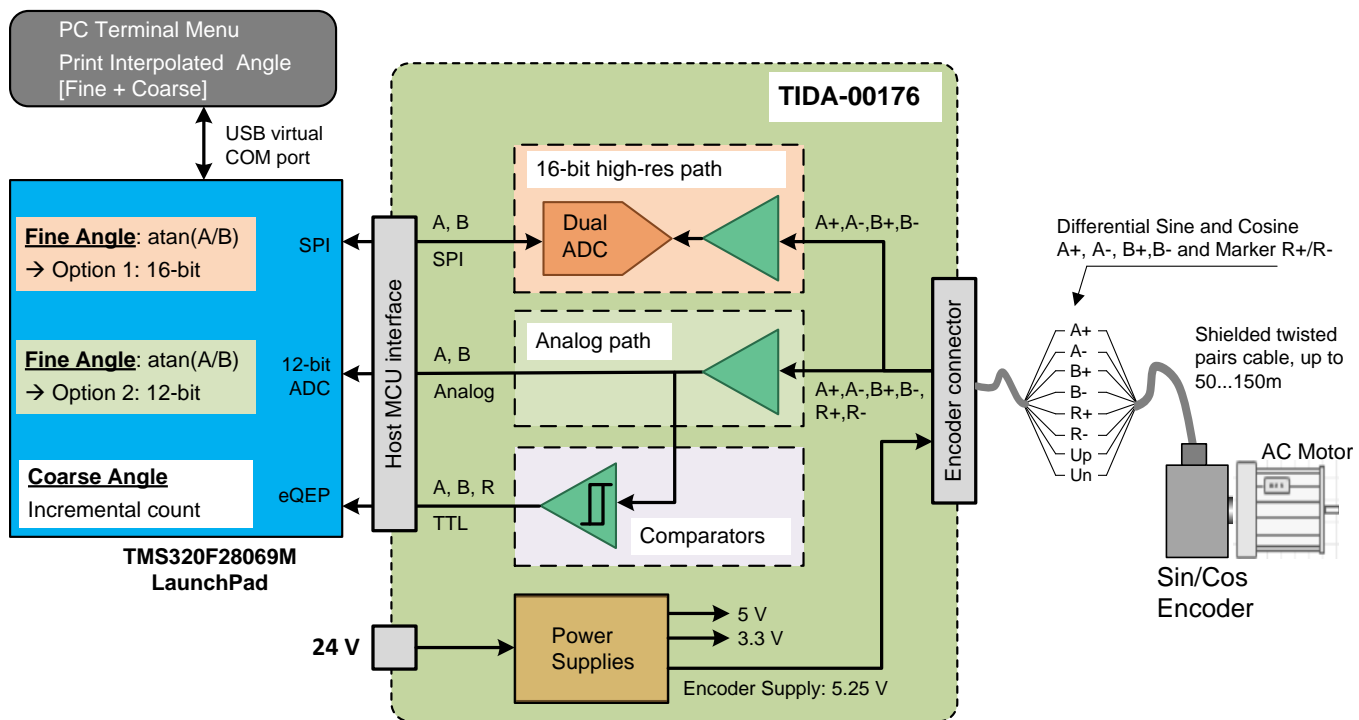


**Figure 1. Simplified System Block Diagram of TIDA-00176 With Piccolo F28069M LaunchPad**

The analog signal chain provides  $120\Omega$  termination with EMC protection. The differential  $1 V_{PP}$  sine and cosine input signals are amplified and level-shifted, respectively. A dual signal path option is provided with an onboard high-speed, high-resolution dual 16-bit simultaneous sampling ADC with SPI and dual analog single-ended outputs with a 1.65-V bias voltage to interface to a microcontroller with embedded dual S/H ADC like the C2000™ Piccolo Real-time MCU family.

The comparator block features high-speed, low propagation delay and adjustable hysteresis for better noise immunity and converts the analog signals A, B, and the marker R into digital signals with a 3.3-V TTL-level to interface to a quadrature encoder pulse module like the QEP module on the C2000 Piccolo MCU.

The onboard wide-input range 24-V power supply provides the necessary voltages for analog signal chain as well as the 5.25-V supply voltage for the Sin/Cos encoder.

The Sin/Cos encoder can be either connected to a 15-pin shielded Sub-D connector or an 8-pin header. The interface to the host processor provides the analog single-ended signals A and B scaled from 0 to 3.3 V with a 1.65-V bias voltage, the digital signals for SPI and A, B, and R with a 3.3-V I/O. The digital output signals A, B, and R are often referred to as "ABZ" signals.

The design is tested for IEC61000-4-2, 4-4, and 4-5 (ESD, EFT, and Surge) as specified in the IEC 61800-3 standard for EMC immunity requirements and specific test methods applicable in adjustable speed, electrical-power drive systems.

## 1.2 Analog Sin/Cos Incremental Encoder

Incremental rotary or linear position encoders are used in many applications to measure angular or linear position and speed. Depending on the application, encoders with TTL/HTL-output signals or analog sinusoidal output signals are used. The latter is often referred as Sin/Cos encoder. Analog Sin/Cos incremental encoders enable high-resolution position measurement. The high quality of the sinusoidal incremental signals permits high interpolation factors for digital speed control. Application areas include electrical motors, machine tools, printing machines, woodworking machines, textile machines, robots, and handling devices, as well as various types of measuring, testing, and inspection devices.

### 1.2.1 Sin/Cos Encoder Output Signals

There are typically two sensing methods implemented with encoders, either based on optical or inductive sensing. With optical rotary encoder, the encoder disc modulates a light beam whose intensity is sensed by photo-electrical cells. These produce two 90-degree phase shifted sinusoidal incremental signals A and B. B lags A with clockwise rotating viewed from the shaft of the encoder. The number of periods of the signals A and B over one mechanical revolution equals the line count N of the encoder. A further track carries the reference marker R, which occurs once per mechanical revolution. The reference marker allows for an absolute angle position measurement.

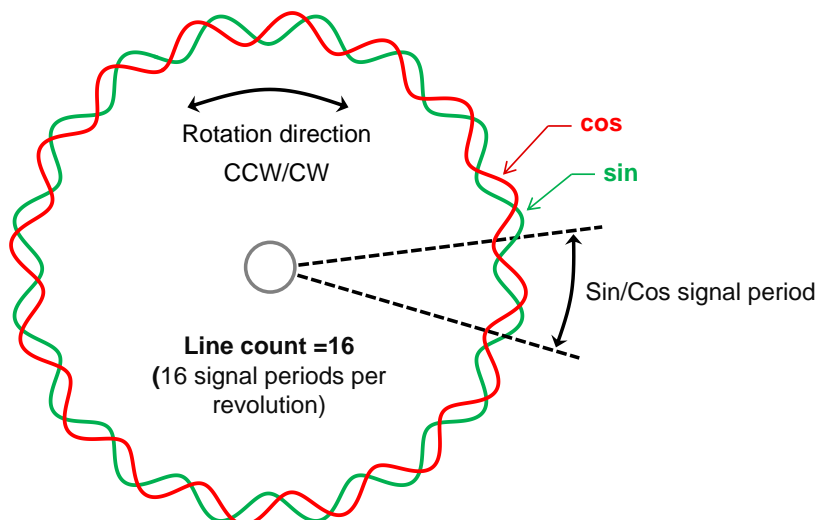


**Figure 2. Simplified Sine and Cosine Signals for a Sin/Cos Encoder Over One Mechanical Revolution for a Line Count of 16**

Sin/Cos encoders with a  $1\text{-V}_{\text{PP}}$  interface provide the differential analog output signals A ( $A_+$ ,  $A_-$ ) and B ( $B_+$ ,  $B_-$ ) with  $1\text{ V}_{\text{PP}}$  and typically a 2.5-V DC-offset. The differential reference mark signal R ( $R_+$ ,  $R_-$ ) is typically slightly lower amplitude and the peak occurs only once per revolution. [Figure 3](#) shows the differential output signals A, B, and R. Note that A, B, and R represent the differential signal of  $A_+$  minus  $A_-$ ,  $B_+$  minus  $B_-$ , and  $R_+$  minus  $R_-$ , respectively.

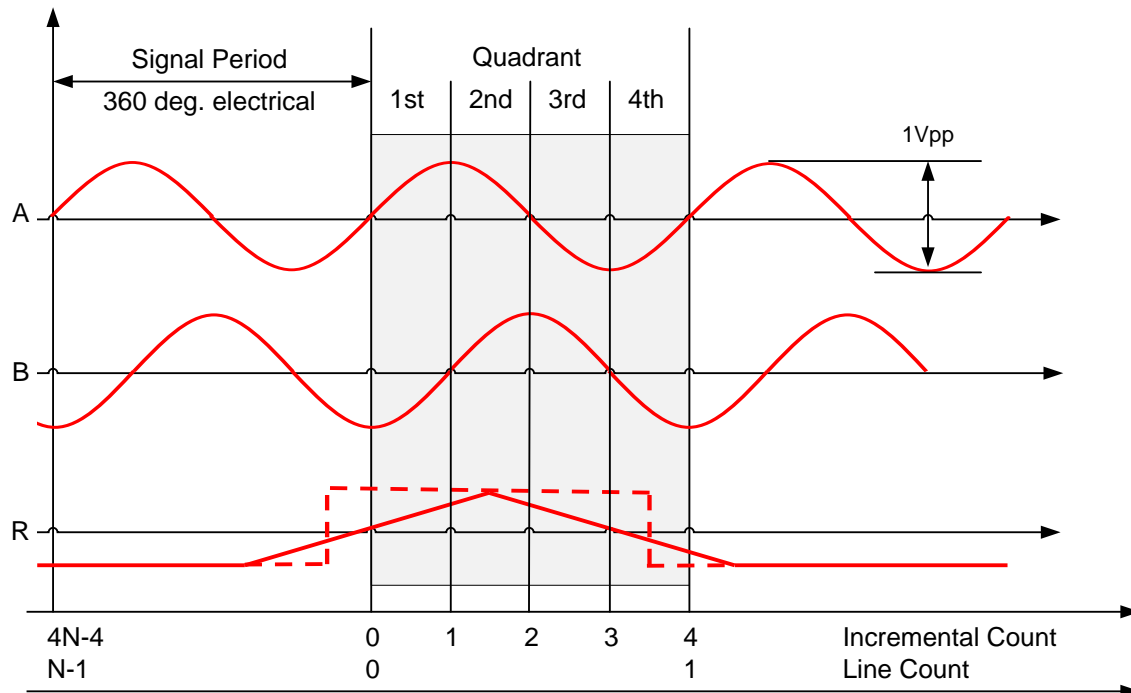


**Figure 3. Output Voltage Signals A, B, and Marker R of Sin/Cos-Encoders With N Line Counts per Revolution**

The frequency of the Sin/Cos encoder's differential output signal depends on the line count of the encoder as well as the mechanical speed, as outlined in [Equation 1](#):

$$f_{A,B} [\text{Hz}] = N \times v[\text{rpm}] \times \frac{1}{60} \quad (1)$$

N represents the Sin/Cos encoder line count and v the encoder shaft mechanical speed in rpm.

[Figure 4](#) provides an overview on the output frequency for encoders with line counts N = 100, 1000, and 2000 versus the mechanical speed.

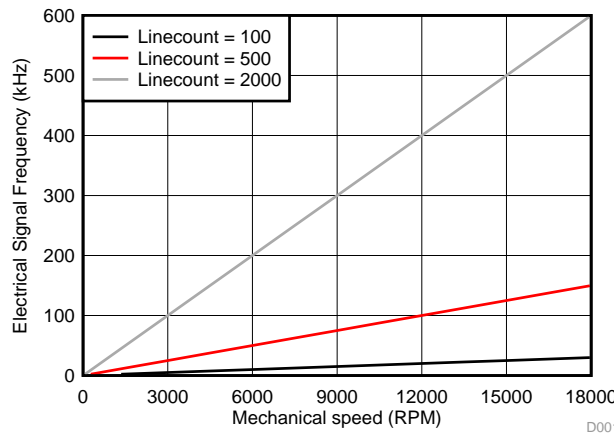


**Figure 4. Electrical Frequency of SinCos Encoder Output Signals A and B versus Mechanical Speed and Line Count**

For example, a Sin/Cos encoder with a line count of N=2000 running at a mechanical speed of 12000 rpm, outputs the signals A and B with a frequency of 400 KHz.

### 1.2.2 Sin/Cos Encoder Electrical Parameter Examples

To understand the requirements for an electrical interface module to Sin/Cos encoders, some example industrial Sin/Cos encoder models have been analyzed. The corresponding parameters are listed in [Table 1](#).

**Table 1. Encoders Supply Voltage Example**

SIN/COS ENCODER MODEL	SUPPLY VOLTAGE	CURRENT CONSUMPTION
1	5-V $\pm$ 0.5-V DC	< 120 mA
2	5 V $\pm$ 10%	150 mA
3	5 V $\pm$ 5%	70 mA (min)

The power supply of the Sin/Cos encoder needs to be within this specification.

The analog signal chain need to be specified to at least meet the requirements listed in [Table 2](#) with respect to signal amplitudes, offset, and maximum frequency.

**Table 2. Encoder Output Signals A, B Example**

SIN/COS ENCODER MODEL	SIGNAL LEVEL A, B	DC OFFSET	LINE COUNT N	LIMIT FREQUENCY (-3 dB)
1	0.6 to 1.2 V <sub>PP</sub> , 1 V <sub>PP</sub> typical	2.5 V $\pm$ 0.5 V	50 to 5000	$\geq$ 180 kHz
2	1 V <sub>PP</sub> (+20%, -40%)	2.5 V $\pm$ 0.5 V		120 kHz
3	1 V <sub>PP</sub> ( $\pm$ 10%)	2.5 V $\pm$ 100 mV	1024 or 2048	400 kHz

**Table 3. Encoder Output Signals Marker R Example**

SIN/COS ENCODER MODEL	USABLE COMPONENT G AT REFERENCE MARK	QUIESCENT VALUE H OUTSIDE REFERENCE MARK	DC OFFSET
1	0.5 V <sub>PP</sub> typical, 0.2 V <sub>PP</sub> min	-1.7 V	2.5 V

**Table 4. Encoder Mechanical Parameter Example**

SIN/COS ENCODER MODEL	SYSTEM ACCURACY	SHAFT MECHANICAL SPEED
1	1/20 of grating period	< 16000 rpm

## 1.3 Method to Calculate High-Resolution Position With Sin/Cos Encoders

### 1.3.1 Theoretical Approach

#### 1.3.1.1 Overview

From a hardware perspective typically two approaches can be realized, which impact mainly the requirements for the A/D converter.

With the "over-sampling method", both sine and cosine signal would be sampled at least four times higher than the maximum sine and cosine frequency. The incremental count as well as the phase calculation would be done by subsequent digital signal processing on a host processor. That method would not need comparators, but rather high-speed dual sampling ADCs.

The typically used "under-sampling" method uses separate hardware blocks to calculate the incremental count and the interpolated incremental phase. The advantage of that method is that the sampling frequency and bandwidth of the ADC can be lower compared to the first method, as it does not impact the incremental count but only the interpolated phase. However, the under-sampling method requires a comparator each, for sine and the cosine, to generate the digital quadrature encoded signals A and B, which drive a directional up and down counter, often referred to as quadrature encoded pulse counter. The analog bandwidth of the dual sampling ADC needs to be at least equal to the maximum sine/cosine frequency. The under-sampling method is outlined in [Figure 5](#).

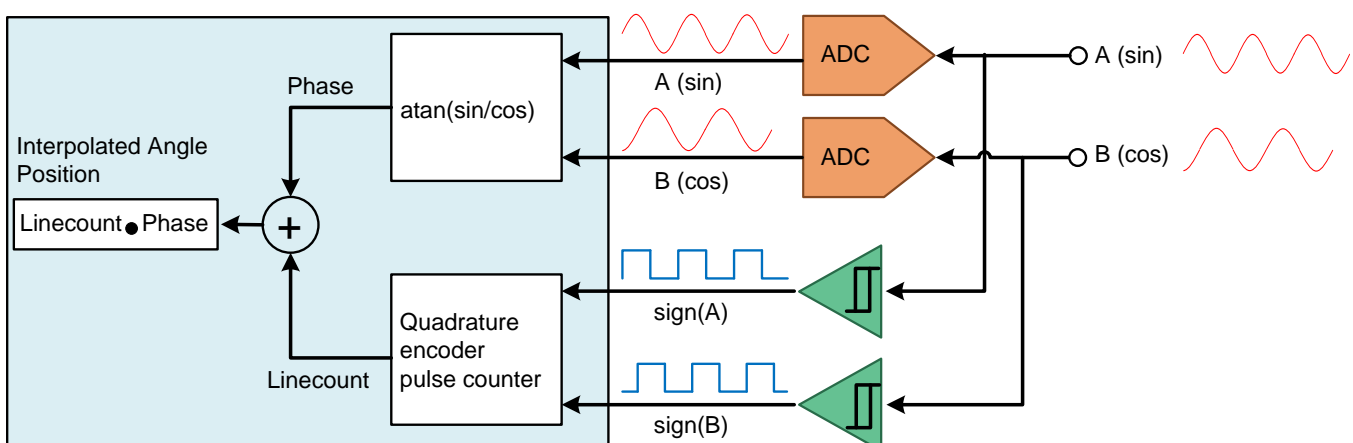


**Figure 5. Signal Processing Block Diagram for Interpolated Angle Calculation**

The total interpolated angular position is composed of coarse and fine angle. The interpolated angle is determined by the actual incremental line count and the phase within this incremental line. The phase within the incremental line is derived from the analog sine and cosine signals A and B at any specific time instant. Both the actual incremental count and the actual analog sine and cosine signals have to be latched at the same time, hence synchronously. The incremental line count provides the coarse angle, while the phase within of the sine and cosine within that incremental line provides the fine angle. The total interpolated angle is a compound of the coarse and fine angle, as shown with a simplified block diagram in [Figure 5](#). The corresponding [Equation 2](#) to [Equation 4](#) are explained in the next paragraph.

### 1.3.1.2 Coarse Resolution Angle Calculation

The incremental count and hence the incremental coarse angle can be determined by a counter, that counts up when A is the leading sequence and counts down when B is the leading sequence. When digitized, both edges of A and B are counted. Hence one incremental count is equivalent to a 90° phase shift of both signals A and B, see [Figure 3](#). The incremental count starts from 0 with the maximum incremental count  $\text{incr}_{\text{MAX}}$  per [Equation 2](#), where N is the line count:

$$\text{incr}_{\text{MAX}} = (4 \times N) - 1 \quad (2)$$

The incremental position  $\Phi_{\text{incr}}$  can be calculated as:

$$\Phi_{\text{incr}} [\text{deg}] = \frac{360}{4 \times N} \times \text{incr} + \Phi_0 \quad (3)$$

Where incr is the actual incremental count, N is the total line count and  $\Phi_0$  the zero angle, determined by the reference marker R, if used.

### 1.3.1.3 Fine Resolution Angle Calculation

The phase  $\phi_{A,B}$  of the sinusoidal signals A and B is used to interpolate the angle between two consecutive line counts, or four incremental steps, which are equivalent to each other. The phase  $\phi_{A,B}$  can be calculated with [Equation 4](#):

$$\phi_{A,B} [\text{deg}] = \begin{cases} 90^\circ + \tan^{-1}\left(\frac{B}{A}\right) & \text{if } A \geq 0 \\ 270^\circ + \tan^{-1}\left(\frac{B}{A}\right) & \text{if } A < 0 \end{cases} \quad (4)$$

Since only the ratio of the amplitudes of A and B is used, which are a common function of the encoder's rotation speed and supply voltage, this result does not affect the result.

### 1.3.1.4 Interpolated High-Resolution Angle Calculation

When the incremental count incr is matched to the phase  $\phi_{A,B}$  according to [Table 5](#), the total interpolated angle  $\Phi_{\text{TOTAL}}$  is calculated with line count N as:

$$\Phi_{\text{TOTAL}} [\text{deg}] = \frac{360^\circ}{N} \left( (\text{incr} \gg 2) + \left( \times \frac{\phi_{A,B}}{360^\circ} \right) \right) + \Phi_0 \quad (5)$$

#### CAUTION

The sinusoidal signals A and B and the incremental count incr must be latched simultaneously.

**Table 5. Example for Relation between Incremental Count to Phase and Phase Quadrant**

INCREMENTAL COUNT	PHASE	QUADRANT
0	0 ≤ Phase < 90	1
1	90 ≤ Phase < 180	2
2	180 ≤ Phase < 270	3
3	270 ≤ Phase < 360	4
4	0 ≤ Phase < 90	1

### 1.3.1.5 Practical Implementation for Non-Ideal Synchronization

Practically, the digitized signals  $A_{TTL}$  and  $B_{TTL}$ , which are input to the quadrature encoder pulse counter, typically have a phase shift compared to the analog signals. This is mainly due to hysteresis and propagation delay of the comparators, as well as due to non-ideal synchronization between latching the incremental count and sampling the analog inputs A and B.

The impact of the hysteresis on the phase shift is almost independent of the signal frequency, but almost inverse proportional to the signal amplitude. The impact of a propagation delay and a non-ideal synchronization between sampling the analog signal and latching the incremental count is almost independent of the amplitude, but proportional to the frequency. Therefore, the maximum phase shift occurs at maximum Sin/Cos encoder frequency with minimum amplitude.

This means that at each transition to the next quadrant, the incremental counter is not updated immediately because of the phase lag, for example, as shown for the first quadrant in [Figure 6](#).

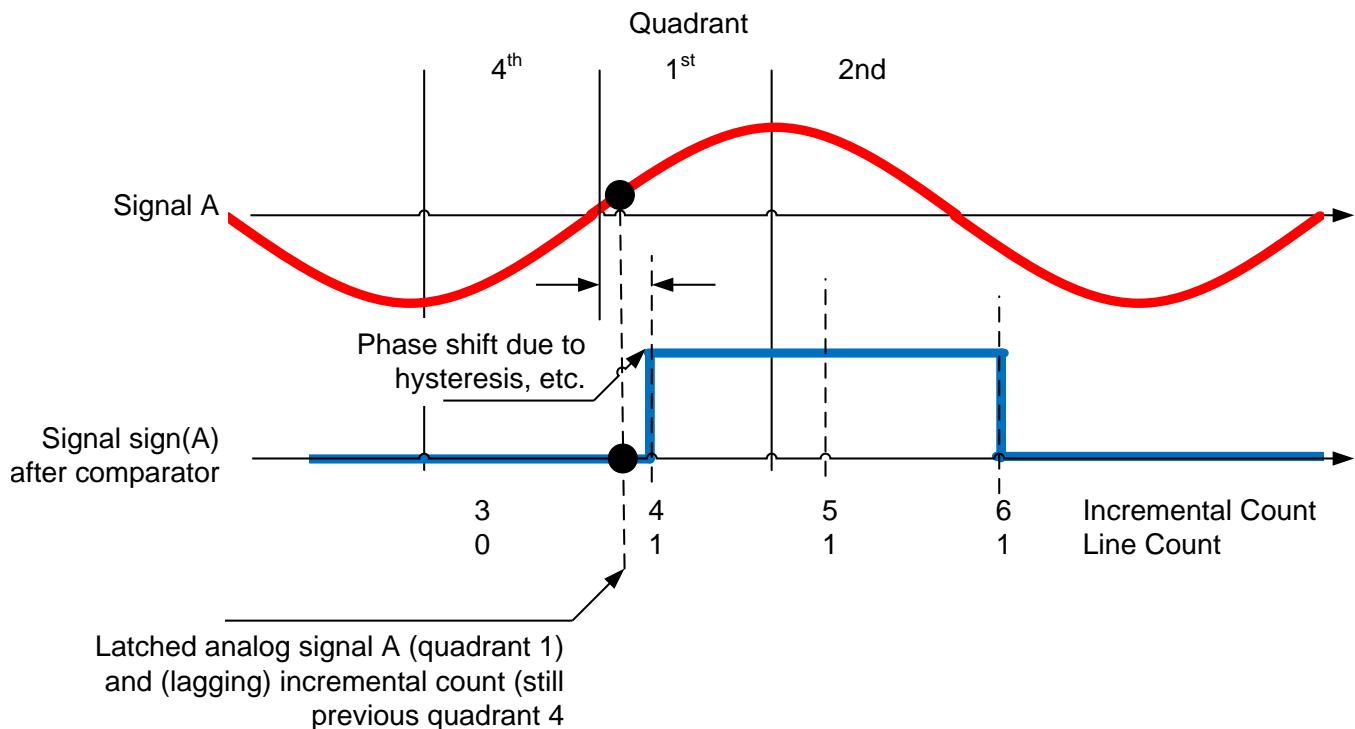


**Figure 6. Phase Shift of  $A_{TTL}$  versus the Analog Signal A, due to Phase Lag**

The factors outlined cannot be omitted and hence a method needs to be applied to detect and correct these corner cases. Due to the ambiguity or the lower two bits of incremental line count and the analog phase, a correction method as outlined in [Table 6](#) can be applied, as long as the phase shift remains less than  $\pm 90^\circ$ .

Since only the phase information is used to identify the quadrant, there are only two exceptions to consider, which occur during the transition from quadrant 4 to quadrant 1, or quadrant 1 to quadrant 4, depending on the rotation direction.

**Table 6. Correction Method**

INCREMENTAL COUNT [incr]	PHASE $\phi_{A,B}$	CORRECTION METHOD
incr%4 = 3	$0 \leq \text{Phase} < 90$	incr = incr+1 if incr > 4 × N - 1 then incr = 0
Incr%4 = 0	$270 \leq \text{Phase} < 360$	incr = incr-1 if incr < 0 then incr = 4 × N - 1

**CAUTION**

The correction method only works if the phase shift between the analog A and B and the digital signal  $A_{TTL}$  and  $B_{TTL}$  is less than  $\pm 90^\circ$ .

A worst case calculation for this design is outlined in [Section 1.4](#).

### 1.3.1.6 Resolution, Accuracy, and Speed Considerations

The ideal interpolated angle resolution is a function of the Sin/Cos encoder's line count and the resolution of the dual ADC. The equivalent interpolated angle resolution can be calculated as:

$$\Phi_{RESOLUTION} [\text{bit}] = \log_2(2 \times N) + \text{ADC}_{RESOLUTION} [\text{bit}] \quad (6)$$

[Figure 7](#) illustrates the achievable interpolated angle resolution as a function of the line count for no interpolation, interpolation with an ideal 12-bit, and a 16-bit dual ADC.

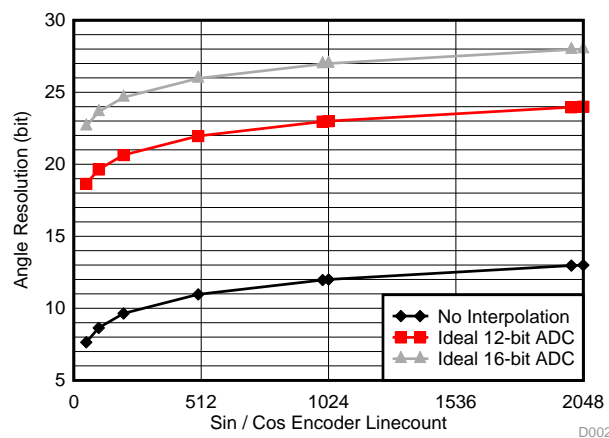


**Figure 7. Ideal Interpolated Angle Resolution versus Line Count versus ADC Resolution**

The ideal resolution with a Sin/Cos encoder with 2048 line counts using a 16-bit dual ADC equals 28-bit, if the ADC's full-scale input range is used.

This high resolution is typically not required for position control, but for very precise speed control, especially at lower mechanical speed. [Figure 8](#) outlines the ideal speed resolution derived at a sample rate of 1.6 kHz without low-pass filtering. This assumes the industrial drive's speed closed-loop control runs 10 times lower than the current closed-loop control and PWM at 16 kHz.

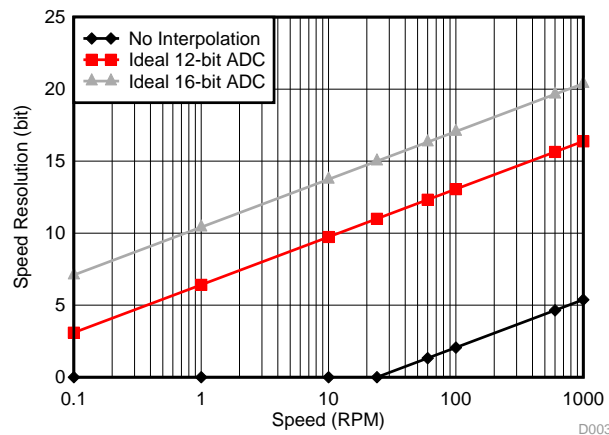


**Figure 8. Ideal Speed Resolution versus Mechanical Speed at 1.6-kHz Sample Rate and Encoder With 1000 Line Count**

Practically, low-pass filtering will be applied and improves resolution and immunity to noise, but with a filter specific propagation (group) delay or latency.

Following the ideal resolution, [Table 7](#), [Figure 9](#), and [Figure 10](#) outline the impact of a quantization, offset, gain, or phase error to the interpolated angle.

**Table 7. Phase Error Examples Analysis**

ERROR SOURCE	EXAMPLE	PHASE ERROR [MAX]
Quantization of signals A and B	12-bit	0.012% [0.045°]
Offset error of signals A and B	0.1%	0.05% [0.18°]
Gain error of signals A and B	0.1%	0.04% [0.15°]
Phase shift between input signals A and B	$90 + 0.36^\circ$ [0.1%]	0.1% [0.36°]

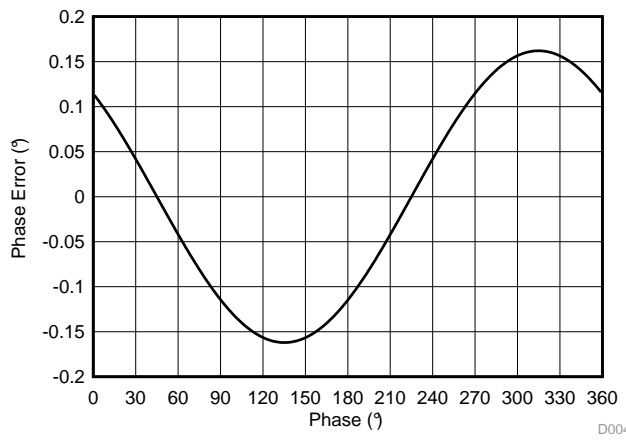


**Figure 9. Phase Error With  $+0.1\%$  Offset With Signals A and B**

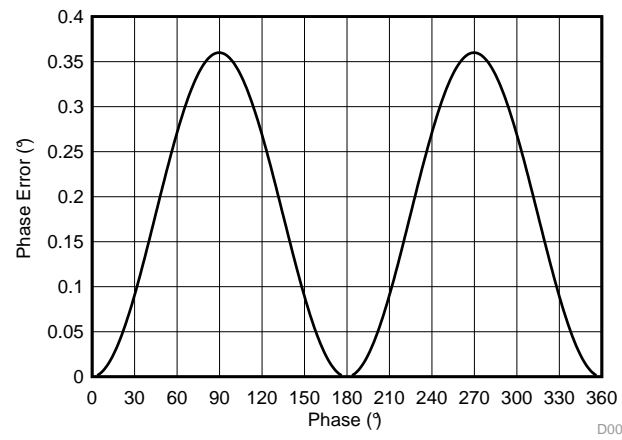


**Figure 10. Phase Error With  $(90 + 0.36^\circ)$  Phase Shift Between Signals A and B**

Note that the phase error introduced due to a phase shift between the input signals A and B exhibits the double period. This signature can be leveraged for detection and correction of a constant phase shift using signal processing algorithms. However, these are beyond the scope of this design guide.

#### 1.4 Sin/Cos Encoder Parameters Impact on Analog Circuit Specification

To specify the analog circuit, as outlined in [Section 4](#), the following Sin/Cos encoder signal parameters (including support for longer cables) have been considered.

- Sin/Cos minimum and maximum peak-to-peak amplitude: Differential 0.3 to 1.2 V<sub>PP</sub>, full-scale input range with at least 50% headroom (1.8 V<sub>PP</sub>)
- Sin/Cos offset voltage range: 2.5 V  $\pm 1$ V
- Sin/Cos maximum frequency: 500 kHz
- Sin/Cos maximum slew rate: >2 V/ $\mu$ s
- Sin/Cos line termination: 120- $\Omega$   $\pm 1\%$
- Encoder supply voltage and current: 5 V  $\pm 5\%$ , 200 mA

#### 1.4.1 Analog Signal Chain Design Consideration for Phase Interpolation

The high-resolution analog signal chain shall support 16-bit resolution to provide a high interpolated angle resolution, especially for precision speed control.

The differential analog amplifier's AC noise floor and distortions should match 16-bit resolution. With respect to a 1-V<sub>PP</sub> input, this equals around 15  $\mu$ V.

- Input voltage noise:  $15 \mu\text{V}/\text{SQRT}(1 \text{ MHz}) = 15 \text{ nV}/\text{SQRT}(\text{Hz})$
- Input current noise:  $15 \mu\text{V}/\text{SQRT}(1 \text{ MHz})/\text{R}_{\text{INPUT}}$ , for  $\text{R}_{\text{INPUT}} = 1\text{k}$  equals  $15 \text{ pA}/\text{SQRT}(\text{Hz})$

Gain and offset are rather DC parameters and their drift is typically very slow as mainly related to temperature or aging. Initial offset and gain can be calibrated during initialization, with specific algorithms even during run-time. Therefore, the requirements for these parameters can be slightly relaxed. The gain and offset drift over temperature shall be each in the range of 10 LSB. With respect to a 1-V<sub>PP</sub> input signal, this equals around 150  $\mu$ V.

- Offset drift [0 to 85°C]:  $150 \mu\text{V}/85^\circ\text{C} \sim 2 \mu\text{V}/^\circ\text{C}$
- Gain drift: [0 to 85°C]:  $160 \text{ ppm}/85^\circ\text{C} \sim 2 \text{ ppm}/^\circ\text{C}$

For the gain setting, matched resistors (same package) are recommended.

#### 1.4.2 Comparator Function System Design for Incremental Count

Referring back to [Figure 5](#): The total propagation delay between the analog signal and the digital signals ATTL and BTTL at 500 kHz should be less than 90°, equivalent to 500 ns. The hardware should not contribute more than around 50 to 70%; equivalent to 250 to 350 ns to leave headroom for example hardware related offset and temperature drift, phase shift due to analog low-pass/decoupling filters and non-ideal synchronization in the subsequent host processor.

The hysteresis contribution to the delay with a 160-mV hysteresis ( $\pm 80 \text{ mV}$ ) at a minimum 0.3-V<sub>PP</sub> input to the comparator is around 32 degree, or 180 ns at a 500-kHz signal frequency.

The comparator's propagation delay adds on top. The lower the comparator's propagation delay the more headroom is available to increase the hysteresis or apply other means to increase the system's noise immunity.

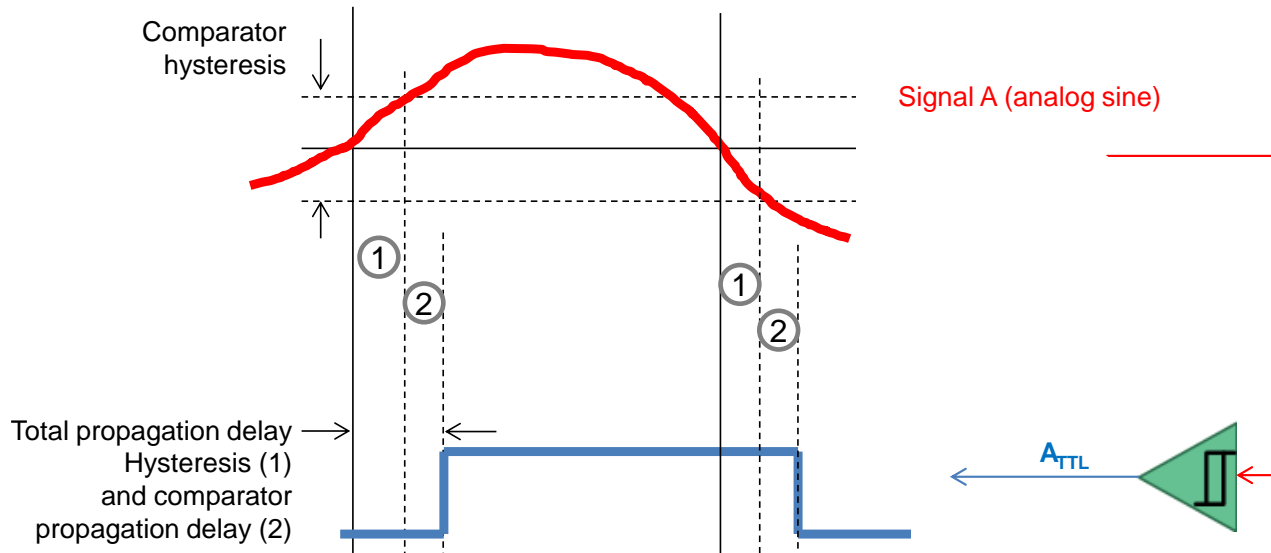


**Figure 11. Signal Delay on Comparator With Hysteresis**

## 2 Design Features

As outlined in [Section 1](#), this TI design realizes an industrial temperature range, EMC-compliant interface to Sin/Cos incremental position encoders with differential  $1\text{-}V_{\text{PP}}$  analog output signals A, B, and index marker R with input frequencies up to 500 kHz and a 5-V supply voltage. The major building blocks of this TI design are the dual path analog signal chain, the high-speed comparator block, the power management block and the interfaces to the Sin/Cos encoder as well as the interface to a host microcontroller for digital signal processing and high-resolution position calculation.

To allow for easy evaluation of this TI design, an example firmware is provided for the TMS320F28069M InstaSPIN-MOTION LaunchPad. The TMS320F28069M calculates the high-resolution angle position for both signal paths, using the external 16-bit ADC through SPI and the analog channel with the internal dual S/H 12-bit ADC and outputs the angle position data with up to 28-bit resolution through a USB virtual COM port.

### TIDA-00176 Features Overview

- Wide input voltage range: 24-V (17 to 36 V) with reverse polarity protection provides the necessary voltages for analog signal chain as well as the 5.25 V for the Sin/Cos encoder.
- Encoder interface: Sub-D15 or 8-pin header interface to 5-V Sin/Cos encoders with differential output signals A, B, and marker R from 0.3 V to  $1.2\text{ V}_{\text{PP}}$  at  $2.5\text{-}V \pm 1\text{-}V$  offset, input bandwidth up to 500 kHz.
- Dual path analog signal processing: Dual path option with an onboard high-speed, high-resolution dual 16-bit simultaneous sampling ADC with SPI and dual analog outputs with a 1.65-V bias voltage to interface to an external dual S/H ADC. High-speed, low propagation delay comparators with an adjustable 160-mV hysteresis for better noise immunity to convert the analog signals A, B, and R to 3.3-V TTL signals often referred as ABZ signals.
- High-resolution interpolated angle position, up to 28-bits resolution, cable length tested up to 70 m.
- EMC immunity: The design is tested for IEC61000-4-2, 4-4, and 4-5 (ESD, EFT, and Surge) as specified in the standard IEC 61800-3 EMC immunity requirements and specific test methods applicable in adjustable speed, electrical-power drive systems.
- Interface to host processor with 3.3-V digital interface signals to MCU QEP and SPI and optional single-ended analog 0 to 3.3-V outputs for MCU embedded dual S/H ADC.
- Evaluation firmware: Example firmware for Piccolo F28069M MCU with high-resolution dual angle position calculation at 16 kHz. The user interface is through USB virtual COM port for easy performance evaluation.

### 2.1 Sin/Cos Encoder Interface

The design offers either a shielded Sub-D15 female connector compatible to HEIDENHAIN encoder test equipment or an 8-pin header connector to interface to 5-V Sin/Cos encoders with differential output signals A, B, and marker R.

**Table 8. Sin/Cos Encoder Interface**

PARAMETER	TYPICAL VALUE	COMMENT
Encoder supply voltage	5.25 V [ $\pm 5\%$ ], 200 mA	5.25 V was chosen for an additional 0.25-V margin to compensate for voltage drop over longer cables. Adjustable to, for example, 5 V through feedback resistor change
Input signals	A+, A-, B+, B-, R+, R-	120- $\Omega$ differential line termination
Input level and common mode voltage range for A+, A-, B+, B-	0.3-V – $1.2\text{ V}_{\text{PP}}$ , 2.5 V $\pm 1.0$ V common mode	
Input level and common mode voltage range for R+, R-	0.2-V – $0.85\text{ V}_{\text{PP}}$ , 2.5 V $\pm 1.0$ V common mode	

## 2.2 Host Processor Interface

The high-resolution path for signals A+, A– and B+, B– features a high-speed, high-resolution dual 16-bit simultaneous sampling ADC with differential input and SPI output. The main features of this functional block are outlined in [Table 9](#).

**Table 9. 16-Bit High-Resolution Channel With ADC and SPI Output**

PARAMETER	TYPICAL VALUE	COMMENT
Gain A, B	5.0 (0.1%)	Matched single package gain setting registers (0.1%)
Gain drift A, B	2 ppm/°C	Matched single package resistors
Offset, A, B	< 10 LSB (@ 16-bit)	Uncalibrated
Offset drift, A, B	< 0.15 LSB/°C	
Bandwidth (-3 dB)	≥500 kHz	
Quantization	16-bit	FSR = ±5 V (ADS8354) Drop-in compatible 14- or 12-bit versions available
Sampling frequency	Up to 700 kSPS	
Data output format A, B	16-bit two's complementary	
Serial interface (SPI slave)	3.3 V, up to 24-Mhz SPI clock	Dual 16-bit data per SPI frame

The parallel, second path for the signals A+, A– and B+ offers a single-ended analog output for A and B with a 1.65-V bias voltage to interface to an external dual S/H ADC, which is for example embedded in microcontrollers like a C2000 Piccolo.

**Table 10. Analog Channel With Single-Ended Analog Output**

PARAMETER	TYPICAL VALUE	COMMENT
Single ended analog output A and B	0-3.3 V, 1.65-V bias voltage [50 ppm/K]	Drop-in compatible 1.5-V reference available to match ADC with 0-3-V input and 1.5-V bias.
Gain (A,B)	1.66 (0.1%)	Adjustable, 0.1% resistors recommended
Offset (A,B)	< 1 mV	Uncalibrated
Offset drift (A,B)	< 2 µV/°C	
Bandwidth (-3 dB)	~ 500 kHz	Adjustable LP filter for bandwidth adjustment

The comparator block features high-speed, low-propagation delay comparators with an adjustable 100-mV hysteresis for better noise immunity to converts the analog signals A, B, and R to 3.3-V TTL.

**Table 11. Comparators**

PARAMETER	TYPICAL VALUE	COMMENT
Digital output signals A, B, and R	3.3-V TTL	
Hysteresis	~160 mV (±80 mV)	For increased noise immunity, adjustable through feedback resistor change
Propagation delay	~ 40 ns	Low propagation delay
Maximum phase delay (propagation delay and hysteresis)	< 60°	at 0.3 V <sub>pp</sub> , 500-kHz input

## 2.3 Evaluation Firmware

To allow for quick evaluation of the TIDA-00176 design an example firmware for Piccolo F28069M MCU is provided, where the interpolated high-resolution angle is calculated for both the 16-bit dual ADC ADS8354 and the F28069M MCU's embedded dual S/H 12-bit ADC. A user interface through USB virtual COM port at 115000 baud allows for easy performance evaluation.

The user interface through virtual COM port at 115000 baud supports the following features:

- Selection of Sin/Cos encoder line count: up to 32000
- Hardware and software synchronized sampling of the external dual sampling 16-bit ADC through SPI, the internal 12-bit dual S/H ADC and the incremental counter with a synchronization delay of less than 100 ns
- High resolution angle in 32-bit, fractional Q28 format. Angle scaled per unit from 0 to 0.9999999, up to 28-bit interpolated angle resolution
- Automatic absolute position initialization after first occurrence of index marker R
- Menu to support display mode at 10 Hz or data dump mode at a 200-Hz update rate for total angle, incremental angle and phase with both, the 16-bit dual ADC (ADS8354) on the TIDA-00176 design, and the C2000 on-chip 12-bit dual S/H ADC
- Diagnostic error message when encoder not connected or when differential input voltage below 0.3 V<sub>PP</sub>

## 2.4 Power Management

The TI design features a 24-V DC input with wide input voltage range from 17 to 36 V and reverse polarity protection. The onboard power management is split into a DC/DC buck that generates an intermediate 6-V rail and three LDOs, which generate the corresponding 3.3-V, 5-V, and 5.25-V rails.

The 5.25-V encoder supply features a LDO with very low noise and an enable pin. Therefore, the Sin/Cos encoder supply voltage can be turned off through the host processor if desired.

**Table 12. TIDA-00176 Voltage Rails**

PARAMETER	VOLTAGE	CURRENT	COMMENT
Input	24 V [17 to 36 V]	150 mA	Wide input voltage with reverse polarity protect
Intermediate rail	6 V [ $\pm 5\%$ ]	500 mA	Intermediate rail. High-efficiency (>80%) DC/DC buck power supply
Encoder supply	5 V [ $\pm 5\%$ ]	250 mA	5.25 V was chosen for an additional 0.25V margin to compensate for voltage drop over longer cables. Adjustable to, for example, 5 V through feedback resistor change
5-V supply rail	5 V [ $\pm 5\%$ ]	100 mA	High precision signal chain supply
3.3-V supply rail	3.3 V [ $\pm 5\%$ ]	100 mA	Low precision signal chain supply

## 2.5 EMC Immunity

The design meets ESD, EFT, and Surge requirements per IEC61000-4-2, 4-4, and 4-5 with levels specified in the IEC 61800-3 standard "EMC immunity requirements for adjustable speed, electrical-power drive systems". It is assumed only the subD-15 connector to the position encoder can be accessed and shielded encoder cables are used to connect to the encoder. Because the encoder cable can exceed 30 m, ESD, EFT, and Surge apply per [Table 13](#) for use in Environment 2.

**Table 13. EMC Immunity Requirements**

PORT	EMC TEST	EMC STANDARD	LEVEL	PERFORMANCE (ACCEPTANCE) CRITERION
Sin/Cos Encoder Interface Connector	ESD	IEC61000-4-2	$\pm 4\text{-kV}$ CD or $8\text{-kV}$ AD, if CD not possible	B
	Fast transient burst (EFT)	IEC61000-4-4	$\pm 2 \text{ kV}/5 \text{ kHz}$ , capacitive clamp	B
	Surge 1.2/50 $\mu\text{s}$ , 8/20 $\mu\text{s}$	IEC61000-4-5	$\pm 1 \text{ kV}$ . Since shielded cable >20 m, direct coupling to shield ( $2\text{-}\Omega$ source impedance)	B

The performance (acceptance) criterion is defined, as follows:

**Table 14. Performance Criterion**

PERFORMANCE (ACCEPTANCE) CRITERION	DESCRIPTION
A	The module shall continue to operate as intended. No loss of function or performance even during the test
B	Temporary degradation of performance is accepted. After the test, the module shall continue to operate as intended without manual intervention.
C	During the test, loss of functions accepted, but no destruction of hardware or software. After the test, the module shall continue to operate as intended automatically, after manual restart, or power off, or power on.

### 3 Block Diagram

The system block diagram of this design is shown in [Figure 12](#). The major building blocks of this TI design are a dual path for the analog signal chain, a high-speed comparator block, the power management and the interfaces to the Sin/Cos encoder and host microcontroller for digital signal processing and high-resolution position calculation. To allow for easy evaluation of the TIDA-00176 design, an example firmware is provided for the F28069M Piccolo LaunchPad, which outputs the angle position through virtual COM port.

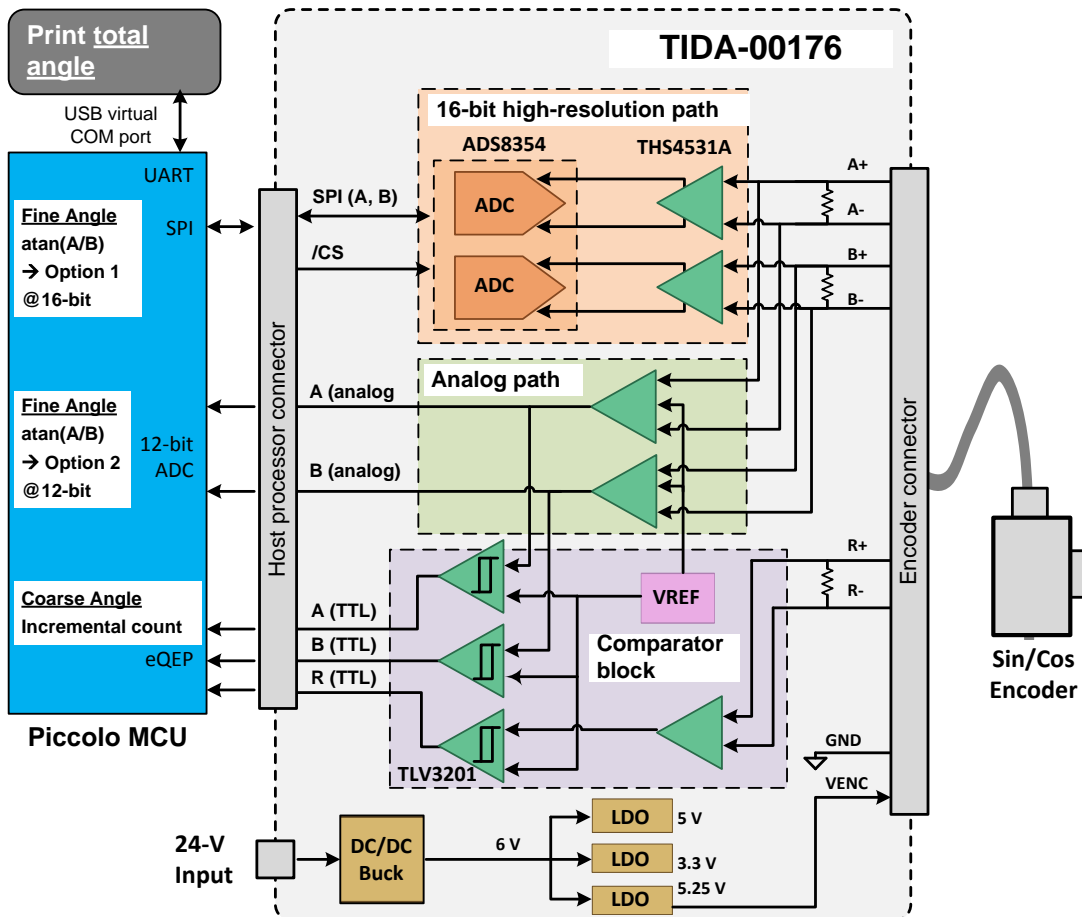


**Figure 12. System Block Diagram of TIDA-00176 With Piccolo F28069M LaunchPad**

The analog signal chain provides  $120\Omega$  termination with EMC protection and amplifies and level shifts the differential  $1-V_{PP}$  sine and cosine input signals, respectively. A dual signal path option is provided with an onboard ADS8354 high-speed, dual 16-bit simultaneous sampling ADC with SPI and an analog path with dual analog outputs with a 1.65-V bias voltage to interface to an external dual S/H ADC, which is for example embedded on MCUs like C2000 Piccolo.

The high-speed, low propagation delay comparator block features adjustable hysteresis for better noise immunity and converts the analog signals A, B, and the marker R into digital signals with 3.3-V TTL-level to interface to a quadrature encoder pulse module like the QEP module on the C2000™ Piccolo MCU.

The onboard wide-input range 24-V power supply provides the necessary voltages for analog signal chain as well as the 5.25 V for the Sin/Cos encoder.

The Sin/Cos encoder interface offers either a 15-pin shielded Sub-D connector or an 8-pin header. The interface to the host MCU offers digital 3.3-V TTL compliant signals for SPI and A, B, and R as well as analog signals A and B scaled from 0 to 3.3 V with a 1.65-V bias voltage.

## 4 Circuit Design and Component Selection

### 4.1 Analog Signal Chain

Figure 13 provides an overview on the analog signal chain sub-system and the comparator subsystem. For the analog signal chain, two paths are implemented:

- A high resolution signal path with increased common mode noise immunity featuring fully differential amplifiers and fully differential dual 16-bit ADC with an SPI output
- An analog path with differential input to single-ended analog output to drive the comparator and additionally for interface to a host processor with embedded ADC

The dual analog path offers the option to either test the design with the onboard 16-bit dual ADC as part of the high-resolution path, or use the analog differential to single-ended path with an MCU with embedded ADC. Additionally the analog path, since decoupled through a buffer from the high-resolution path, ensures an ideal decoupling of the comparator path. This avoids x-talk into the high-resolution analog path when switching the output level during sine and cosine zero crossing.

Another use case would use both paths. One path would have improved noise immunity with a reduced bandwidth to filter out HF noise, while the other path would offer standard bandwidth up to maximum speed. The lower bandwidth with improved noise immunity would be dedicated to the high-resolution 16-bit ADC, while the other path with standard bandwidth would be connected to the MCU with embedded ADC. The interpolated phase (arc tangent) would then be taken from the high-resolution path when the motor speed is low (below the configured cut-off frequency), while at higher speed the interpolated phase from the other path would be used. The host processor will decide which angle to use pending motor speed.

The comparator sub-system will generate TTL level outputs for signals A, B, and R, at a very low-propagation delay. Each sub-system is explained in the following sections.

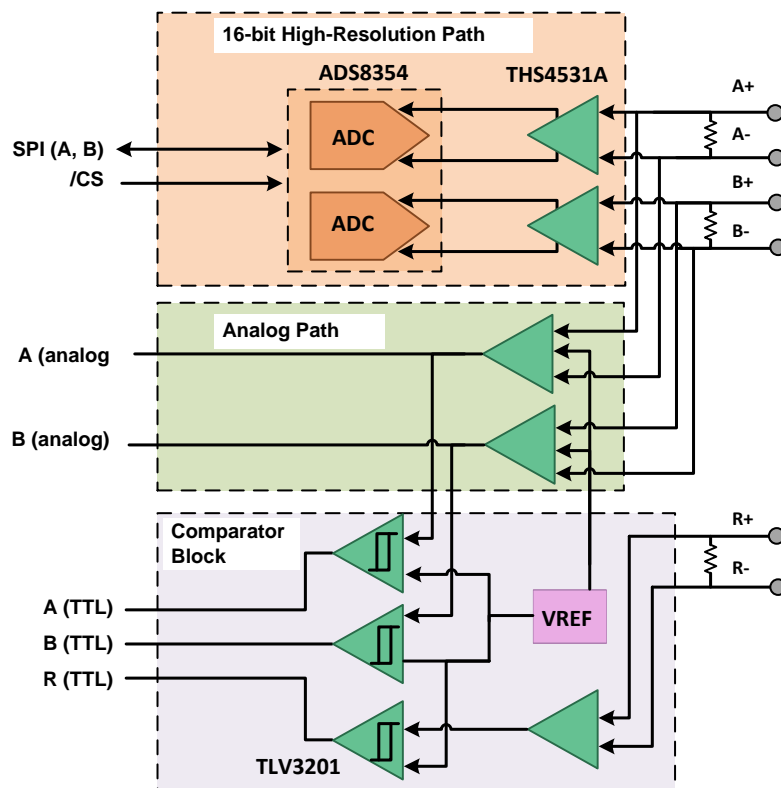


**Figure 13. Analog Signal Chain**

## 4.1.1 High-Resolution Signal Path With 16-Bit Dual Sampling ADC

### 4.1.1.1 Component Selection

A high-precision dual channel ADC is required to fulfill the design requirements. The ADS8354 has been selected for the following reasons:

- High resolution (16-bit) with high precision (superb THD and SNR performance of  $-93$  dB SNR,  $-100$  dB THD)
- Drop-in pin-compatible 14-bit and 12-bit versions for flexibility pending required resolution versus cost optimization
- High speed (700 kSPS) and bandwidth to support at least 500-kHz analog input signals
- Dual channel with true differential inputs and dual/independent reference voltages to improve immunity against common mode noise
- Dual channel, simultaneous sampling of two channels to ensure zero phase shift between the sin and cos input signals A and B
- Sample point triggered by hardware (falling edge of /CS) allows host processor to precisely synchronize the sample point with the incremental counter latch.
- Sample-and-hold circuit returns to sample mode after completing the conversion process, hence relative long sample times to settle to 16-bit accuracy
- Dual, programmable, and buffered 2.5-V internal reference to provide common mode bias voltage to amplifier to almost cancel offset and offset drift related errors.
- Serial interface to host processor (dual data) with up to 24-MHz clock frequency to minimize latency
- Fully-specified over the extended industrial temperature range:  $-40^{\circ}\text{C}$  to  $125^{\circ}\text{C}$
- Small package

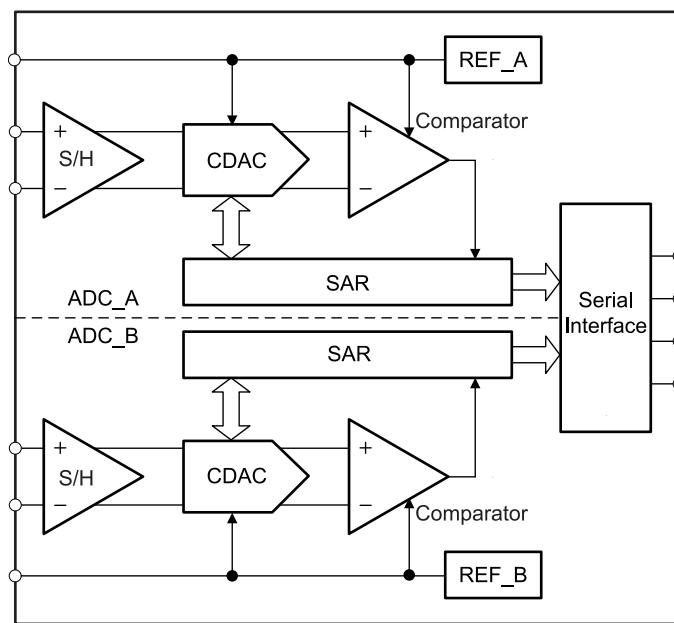
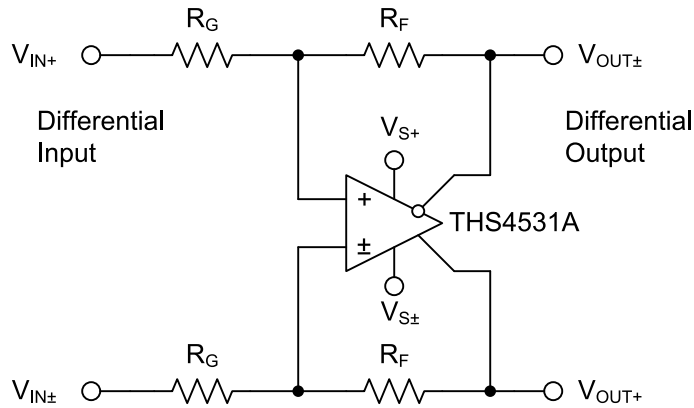


Figure 14. ADS8354 Block Diagram

To leverage the ADS8354 performance, a fully differential high-speed amplifier with configurable output common mode voltage, like the THS45xx family, is required.



**Figure 15. Differential Input to Differential Output Amplifier**

The signal remains fully differential, the gain and optional filtering is defined by the input and feedback resistors and capacitors. The gain is set by the ratio of  $R_F/R_G$  and the output common mode voltage is set by the input signal  $V_{OCM}$ .

The THS4531A was chosen as it meets the topology, can drive the ADS8354, and meets the AC and DC requirements specified in [Section 1.4](#). A single amplifier topology per package was used instead of the dual differential amplifier per package like the THS4532 for flexibility and easier PCB routing.

The key parameters of the THS4531A for use in this design are:

- Fully differential architecture with adjustable output common mode voltage
- High gain bandwidth: 27 MHz (6 MHz at  $G = 5$ )
- Low distortions, THD –120 dBc at 1 kHz ( $1 V_{RMS}$ ,  $R_L = 2 k\Omega$ )
- Low input voltage noise:  $10 nV/\sqrt{Hz}$  ( $f = 1 kHz$ )
- Very low offset,  $V_{OS}$ :  $\pm 100 \mu V$
- Very low offset drift,  $V_{OS}$  Drift:  $\pm 2 \mu V/^{\circ}C$  (Industrial temperature range)
- Single 5-V supply to leverage same supply than the ADS8354
- Rail-to-rail output (RRO) and negative rail input (NRI) to maximize input and output signal swing

#### 4.1.1.2 Input Signal Termination and Protection

The differential input signals are terminated with  $120\Omega$  resistors each. COG capacitors are added for differential and common mode HF noise rejection. The differential low-pass filter's cut-off frequency ( $-3\text{ dB}$ ) is around 6 MHz. The  $10\Omega$  (1%) pulse-proof resistor in conjunction with Schottky-diodes clamp to the 5-V rail or GND, for ESD protection with input current limitation. Figure 16 shows the TIDA-00176 schematics of the input stage for the encoder's differential signals A+ (sine) and A- (cosine).

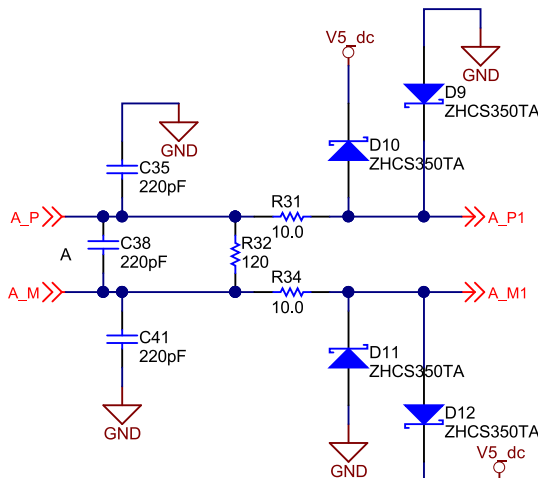


**Figure 16. Termination for Analog Inputs**

Looking at the encoder signals A+/A- (named "A\_P – A\_M" in the schematic) signal conditioning block schematic from left to right we can distinguish the following parts/functions:

- The HF noise suppression COG capacitors: C35, C38, and C41. For higher common mode rejection, an additional 2-nF COG capacitor might be placed in parallel to the 220-pF capacitor from each differential input to GND. The low-pass cut-off frequency ( $-3\text{ dB}$ ) is around 6 MHz.
- The impedance matching/termination resistor  $120\Omega$ : R32
- Current limiting resistors with pulse proof current: R31, R34
- Clamping diodes / op-amp input protections (D9 to D12) to the 5-V rail and GND

The LP filters are designed to guarantee the proper functionality and performance at the speed provided in the system specifications.

#### 4.1.1.3 Differential Amplifier THS4531A and 16-Bit ADC ADS8354

The two primary circuits, required to maximize the performance of a high-precision, successive approximation register (SAR) ADCs, are the input driver and the reference driver circuits. For details on selecting the amplifier, refer to the ADS8354 datasheet, Section 9.1.

The THS4531A has been minded to work in combination with the ADS8354. Indeed, the common mode or DC-level of the input signal (2.5 V nominal) is provided to the THS4531A directly from the reference output of the ADS8354 itself to minimize potential offset and drift errors.

The differential input full scale range of the ADS8354 was configured to  $\pm 2 \times V_{REF}$ . With the reference voltage of  $V_{REF} = 2.5$  V, this yields a FSR of  $\pm 5$  V. The maximum Sin/Cos encoder's differential input voltage is  $1.2 V_{PP}$ . A voltage of higher than  $1.35 V_{PP}$  should still be detected as failure. A safety margin of 50% is added to the maximum peak-to-peak voltage, which is then  $1.8 V_{PP}$ . To match the ADC full-scale input range, the gain of the THS4531A should be 5.5. However, to remain in the linear output voltage range of the THS4531A at a 5-V supply, which is at least 0.25 to 4.8 V, the gain should be reduced by around 10%, hence the ideal differential amplifier gain would be 5.

To ensure the minimum gain error and especially drift between the channels, high-precision, matched resistors with 0.1% accuracy and 2-ppm/K temperature drift are required. To minimize noise, the feedback resistors should be chosen in the lower  $k\Omega$  range (see [Section 1.4](#)).

A precision matching resistor divider is used to keep potential gain errors as small as possible. Refer to the MPMT10015001AT1 datasheet for details.

Due to the gain of 5, a typical  $1-V_{PP}$  input signal leverages around 50% of the ADC full-scale range (FSR), which results in a loss of 1-bit of precision, therefore yielding an equivalent 15-bit resolution. The lower input voltage of  $0.6 V_{PP}$  will leverage around 25% of the FSR, which equals typically 14-bit resolution.

[Figure 17](#) shows the schematics of the high-precision analog signal path; the matched gain setting resistors are R18, R27, R30, and R37.

The series  $10\Omega$  resistors R21, R25 and the  $2.2-nF$  capacitor C29 (R33, R36, and C39 for ADS8354 channel B) from the anti-aliasing filter. The filter capacitor C29 (C39), connected across the ADC inputs, filters the noise from the front end drive circuitry, reduces the sampling charge injection and provides a charge bucket to quickly charge the internal sample-and-hold capacitors during the acquisition process. As a rule of thumb, the value of this capacitor should be at least 10 times the specified value of the ADC sampling capacitance. For these devices, the input sampling capacitance is equal to 40 pF. The capacitor should be a COG- or NPO-type because these capacitor types have a high-Q, low-temperature coefficient, and stable electrical characteristics under varying voltages, frequency, and time. To avoid amplifier stability issues,  $10\Omega$  series isolation resistors R21, R25 (R31, R39) are used at the output of the amplifiers. For details, refer to the Section 9.1 of the ADS8354 datasheet.

To minimize the impact of an offset drift of the ADC reference REFIO\_A and REFIO\_B, the ADC references are used to bias the common mode output voltage of the THS4531A. To buffer and decouple the  $V_{OCM}$  signal at the THS4531A, small RC filters R24/C32 and R35/C42 R28, R29, C36, and C37 are added close to each pin.

The ADS8354 reference voltages REFIO\_A and REFIO\_B are decoupled with a  $10-\mu F$  capacitor C36 and C37, respectively and a  $0.22\Omega$  resistor is added in series to avoid high-frequency oscillations.

To optimize the layout for cross-talk with minimum use of via for the critical signals A+, A- and B+, B-, the following connections have been made.

1. The differential input signal A (A+, A-) has been inverted at the input of the THS4531A and fed into the ADS8354 input channel B.
2. The differential output signal of the THS4531A, B+ and B- have been connected inverted to the ADS8354 input pins AINP\_A to B- and AINM\_A to B+

This results in the following hardware relationship: The ADS8354 channel B equals the inverted Sin/Cos encoder signal A; the ADS8354 channel A equals the inverted Sin/Cos encoder signal B.

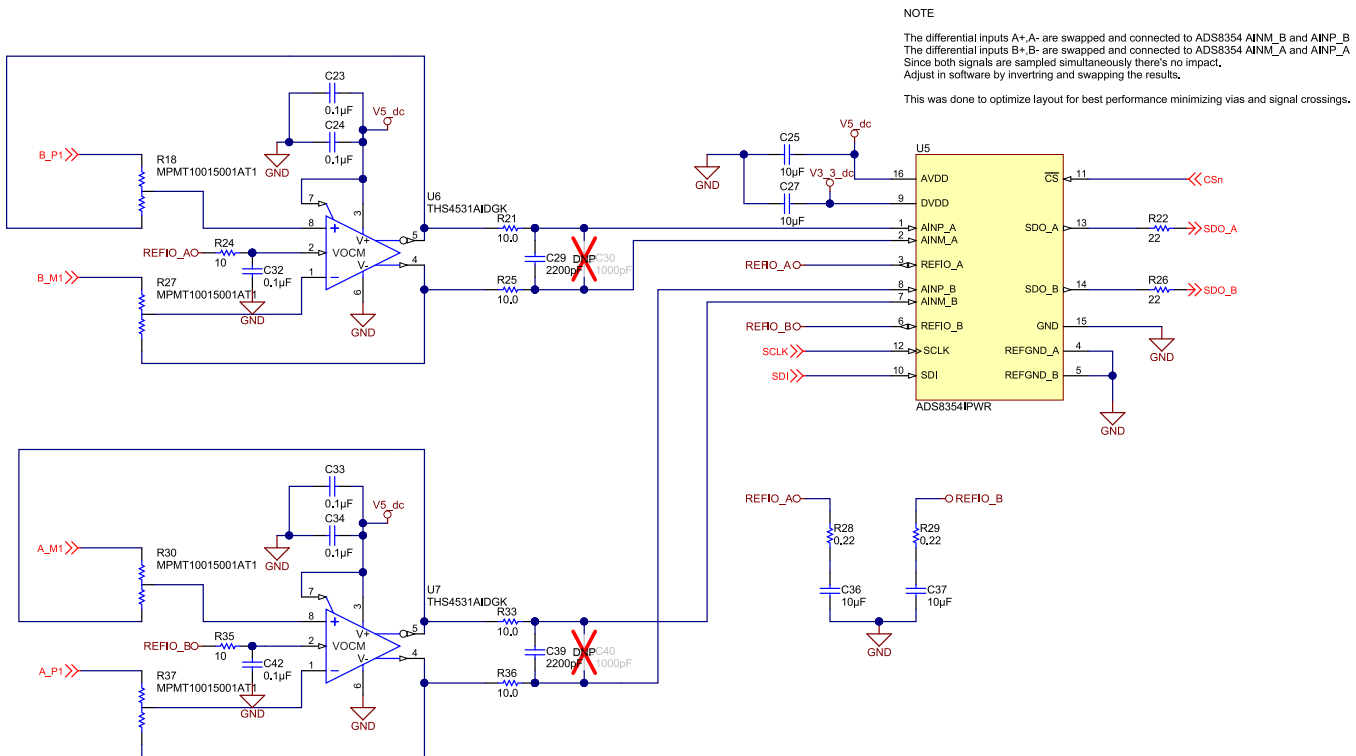


**Figure 17. Sin and Cos Signal Chain With Dual THS4531A and ADS8354**

---

**NOTE:** Channels are inverted and swapped for optimum performance layout and minimize the numbers of vias.

---

To achieve a higher noise immunity with reduced bandwidth, a capacitor of 10 pF (1% or better) or higher, pending desired bandwidth is recommended in the feedback path in parallel to the 5 kΩ. See [Section 4.5](#).

The configuration of the ADS8354 registers through serial interface is explained in [Section 4.3](#).

#### 4.1.2 Analog Signal Path With Single-Ended Output for MCU With Embedded ADC

The parallel analog signal path should not impact the high-resolution path and especially the differential amplifier. Therefore, the differential signals A+, A–, B+, and B– are tapped off after the input termination and protection and are buffered using unity gain amplifiers with very low offset and especially offset drift. The following amplifier should convert the differential signals into a single-ended signal. The minimum bandwidth should be least 500 kHz, ideally higher to support incremental encoders with higher than 500-kHz output signals. The phase delay for the path to the comparator should be similar than the high-resolution path to ensure minimum analog signal phase shift.

The supply voltage should be a single supply 5 V.

To match the high-resolution channel, the sum of the offset drift of both op-amps should be at least 12-bit equivalent accuracy, ideally match the analog performance of the high-resolution channel. For the input buffer and the differential to single-ended conversion, the OPA2365 has been selected due to:

- 2.2-V TO 5.5-V operation to leverage 5-V rail
- Rail-to-rail I/O
- Very low offset and offset drift: 200  $\mu$ V (max) and 1  $\mu$ V/K (typically)
- Low voltage and current noise: 4.5 nV/SQRT(Hz) and 0.004 pA/SQRT(Hz)
- Excellent THD+N: 0.0004%
- High common mode rejection, CMRR: 100 dB (min)
- Slew rate: 25 V/ $\mu$ s
- Fast settling: 300 ns to 0.01% to drive external ADC

Another option is the OPA2322, which is a lower cost alternative, with 2-mV offset voltage and slightly reduced AC and DC performance.

The analog output voltage should be scaled from 0 to 3.3 V with a 1.65-V common mode. Applying the same criteria in [Section 4.1.1](#) with a maximum 1.8-V<sub>PP</sub> input voltage, and a 10% margin with regards to the 3.3-V FSR, the gain yields 1.66.

[Figure 18](#) shows the analog signal chain for channel A. The channel B is identical.

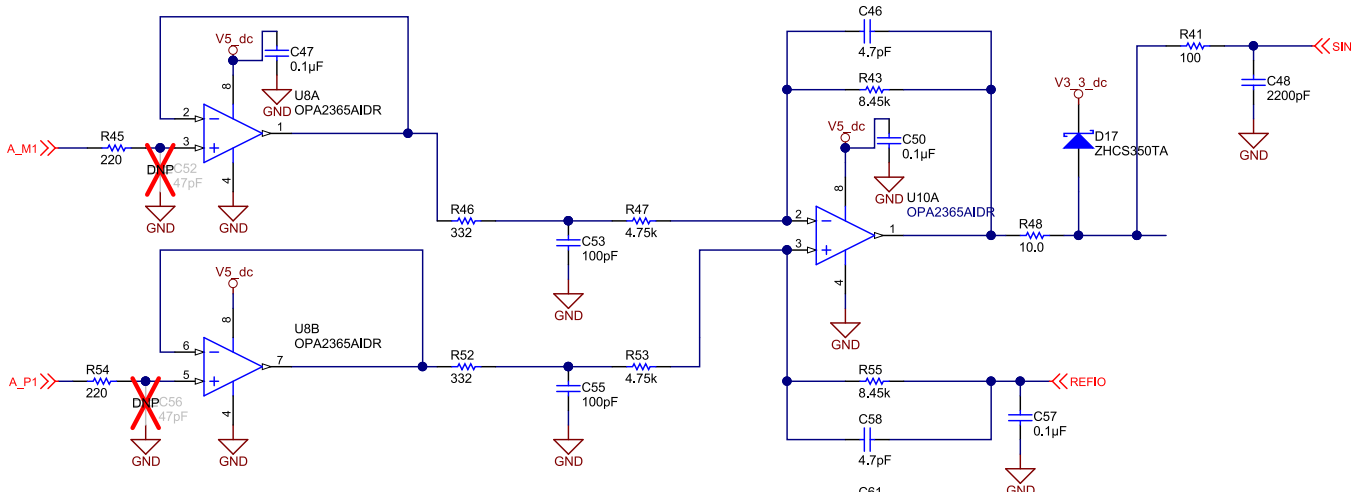


**Figure 18. Analog Signal Path With Differential Input to Single-Ended Output for Signal A (sin), Signal B (cos) Not Shown**

The differential signals A\_P and A\_N are connected through a 220- $\Omega$  resistor to the non-inverting input of the OPA2365 (U8A and U8B). The OPA2365 (U8A and U8B) are configured as unity-gain buffer to avoid loading the source and introducing distortions. The 220- $\Omega$  series resistor limits the current into the non-inverting input of the OPA2365 in case of an over- or undervoltage event. The output of each buffer employs a small, adjustable RC-filter with, for example, R46 and C53 in above picture with f-3dB ~ 5 MHz for high-frequency noise reduction.

The following OPA2365 (U10A) is configured as differential to single-ended amplifier and level shifter. The gain is set to 1.66 and the output common mode voltage to 1.65 V through a low-drift voltage reference REF2033. An adjustable 5.6-pF feedback capacitor is added in parallel to the feedback resistor for HF noise filtering (f-3dB ~ 3.5 MHz), ideally matched to the THS4531A bandwidth. See [Section 4.5](#).

Since the OPA2365 is supplied with 5 V, the output of the amplifier is clamped to 3.3 V (D17) with a series 10- $\Omega$  current limiting resistor (R48). This is to protect the following comparator (TLV3202/1) and an external ADC, which typically are 3.3-V I/O.

An anti-aliasing and decoupling RC network (R41/C48) is added to drive an external ADC. The filter was optimized for use with the embedded 12-bit dual S/H ADC in the C2000 Piccolo MCU family. For other ADCs, the filter has to be adjusted accordingly.

The 1.65-V bias voltage is decoupled with a 100-n capacitor (C57). Furthermore, LP RC filters have been added to reduce more and more HF noise components, in particular the one potentially coming from the switcher TPS54040A.

#### 4.1.3 Comparator Subsystem for Digital Signals A, B, and R

The comparators are required to detect the zero-crossing of the analog signals A and B, as well as the zero index pulse with the marker R and generate the corresponding digital 3.3-V TTL-compatible signals  $A_{TTL}$ ,  $B_{TTL}$ , and  $R_{TTL}$ , often referred to as ABZ. As outlined in [Section 1.4](#) a low propagation delay comparator offers additional margin to the system.

The comparators selected are the TLV3201 (single) and TLV3202 (dual), 40 ns, microPOWER, push-pull output comparators, with the following main characteristics:

- Low propagation delay of typical 40 ns
- Low input offset voltage of typical 1 mV, to ensure minimum drift of switching threshold
- Push-pull outputs, to drive the input of a 3.3-V I/O host processor
- Industrial temperature range

The TLC372 dual comparator with 250-ns propagation delay is a lower cost option, depending overall system propagation delay and maximum frequency. The advantage of the TLV320x family is that it allows other components to add more delay while still keep the required 500-ns maximum delay at 500 kHz. For example, a larger hysteresis would increase the propagation delay while improve immunity against noise.

##### 4.1.3.1 Non-Inverting Comparator With Hysteresis

The input signals to all comparators are derived from the output of the single-ended to differential amplifier. The output signal is clamped to 3.3 V, as described earlier, and decoupled with a RC network (like R49, C54 in figure 19 for signal A) to avoid cross-talk to the analog single-ended signals A and B respectively.

To match the phase between the high-resolution path and this path, the RC decoupling network at the input to the comparator matches the RC filter ( $2 \times 10 \Omega$  and  $2.2 \text{ nF}$ ) at the THS4531A output.

The TLV370x is configured as non-inverting comparator to detect the zero-crossing of the analog sin and cosine signals A and B as well as the index pulse R. [Figure 19](#) shows the corresponding schematics for the signal A.

The switching threshold is set by the reference voltage  $V_{REF} = 1.65 \text{ V}$  (REF2033), which is also used to bias the single-ended analog signals for the differential to single-ended amplifiers. For each comparator, the reference input is taken from the REF2033 and decoupled with a  $10\Omega$  series resistor and a 100-n capacitor.

A hysteresis is added for better noise immunity. The hysteresis ( $V_{TH+} - V_{TH-}$ ) of a non-inverting comparator can be calculated per [Equation 7](#):

$$V_{Hysteresis} = (V_{Out\_High} - V_{Out\_Low}) \times \frac{R_G}{R_F} \quad (7)$$

with  $V_{Out\_High}$  the high-level and  $V_{Out\_Low}$  the low level comparator output voltage,  $R_F$  the feedback and  $R_G$  the input resistor into the non-inverting comparator input.

For the configuration of this design as outlined in [Figure 19](#), the hysteresis has been set to around 160 mV per [Equation 8](#). Since R49 and R48 are magnitudes lower than R50, they can be neglected.

$$V_{Hysteresis} = 3.3 \text{ V} \times \frac{R_{50}}{R_{51}} \sim 160 \text{ mV} \quad (8)$$

The upper and lower switching thresholds  $V_{TH+}$  and  $V_{TH-}$  are defined per [Equation 9](#) and [Equation 10](#) with the reference voltage  $V_{REF} = 1.65$  V.

$$V_{TH+} = 1.65 \text{ V} \times \left(1 + \frac{R50}{R51}\right) = 1.73 \text{ V} \quad (9)$$

$$V_{TH-} = (3.3 \text{ V} - 1.65 \text{ V}) \times \left(1 - \frac{R50}{R51}\right) = 1.57 \text{ V} \quad (10)$$

### CAUTION

The lower threshold is a function of the supply voltage. However, the supply voltage tolerance of this design 5%, as typical with most designs. A  $\pm 5\%$  tolerance with the 3.3-V supply voltage would affect the lower threshold by only by  $\pm 16$  mV, resulting  $V_{TH-}$  range from approximately 1.56 to 1.59-V, hence still acceptable.

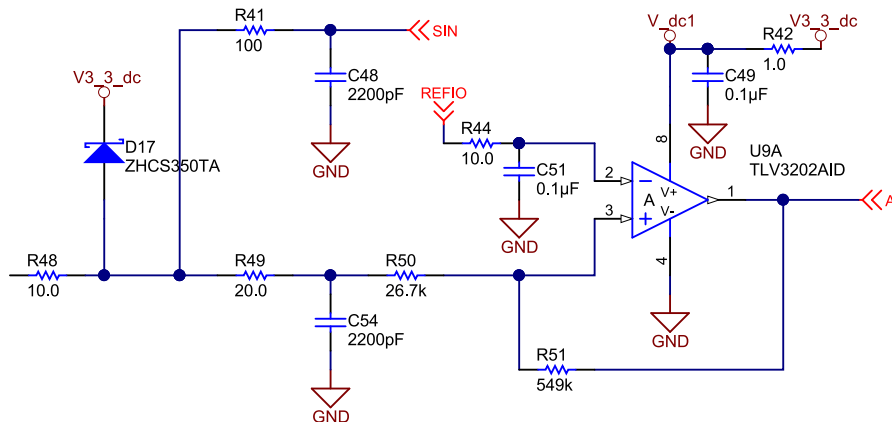


**Figure 19. Signal A Comparator With Hysteresis**

The 3.3-V supply of each comparator is decoupled with a 1- $\Omega$  series resistors and 100-nF capacitor to minimize cross-talk through the 3.3-V rail to other comparators. The RC low pass comprised of R49 and C54 is added to decouple the comparators switching node from the analog signal A/sin, which will be connected to an external ADC.

The hysteresis allows for a clean digital signal, which means it avoids fast switching due to noise around the zero crossing point. The hysteresis however introduces an additional propagation delay, which is depending on the analog signal amplitude  $V_{IN\_PEAK-PEAK}$  at the comparator input.

$$f_{Hysteresis} \sim \sin^{-1} \left( \pm \frac{160 \text{ mV}}{V_{IN\_PEAK-PEAK}} \right) \quad (11)$$

Assuming minimum input voltage of 0.3  $V_{PP}$ : The output of the differential- to single-ended amplifier (gain = 1.66) will have an amplitude of 0.5  $V_{PP}$  (0 to 100 kHz) and around 0.32  $V_{PP}$  at 500 kHz due to low-pass filter attenuation. The hysteresis corresponding phase delay of the digital signals A, B, and R will be around 30 degrees for a 0.32  $V_{PP}$  input at the comparator. At 500 kHz, this would translate into a total propagation delay of the comparator of around 170 ns + 40 ns = 210 ns.

Due to the low propagation delay of the TLV3201 with 40 ns only, the overall delay of the comparator block remains below 45 degrees up to 500 kHz.

The comparators for the signals B and R have the same settings. Also the buffering and gain stage for the index marker R is identical to the signals A and B. This is to ensure the phase of the index marker R is exactly in sync with the signal A and B up to a 500-kHz signal frequency. This ensures the zero Index Marker R will occur as specified, slightly before the rising edge of signals A and B. The index marker R defines the absolute zero position, and hence exact relation to signals A and B is required to avoid any position offset.

## 4.2 Power Management

The power management consists DC/DC buck to generate a 6-V intermediate rail from the 24-V input voltage. The encoder supply voltage and the 5-V and 3.3-V rails are derived from the intermediate voltage, as shown in [Figure 20](#).

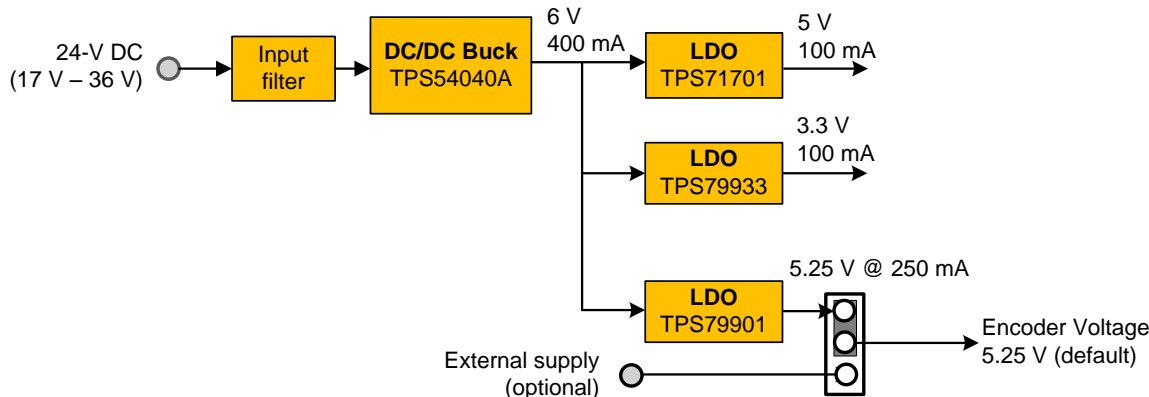


**Figure 20. Power Management Solution**

Because of the high performance required by the system and solution, most of the power rails are provided by low-noise LDOs. The drawback is the limited efficiency and low output current capability. The maximum output current is limited by the thermal performance, due to the high power losses.

To reduce the voltage drop across the LDO a high-efficiency DC/DC switching converter to generate a 6-V intermediate rail from the 24-V input is used. Pay attention to minimize the noise introduced by the switcher solution by proper layout and component selection.

### 4.2.1 24-V Input to 6-V Intermediate Rail

A switching DC-DC converter is provided to achieve the intermediate voltage rail of 6 V that supplied the three LDOs. This is a basically mandatory choice since the high VIN / VOUT ratio makes any LDO unsuitable for the power conversion. Indeed the efficiency of any LDO could be simply calculated as  $V_{OUT} / V_{IN}$  that, in the worst case (maximum VIN) would lead to  $5.25 \text{ V} / 36 \text{ V} \approx 14\%$ . The remaining 86% of the power consumption is dissipated by the LDO package: having indeed a maximum current of 200 mA would lead to  $36 \text{ V} \times 200 \text{ mA} \times 86\% = 6.2\text{-W}$  power dissipated on the LDO package that would simply and quickly blow up any reasonable package.

Starting with the input filter, it is widely known that conducted EMI are generated by the normal operation of switching circuits. Large discontinuous currents are generated by the power switches turn on and off very fast. In a buck topology, large discontinuous currents (high di/dt) are present at the input of the converter. The selected values for the input filter are shown in [Figure 21](#).

For more details about how to design an input EMI filter, please refer to the application report, AN-2162 *Simple Success With Conducted EMI From DC/DC Converters* ([SNVA489](#)).

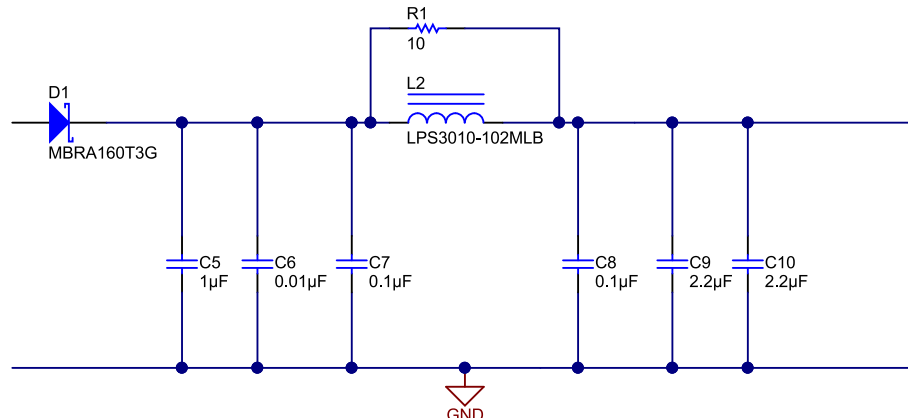


**Figure 21. Input Filter Including Reverse Polarity Protection**

The DC/DC buck converter has been designed to meet the following specifications:

- Input voltage:  $V_{IN} = 17$  to  $36$  V,  $24$  V nominal
- Output voltage:  $6$  V @  $500$  mA
- Switching frequency:  $500$  kHz nominal
- Output voltage ripple:  $25$  mV<sub>PP</sub> max
- Efficiency: >  $80\%$  at full load
- Non-isolated topology

The TPS54040A is selected for the purpose: this is a buck converter with an integrated FET, 3.5 to 42-V input voltage, and 0.8 to 39-V output voltage at a 500-mA output current. Its frequency can be adjusted from 100 kHz to 2.5 MHz or can be synchronized with an external clock. It can also be enabled and disabled. These features make the TPS54040A a very good fit to the requirements/specifications listed above.

Note that the TPS54040A is pin-to-pin compatible with the TPS5401, which is a lower cost version of the TPS54040A with similar performance but a less accurate output voltage and enable threshold.

Also note that the TPS54040A is pin-to-pin compatible also with the TPS54140A, TPS54240, TPS54340, and TPS54540: this widens the part selection and offers the possibility to modulate costs and power level (in case of future system upgrades).

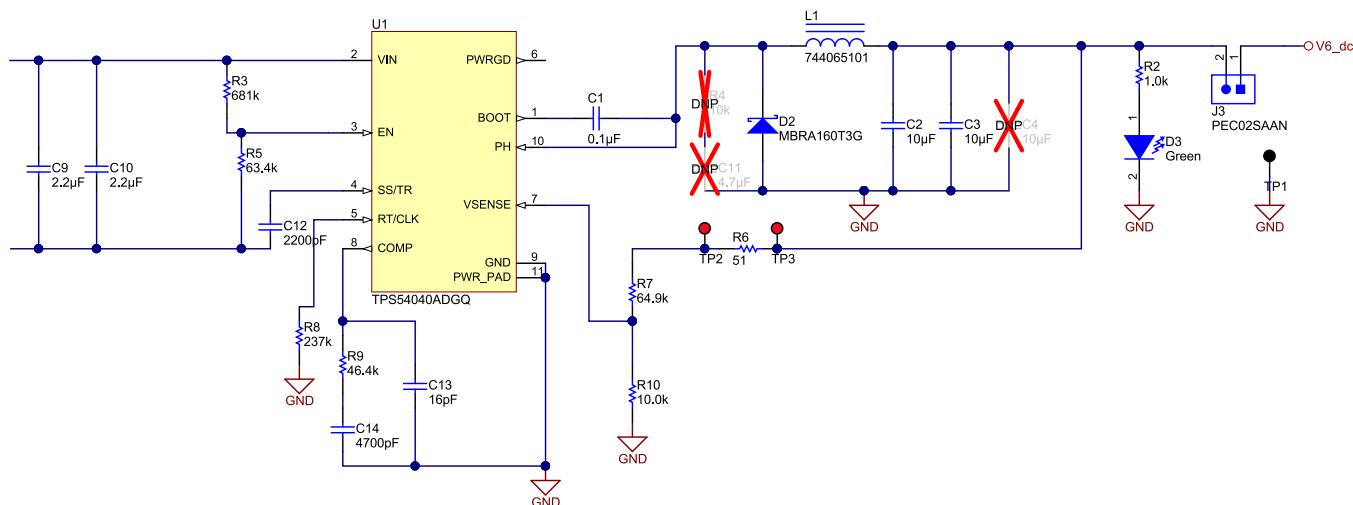


**Figure 22. Schematic of 24-V to 6-V DC-DC Buck Converter With TPS54040A**

For a detailed explanation of the design process, refer to the TPS54040A datasheet or the TI Design TIDA-00180.

On a typical application the output voltage is set thanks to a simple resistor divider network. [Equation 12](#) gives the value of the upper resistor according to the output voltage, the reference voltage (0.8 V for the TPS54040A) and the lower resistor (with R10 usually fixed to 10 kΩ).

$$R7 = R10 \times \frac{V_{OUT} - 0.8 \text{ V}}{0.8 \text{ V}} \quad (12)$$

With  $V_{OUT} = 6 \text{ V}$  and  $R10 = 10 \text{ k}\Omega$ ,  $R7$  yields 65 kΩ.

The tolerance of the 6-V output voltage will be  $6 \text{ V} \pm 4\%$ . This assumes feedback resistors with a 1% tolerance and the internal bandgap tolerance from the TPS54040A of  $\pm 2\%$ .

The switching frequency is set with  $R8 = 237 \text{ k}\Omega$  to 500 kHz.

On the TPS54040A schematics, some components are marked as do not populate (DNP). This is the case of the snubber network formed by R4 and C11. The snubber network is not needed with the TPS54040A design. A snubber network is a solution to reduce the ringing on the switch node and overshoot of the MOSFET if needed. For more details of other option, refer to the application note *Ringing Reduction Techniques for NexFET™ High Performance MOSFETs* ([SLPA010](#)) on how to use and calculate the snubber network.

#### 4.2.2 Encoder Supply

A 5.25-V supply for the encoder has been selected in order to meet a typical 5-V ( $\pm 5\%$ ) encoder supply specification and have a 0.25-V additional margin to compensate for voltage drop across longer cables used to connect the encoder.

The LDO that provides the 5.25 V to the encoder has to provide also an enable pin. In this way, it is possible to power-cycle the turn-off or power-cycle the encoder supply from a host processor, if desired to for example turn-off the voltage at the encoder connector in case no encoder is connected.

The LDOs do not need specific description, except for the allowed range of output cap/ESR for stability purpose; while the main design involves the SMPS, as this affects all the main performances (noise, EMI, efficiency, cost, and board space).

The TPS79901 has been designed to provide a little higher voltage than the nominal 5 V (5.25 V), using part of the greater accuracy of the LDO to reduce the thermal stress on it. In brief  $5.25 \text{ V} \pm 2\%$  is within the allowed supply range of the encoder (5 V  $\pm 5\%$ ). In this way, the power it has to dissipate is

$$P_{LDO,MAX} = (V_{LDO,IN} - V_{LDO,OUT}) \times i_{LDO,MAX} = (6 \text{ V} - 5.25 \text{ V}) \times 250 \text{ mA} = 187 \text{ mW} \quad (13)$$

With a 5-V encoder voltage, the maximum power dissipation would increase to 250 mW.

Indeed with a  $R_{thja} \approx 180^\circ\text{C}/\text{W}$  it means that the TPS79901 junction temperature will increase less than  $34^\circ\text{C}$  versus ambient temperature when working at maximum load current of 250 mA. For example at  $85^\circ\text{C}$  ambient, the junction will be  $120^\circ\text{C}$ .

The output voltage of the TPS79901 LDO is set with 1% feedback resistors R11 and R13 according to [Equation 13](#), where 1.193 V is the nominal value of the TPS79901 reference voltage:

$$V_{ENC\_VCC} = 1.193 \text{ V} \times \left(1 + \frac{R11}{R13}\right) = 1.193 \times \left(1 + \frac{340k}{100k}\right) = 5.25 \text{ V} \quad (14)$$

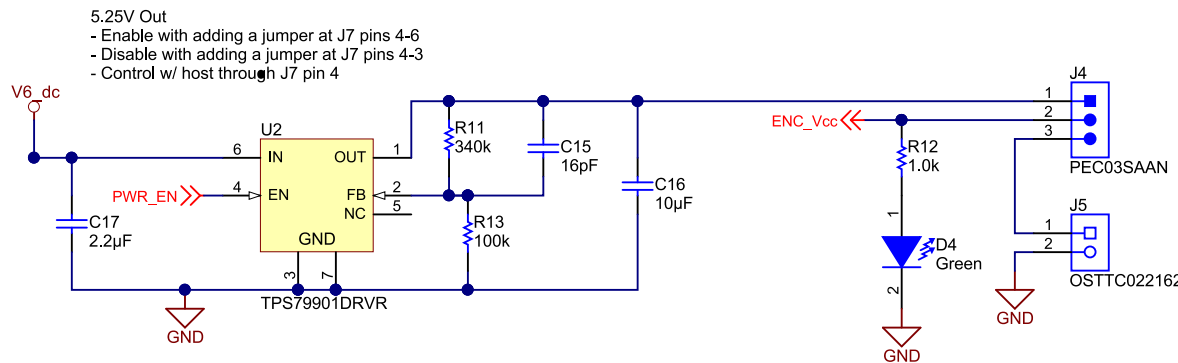


**Figure 23. Schematic of 5.25-V LDO for Encoder Supply**

A jumper selects between the 5.25-V LDO output and an optional external supply, if desired. The signal PWR\_EN is default pull-up, but can be asserted to low from a host microcontroller to disable or power-cycle the encoder supply voltage (see [Section 4.3](#)).

#### 4.2.3 Signal Chain Power Supply 5 V and 3.3 V

Because of the low current demanded by the analog signal chain, as described in [Section 4.1](#), and to achieve high-performance with very low noise, the LDO is again a mandatory choice. Indeed, because of the high PSRR featured by TI LDOs, the AC noise generated by the switcher is blocked and does not affect the noise sensitive analog parts, like the ADCs and the input buffers and amplifiers.

The 5-V rail is dedicated to the analog buffers and amplifiers as well as to the analog supply voltage of the ADS8354 ADC. The 3.3 V is dedicated to the digital supply of the ADS8354 and the comparators to ensure a 3.3-V interface to the host processor without the need for I/O level-shifters. Because of the low power consumptions of the selected components, an LDO each was selected for the 3.3-V and 5-V rail with a nominal output current of 100 mA.

A fixed 3.3-V LDO TPS79933 was used for the 3.3-V rail, the TPS71701 was used for the 5-V rail. The schematic is shown in [Figure 24](#). The 5-V output voltage is set by the feedback resistors R15 and R16 with the TPS71701  $V_{REF} = 0.8$  V, according to [Equation 15](#).

$$V_{5V} = V_{REF} \times \left(1 + \frac{R15}{R16}\right) = 0.8 \text{ V} \times \left(1 + \frac{845\text{k}}{160\text{k}}\right) = 5.02 \text{ V} \quad (15)$$

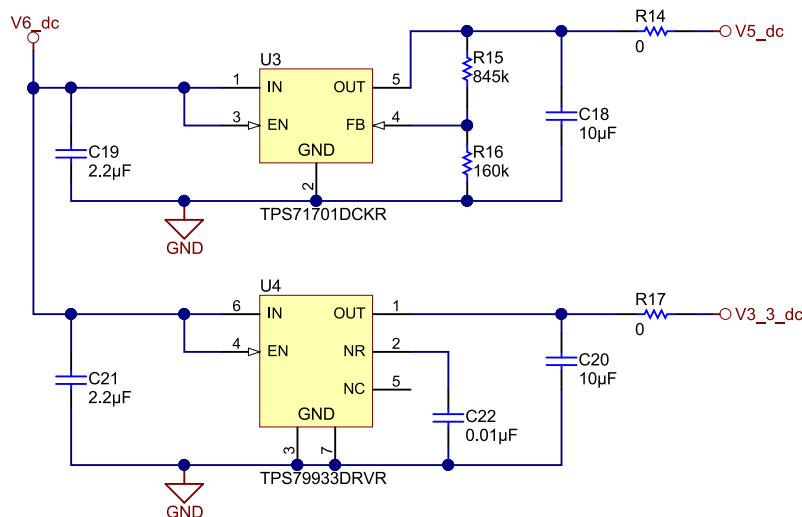


**Figure 24. Schematic for 5-V and 3.3-V PoL for Signal Chain**

## 4.3 Host Processor Interface

### 4.3.1 Signal Description

A 10-pin header interface is available to connect to a host processor. The header provides the necessary signals to calculate the high-resolution interpolated angle for both signal paths, using the ADS8354 dual 16-bit ADC and an embedded dual S/H ADC, if available.

The interface is compliant to 3.3-V I/O systems. To have a solid GND connection, all odd pins are assigned to GND. The signals available are listed in [Table 15](#).

**Table 15. TIDA-00176 Interface Connector to Host MCU**

FUNCTION	SIGNALS	I/O (3.3 V)	COMMENT
16-bit high-resolution output channel for A, B with ADS8354 and SPI (Slave)	SDI (I)	Digital input	Data input for serial communication. Used for configuration of dual sampling mode
	/CS (I)	Digital input	Chip-select signal; active low. Falling edge of /CS latches the analog input (Hold) and initiates a new conversion. Use falling edge of /CS to latch QEP counter on host processor synchronously, like on Piccolo MCU
	SCLK (I)	Digital input, up to 24 MHz	Clock for serial communication
	SDO_A (O)	Digital output	Data output for serial communication, channel A and channel B. 16-bit 2's complementary data on each channel A and channel B. Input to output signal gain = 5.
	SDO_B (O)	Digital output	Data output for serial communication channel B
Digital quadrature encoded signals A, B and index Marker R	ATTL (O)	Digital output	160mV hysteresis for A, B, and R, configurable
	BTTL (O)	Digital output	
	RTTL (O)	Digital output	
Analog single-ended output channel for A and B	A/sin (O)	Analog output: 0 to 3.3 V, 1.65-V bias (single-ended)	Nominal output range: 0.82 V – 2.48 V ( $1.65 \pm 0.83$ V) for $V_{PP}$ , gain = 1.66, bias voltage = 1.65 V
	B/cos (O)	Analog output: 0 to 3.3 V, 1.65-V bias (single-ended)	Nominal output range: 0.82 V – 2.48 V ( $1.65 \pm 0.83$ V) for $V_{PP}$ , gain = 1.66, bias voltage = 1.65 V

For details on the connector pin assignment, refer to [Section 6](#).

#### CAUTION

To synchronize the analog input sample of the ADS8354 16-bit dual sampling ADC with a QEP incremental counter module, use the /CS signal to the ADS8354 to latch the QEP counter as well. For an MCU like Piccolo, the /CS need to be connected to the eQEP Strobe input pin EPEPxS, where x is the module number. The Piccolo eQEPx module can be configured to latch the QEP counter on a falling edge of the EQEPxS pin.

#### 4.3.2 High-Resolution Path Using 16-Bit Dual ADC ADS8354 With Serial Output

This section outlines the configuration of the ADS8354 through the serial interface. This is split into programming the full-scale input voltage range with the internal ADS8354 reference as well as the serial data transfer.

##### 4.3.2.1 ADS8354 Input Full Scale Range Output Data Format

For use in this design, the ADS8354 is intended to be configured for  $\pm 2 \times V_{REF}$  input range. The internal reference voltage  $V_{REF}$  should be set to 2.5 V, to yield a  $\pm 5$ -V FSR.

**Table 16. ADS8354 Transfer Characteristic for TIDA-00176**

INPUT VOLTAGE: AINP_x – AINM_x	MODE	INPUT VOLTAGE	OUTPUT CODE (HEX)
< -5 V	$\pm 2 \times V_{REF}$ RANGE	NFSC	8000
-5 V + 1 LSB		NFSR	8001
-1 LSB		-1 LSB	FFFF
0		0	0000
> 5 V – 1 LSB		PFSR – 1 LSB	7FFF

The output date format for each channel A and B is 16-bit signed integer output (2's complementary).

##### 4.3.2.2 ADS8354 Serial Interface

The ADS8354 uses the serial clock (SCLK) for synchronizing data transfers in and out of the device. The CS signal defines one conversion and serial transfer frame. A frame starts with a CS falling edge and ends with a CS rising edge. Between the start and end of the frame, a minimum of N SCLK falling edges must be provided to validate the read or write operation. As shown in [Table 17](#), N depends upon the interface mode used to read the conversion result. When N SCLK falling edges are provided, the write operation attempted in the frame is validated and the internal user-programmable registers are updated on the subsequent CS rising edge. This CS rising edge also ends the frame. If CS is brought high before providing N SCLK falling edges, the write operation attempted in the frame is not valid.

**Table 17. ADS8354 SCLK Falling Edges for a Valid Write Operation**

INTERFACE MODE	MINIMUM SCLK FALLING EDGES REQUIRED TO VALIDATE WRITE OPERATION N
32-CLK, dual-SDO mode (default)	32
32-CLK, single-SDO mode	48
16-CLK, dual-SDO mode	16
16-CLK, single-SDO mode	32

The example firmware on the F28069M Piccolo MCU initializes the ADS8354 in the 32-CLK, single SDO mode.

For more details on the serial interface mode and read and write operations, refer to the ADxx54 data sheet.

#### 4.3.2.3 ADS8354 Conversion Data Read

As outlined in [Table 17](#), the device provides four different interface modes to the user. These are applicable for reading the conversion result too. These modes offer flexible hardware connections and firmware programming. In the 32-CLK interface modes, the device uses an internal clock to convert the sampled analog signal. The conversion is completed during the first 16 periods of SCLK and the conversion result can be read on the subsequent SCLK falling edges. All devices in the family (that is, ADS8354, ADS7854, and ADS7254) support the 32-CLK interface modes. In addition to the 32-CLK interface modes, the ADS7854 and ADS7254 also support the 16-CLK interface modes. By using the 16-CLK interface modes, the same throughput can be achieved at much lower SCLK speeds.

The example firmware on the F28069M Piccolo MCU initializes the ADS8354 in the 32-CLK, single SDO mode.

The 32-CLK, single-SDO mode provides the option of using only one SDO pin (SDO\_A) to read conversion results from both ADCs (ADC\_A and ADC\_B). SDO\_B remains in 3-state and can be treated as a no connect (NC) pin. [Figure 25](#) shows a detailed timing diagram for this mode.

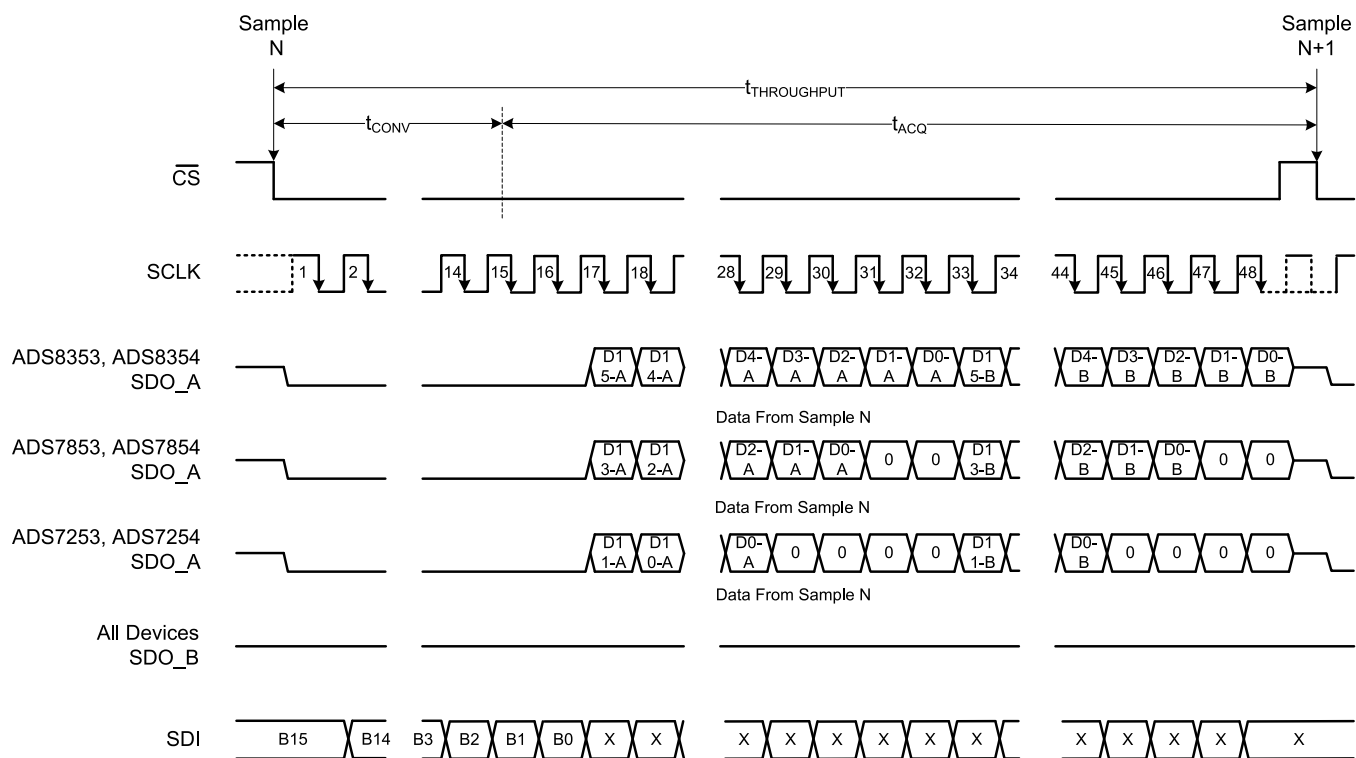


**Figure 25. 32-CLK, Single-SDO Mode Timing Diagram**

A CS falling edge brings the serial data bus out of 3-state and also outputs a 0 on the SDO\_A pin. The device converts the sampled analog input during the conversion time ( $t_{CONV}$ ). SDO\_A reads 0 during this period. After completing the conversion process, the sample-and-hold circuit goes back into sample mode. The device outputs the MSB of ADC\_A on the SDO\_A pin on the 16<sup>th</sup> SCLK falling edge. The subsequent SCLK falling edges are used to shift out the conversion result of ADC\_A followed by the conversion result of ADC\_B on the SDO\_A pin. In this mode, at least 48 SCLK falling edges must be given to validate the read or write frame. A CS rising edge ends the frame and puts the serial bus into 3-state.

Refer to the ADSxx54 datasheet for more details.

#### 4.3.2.4 ADS8354 Register Configuration

To select the modes as outlined in the previous sections, the ADS8354 registers REFDAC\_A, REFDAC\_B, and CFR are programmed as follows.

REFDAC\_X and CFR are 16-bit registers and are programmed as shown in [Table 18](#), with the upper 4 bits selecting write/read mode and its corresponding register.

**Table 18. ADS8354 Register Configuration**

REGISTER	DATA (HEX)	COMMENT
REFDAC_A	9FF8	Write mode to REFDAC_A, selects VREF_A = 2.5 V
REFDAC_B	AFF8	Write mode to REFDAC_B, selects VREF_B = 2.5 V
CFR	8640	Write mode to CFR, selects 32-CLK dual SDO mode with A and B on SDO_A, FSR = $\pm 2 \times V_{REF}$ , select internal $V_{REF}$

Refer to the ADSxx54 datasheet for more details.

#### 4.4 Encoder Connector

Two connector options are available for interface to Sin/Cos encoders. The default connector is a shielded SubD-15 female connector. The other option is an 8-pin header. For details on the connector assignment, refer to [Section 6](#).

#### 4.5 Design Upgrades

High-resolution path: To further increase the noise immunity of the high-resolution channel, a first order low-pass filter is recommended with the differential amplifier THS4531A. To use the high-resolution channel up to 500 kHz, a 33-pF, 1% NPO/COG capacitor each is recommended in the THS4531A feedback path in parallel to the 5-kΩ matched resistor. For lower cut-off frequencies, the capacitor value should be higher, respectively.

The 5.25-V LDO with output enable through signal PWR\_EN: Although a connector J-7, pin 4 is available to ensure the input to the LDO is always terminated with either pulled-up (Jumper: J7 4-6) or pulled-down (Jumper: J7 4-3) an additional pull-up of 10k from U2, pin 4 to 3.3 V (V3\_3\_dc) is recommended.

## 5 Software Design

### 5.1 Overview

Any embedded processor or microcontroller with an embedded quadrature encoded pulse counter and SPI can be used in conjunction with the TIDA-00176 hardware design.

However, to allow for easy evaluation of the TIDA-00176 hardware reference design, an example firmware is provided for the C2000 F28069M Piccolo LaunchPad, which allows for evaluating TIDA-00176 with Sin/Cos incremental position encoders. A user menu through USB virtual COM port is provided to initialize the line count of selected Sin/Cos encoder and print the calculated high-resolution angle information along with other user selectable data.

The main peripherals leveraged on the F28069M are the SPI-A peripheral to read the dual high-resolution 16-bit data signals  $A_{16\text{-bit}}$  and  $B_{16\text{-bit}}$ . The embedded dual S/H ADC is used to convert the single-ended analog signals  $A_{12\text{-bit}}$  and  $B_{12\text{-bit}}$ . The quadrature encoder pulse (eQEP2) module is used for directional up-down incremental count based on the signals  $A_{\text{TTL}}$  and  $B_{\text{TTL}}$  and the zero index marker  $R_{\text{TTL}}$  for absolute position initialization. The ePWM1 timer is used to generate periodic interrupts to trigger a new angle measurement. A 16-kHz period was chosen. The SCI-A peripheral was used to implement the UART-based user interface at 115000 baud through virtual COM port.

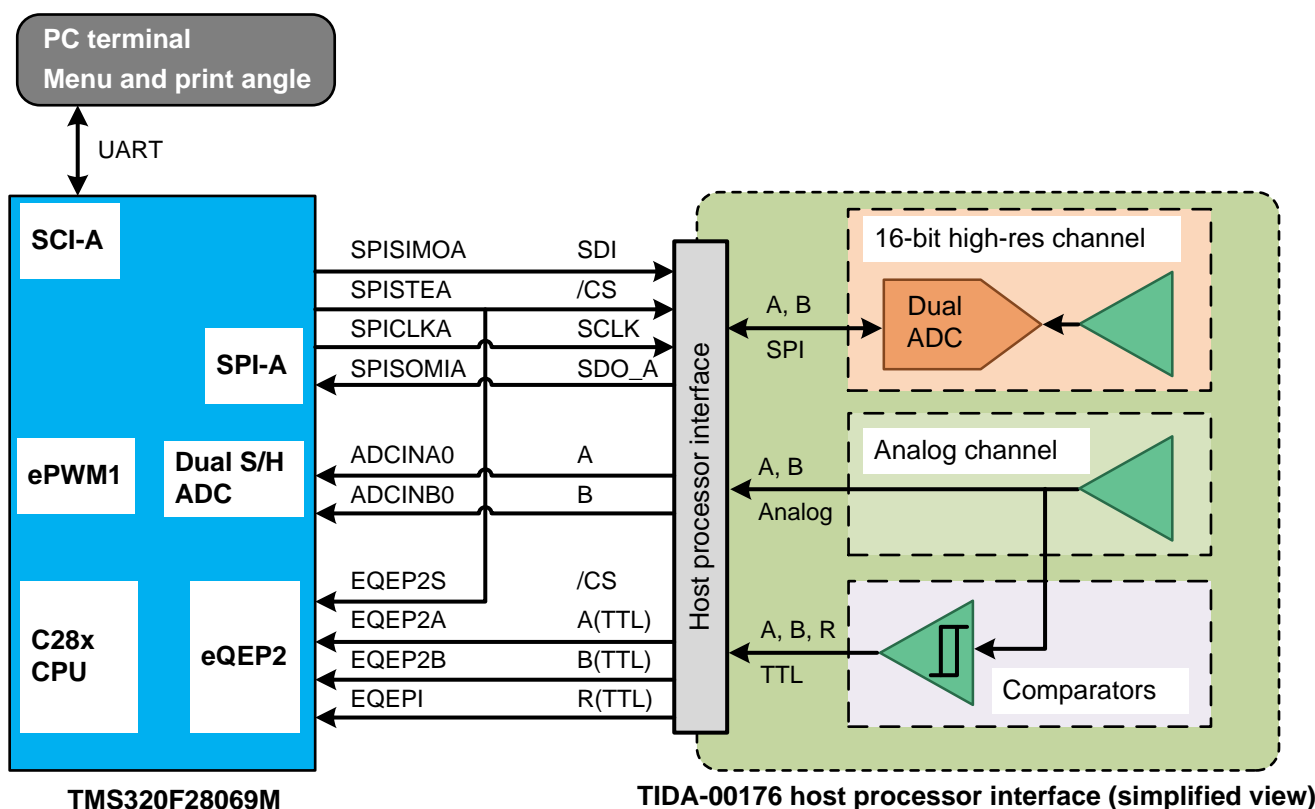
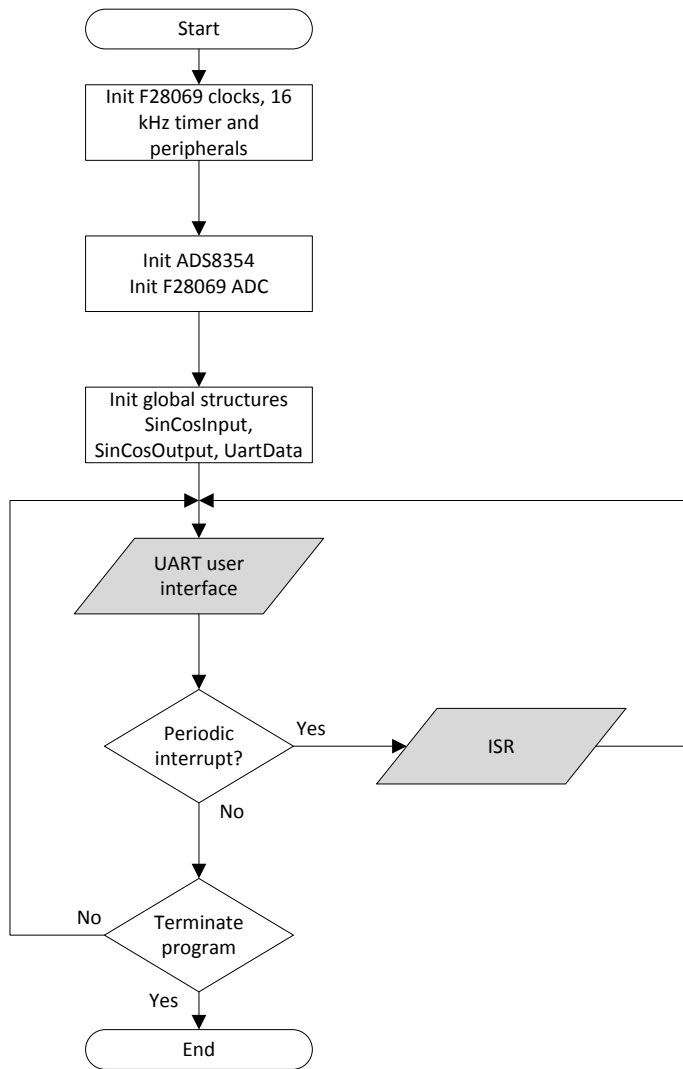


Figure 26. TMS320F28069M Peripheral Module and Pin Assignment to TIDA-00176 Host Processor Interface

## 5.2 C2000 Piccolo Firmware

The example firmware is developed and compiled for the Piccolo TMS320F28069M and leverages the peripheral modules outlined in [Figure 26](#).

The firmware leverages C2000 controlSUITE™. The firmware basically consists of three functional blocks. The F28069M framework, as outlined in [Figure 27](#), the algorithm to synchronously sample the required data and calculate the interpolated angle, as well as the UART terminal based user interface.



**Figure 27. Flowchart of Sin/Cos Encoder Framework**

The TMS320F28069M framework initializes the TMS320F28069M CPU clock to 80 MHz, the GPIO multiplexers, the peripherals like SPI-A, SCI-A (UART), the ePWM1-based periodic timer and interrupt, the embedded 12-bit dual S/H ADC. It also configures the external 16-bit dual ADC ADS8354 through SPI-A as outlined in [Section 4.3.2.4](#). The SPI-A is configured as SPI Master with the serial clock of 10 MHz. This is the maximum SPI clock for the Piccolo F28069M. For other processors like Sitara AM437x or Delfino F287x, the SPI clock can be up to 24 MHz.

After initialization the program invokes the UART-based user interface and serves the period interrupt service routine (ISR). The period ISR implements the synchronized data capture, calculation of intermediate phase, and total interpolated angle based on both the external 16-bit ADC ADS8354 and the internal 12-bit ADC. It follows the algorithms outlined in [Section 1](#). The code is written with 32-bit integer fractional Q28 numbers using TI's IQmath library. The advantage of 32-bit fractional numbers versus

32-bit IEEE floating point is that the resolution remains constant independent of the data range. Since the data range is limited from 0 to 1.0 for the angle (per unit), as well as for the ADC input data, which is scaled to maximum of  $\pm 5$  (V), Q28 numbers with an integer range  $\pm 8.0$  provide enough headroom, while accuracy remains constant for all data.

The flowchart of the ISR is shown in Figure 28.

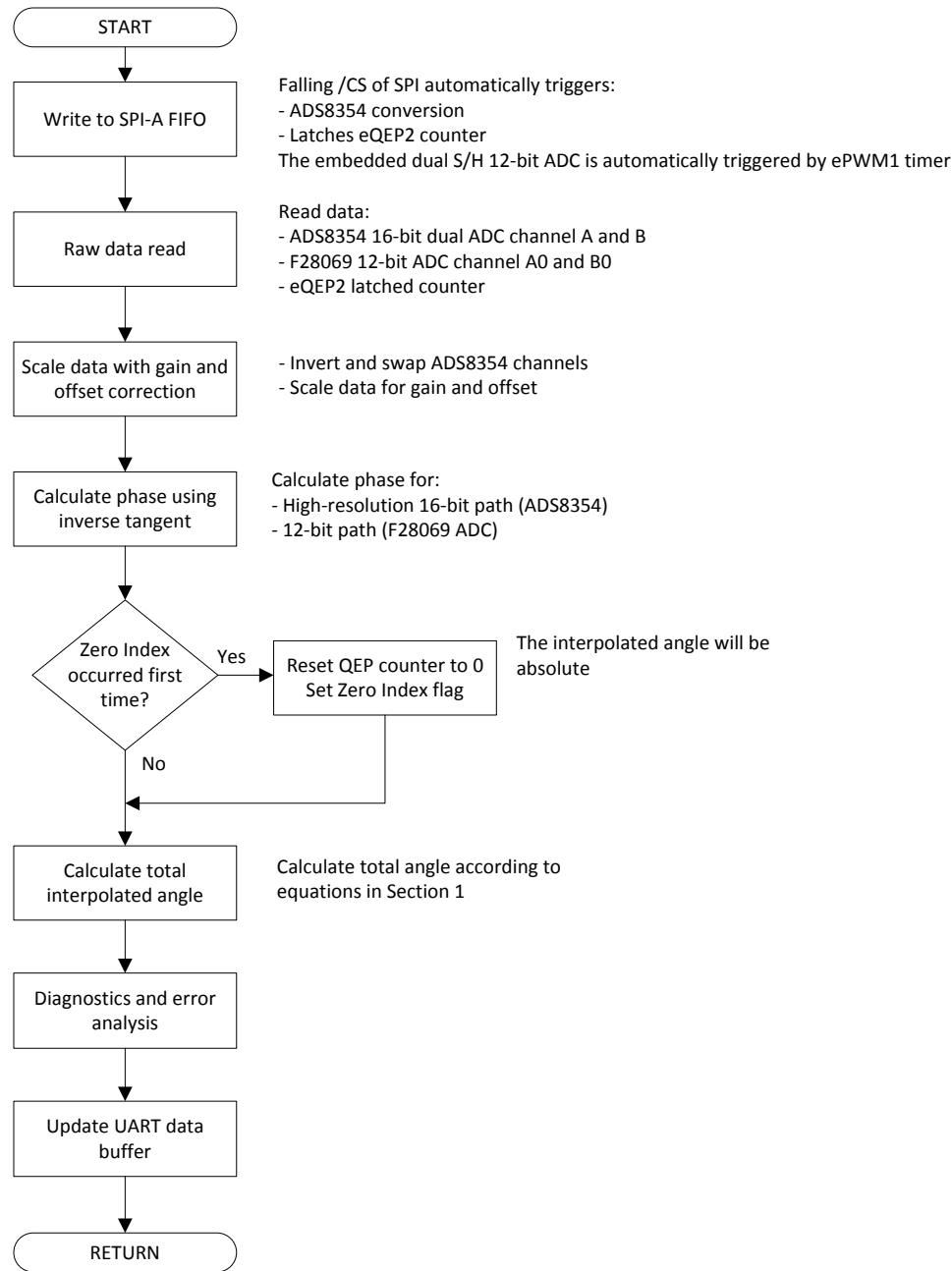


**Figure 28. Flowchart of Sin/Cos Encoder Main ISR With Interpolated Angle Calculation**

### 5.3 User Interface

To allow for quick evaluation a virtual COM port based user interface was implemented. Any terminal interface at 115000 baud like Tera Term can be used.

The user interface allows the user to enter the line count of the connect Sin/Cos encoder before the program reaches the main menu. The menu provides menu item options for the user to select either a basic display mode with just the high-resolution angle printed or an expert display mode, both with a 10-Hz update rate. Further menu items are data dump modes at a 200-Hz update rate, intended write to a file for post analysis.

The flowchart of the user interface is shown in [Figure 29](#).

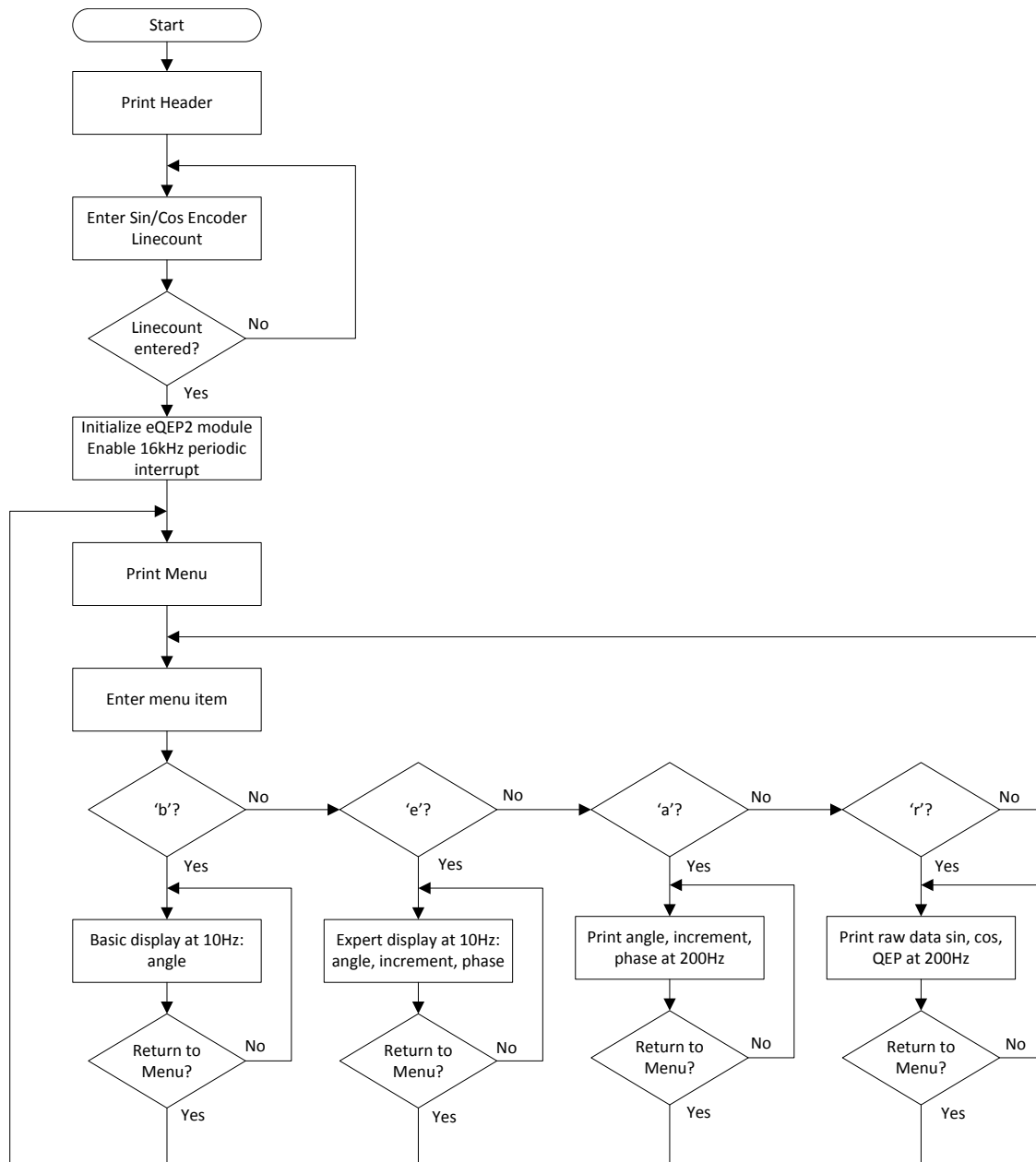


**Figure 29. Flowchart of UART Terminal User Interface**

**Table 19** through **Table 22** outlines the data output format for each of the four menu items. In data dump mode, a "tab" is included as delimiter between the data in each row.

**Table 19. Basic Display Mode Output Format and Data Scaling**

MENU	COLUMN 1	COLUMN 2	COLUMN 3	COLUMN 4	COLUMN 5
"b" basic display	Total angle with ADS8354 (Scale)	—	—	—	—
Data format	Float (0 to 360 degrees)	—	—	—	—

**Table 20. Expert Display Mode Output Format and Data Scaling**

MENU	COLUMN 1	COLUMN 2	COLUMN 3	COLUMN 4	COLUMN 5
"e" expert display	Total angle with ADS8354 (Scale)	Marker index R occurred	Incremental count	Phase ADS8354 (scale)	Phase F28069M ADC (scale)
Data format	float (0 to 360 degrees)	Flag (Yes/No)	Integer	Float (0 to 1.0)	Float (0 to 1.0)

**Table 21. Angle Data Dump Menu Format and Scaling**

MENU	COLUMN 1	COLUMN 2	COLUMN 3	COLUMN 4	COLUMN 5	COLUMN 6
"d" angle dump	Total angle with ADS8354 (scale)	Total angle with F28069 ADC (scale)	Incremental count	Phase ADS8354 (scale)	Phase F28069M ADC (scale)	Periodic tick (scale)
Data format	Float (0 to 360 degrees)	Float (0 to 360 degrees)	Integer	Float (0 to 1.0)	Float (0 to 1.0)	Integer (66 µs)

**Table 22. Raw Data Dump Menu Format and Scaling**

MENU	COLUMN 1	COLUMN 2	COLUMN 3	COLUMN 4	COLUMN 5	COLUMN 6	COLUMN 7
"r" raw data	Incremental count (SW)	Incremental count (Latch on /CS)	Input A+/A-, ADS8354 (scale)	Input B+/B-, ADS8354 (scale)	Input A+/A-, F28069 (scale)	Input A+/A-, F28069 (scale)	Periodic tick (scale)
	Integer	Integer	Float (V <sub>PP</sub> )	Float (V <sub>PP</sub> )	Float (V <sub>PP</sub> )	Float (V <sub>PP</sub> )	Integer (66 µs)

## 6 Getting Started

### 6.1 TIDA-00176 PCB Overview

Figure 30 shows a photo of the top side of the TIDA-00176 PCB. The headers and default jumper settings are explained in [Section 6.2](#).

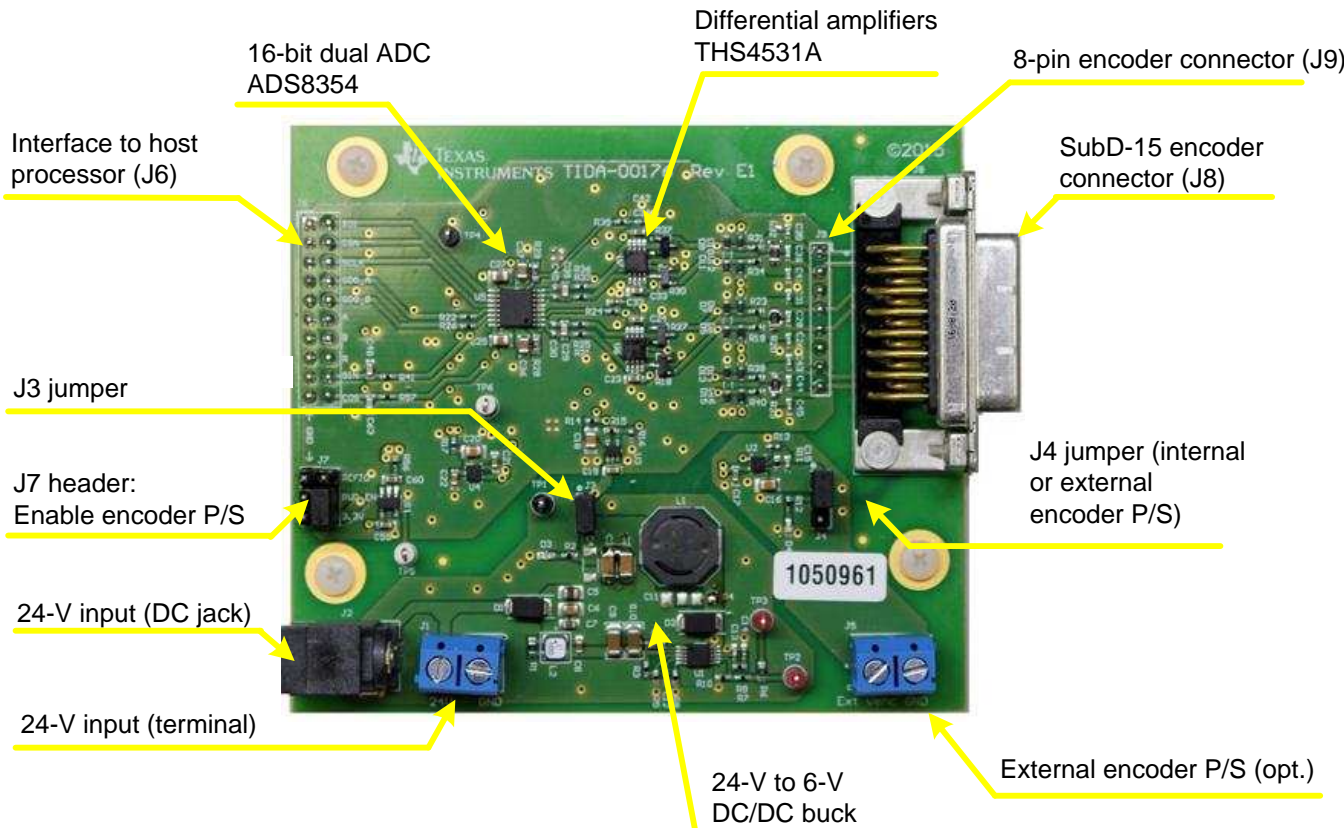


**Figure 30. TIDA-00176 Board Picture**

## 6.2 Connectors and Jumper Settings

### 6.2.1 Connector and Jumpers Overview

The connector assignment and jumper settings are outlined in [Table 23](#) through [Table 26](#).

The 24-V nominal input voltage can be supplied through either connector J1 or J2.

**Table 23. Connector Assignment and Jumper Settings (J1 to J4)**

CONNECTOR AND PIN ASSIGNMENT	DESCRIPTION	
<b>24-V INPUT (TERMINAL; J1)</b>		
1	24-V input voltage (17 to 36 V)	
2	GND	
<b>24-V INPUT (DC JACK; J2)</b>		
Internal	24-V input voltage (17 to 36 V)	
External	GND	
<b>J3</b>		
1	Output of TPS54040A (default 6 V)	
2	6-V supply rail	
<b>J4</b>		
1	5.25-V supply (default)	
2	V_ENC (encoder supply voltage)	
3	External supply	

If desired, an external supply voltage other than the 5.25-V encoder supply voltage can be applied through connector J5.

**Table 24. External Encoder Supply Connector (J5)**

PIN	DESCRIPTION	
1	Encoder supply VCC	
2	Encoder supply GND	

**Table 25. Host Processor Interface (J6)**

PIN	DESCRIPTION	PIN	DESCRIPTION (3.3-V I/O)
1	GND	2	SDI (ADS8354)
3	GND	4	/CS (ADS8354)
5	GND	6	SCLK (ADS8354)
7	GND	8	SDO_A (ADS8354)
9	GND	10	SDO_B (ADS8354)
11	GND	12	A (TTL)
13	GND	14	B (TTL)
15	GND	16	R (TTL)
17	GND	18	A (single ended analog 0 to 3.3 V)
19	GND	20	B (single ended analog 0 to 3.3 V)

For detailed signal descriptions on the host processor interface, refer to [Section 4.3](#).

**Table 26. Connector Assignment and Jumper Settings (J7 to J9)**

PIN	DESCRIPTION	PIN	DESCRIPTION
<b>HEADER J7 WITH ENCODER SUPPLY ENABLE (J7)</b>			
1	GND	2	REFIO (1.65 V)
3	GND	4	ENABLE encoder supply voltage (5.25 V)
5	GND	6	3.3 V
<b>ENCODER DSUB15 CONNECTOR (J8)</b>			
1	A+	2	Encoder supply GND
3	B+	4	Encoder supply VCC (default 5.25 V)
5	NC	6	NC
7	R-	8	NC
9	A-	10	Reserved
11	B-	12	Reserved
13	NC	14	R+
15	NC	—	—
<b>ENCODER 8SIL100 CONNECTOR (J9)</b>			
1	A+	2	A-
3	Encoder Supply GND	4	B-
5	B+	6	Encoder supply VCC (default 5.25 V)
7	R-	8	R+

### 6.2.2 Default Jumper Configuration

Prior to working with the TIDA-00176 board, ensure the below default jumper settings are applied. Refer to the board picture [Figure 30](#).

**Table 27. Default Jumpers Settings**

HEADER	JUMPER SETTING
J3	Insert a jumper between J3 pins 1-2 to enable the 6-V intermediate rail connected the three LDOs
J4	Insert a jumper between J4 pins 1-2 to route the onboard 5.25-V encoder supply to the encoder connectors
J7	Insert a jumper between J7 pins 4-6 to enable the 5.25-V encoder supply.

## 6.3 Design Evaluation

### 6.3.1 Prerequisites

The following hardware equipment and software are required to allow an evaluation of the TIDA-00176 TI design.

**Table 28. Prerequisites**

EQUIPMENT	COMMENT
24-V power supply	24-V output power brick with at least 250-mA output current Output connector 2.1-mm I.D. × 5.5-mm O.D. × 9.5-mm female
TIDA-00176 hardware	For default jumper settings per Section 6.2.
Three jumpers for board settings	2 pins, 100 mil
TIDA-00176 firmware	Download from TIDA-00176 design folder
InstaSPIN-MOTION F28069M LaunchPad	Available through TI eStore
USB cable	Mini USB type A to USB type A cable
TIDA-00176 to LaunchPad adapter	Internal TI (optional)
Code Composer Studio 6	Download from <a href="http://www.ti.com">www.ti.com</a>
PC terminal program	Any terminal program, like for example Tera Term
Sin/Cos encoder with 1-V <sub>PP</sub> output signals	For example, ROD480

### 6.3.2 Hardware Setup

The following connections are required between the TIDA-00176 and the InstaSPIN-MOTION LaunchPad.

**Table 29. TIDA-00176 Host Processor Interface (J6) to InstaSPIN-LaunchPad**

TIDA-00176 HOST PROCESSOR INTERFACE (J6)		CONNECTS TO →	InstaSPIN-MOTION LAUNCHPAD	
J6-PIN	DESCRIPTION		HEADER-PIN	DESCRIPTION (3.3-V I/O)
1	GND		J3-Pin 22	GND
19	GND		J2-Pin 20	GND
2	SDI (ADS8354)		J2-Pin 15	GPIO16/SPISIMOA
4	/CS (ADS8354)		J2-Pin 19 J6-Pin 59	GPIO27/eQEP2S and GPIO19/SPISTEA
6	SCLK (ADS8354)		J1-Pin 7	GPIO18/SPICLKA
8	SDO_A (ADS8354)		J2-Pin 14	GPIO17/SPISOMIA
10	SDO_B (ADS8354)	NC	NC	NC
12	A (TTL)		J6-Pin 55	GPIO24/eQEP2A
14	B (TTL)		J6-Pin 54	GPIO25/eQEP2B
16	R (TTL)		J6-Pin 58	GPIO26/eQEP2I
18	A (single ended analog 0 to 3.3 V)		J3-Pin 27	ADCIN_A0
20	B (single ended analog 0 to 3.3 V)		J3-Pin 28	ADCIN_B0

Follow these steps to setup the hardware:

1. Connect the TIDA-00176 board with the InstaSPIN-MOTION LaunchPad using the proper connector or adapter.

---

**NOTE:** For the internal testing an adapter board has been designed to interface between the TIDA-00176 and the InstaSPIN-MOTION LaunchPad as shown in [Figure 31](#).

2. Verify the TIDA-00176 is configured with the default three jumper settings per [Section 6.2.2](#).
3. Connect a Sin/Cos encoder to the board, by using either the SubD-15 connector (J8) or the SIL-8 connector (J9).
4. Insert the 24-V input from the power brick in the J1 connector or use J2 connector in case of an external power supply (17 to 36 V) is preferred.
5. Connect the USB mini cable from the InstaSPIN-MOTION LaunchPad to the PC.

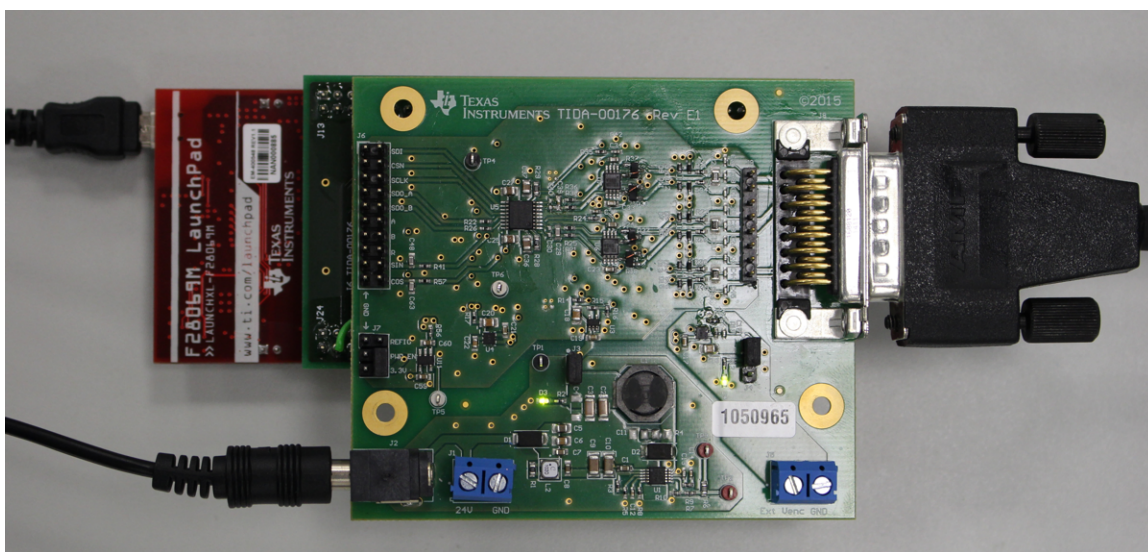


**Figure 31. TIDA-00176 Board Mounted on InstaSPIN-MOTION LaunchPad**

Also refer to the InstaSPIN-MOTION LaunchPad prerequisites at: <http://www.ti.com/tool/launchxl-f28069m>

Ensure the following jumpers on the F28069 LaunchPad are set: JP1, JP2, JP3 and JP7. Do not set JP4, JP5 and JP6; these have to be not connected.

### 6.3.3 Software Setup

Follow these steps to setup the software:

1. If not done yet, download the TIDA-00176 SinCosEncoder Firmware from the TIDA-00176 design folder and extract to a folder such as c:\ti\tida-00176\bin.
2. Invoke a Terminal program, like Tera Term, that can connect to the virtual COM port.
3. Setup the Terminal program in Serial Console mode and set the parameters to:
  - Baud Rate = 115200, Data = 8-bit, Parity = None, Stop = 1-bit, Flow Control = None
4. Launch Code Composer Studio (CCS).
5. In CCS, setup the XDS100 JTAG target with the InstaSPIN-MOTION F28069M LaunchPad.
6. In CCS, connect to the TMS320F28069M and download TIDA-00176 binary output file. Run → Load Program → TIDA-00176\_SinCosEncoder\_Firmware\_rev1\_0.out
7. In CCS, run the target.

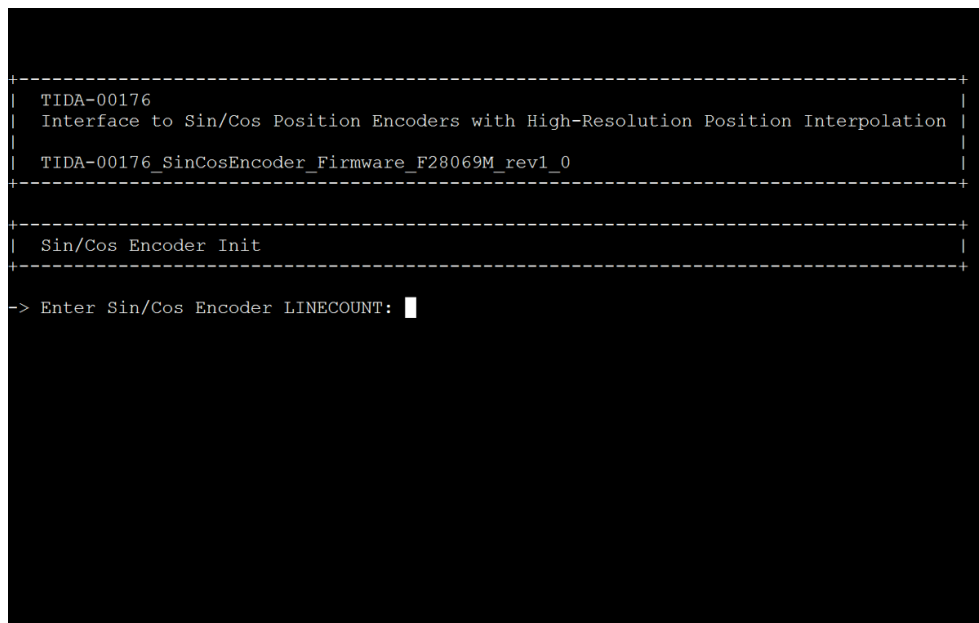
The terminal program should display the start screen of TIDA-00176 as shown in [Figure 32](#).

---

**NOTE:** After the binary file has been loaded to the F28069M, Steps 4 through 7 are not required anymore. Simply reset the LaunchPad to restart the program. Ensure the F28069M is configured to boot from internal flash. Refer to the InstaSPIN-MOTION LaunchPad documentation.

---

Trouble-shooting: If no connection gets established, the VCP driver of the USB virtual Com port TI XDS100 Channel B needed to be enabled under Windows® 7 Device Manager. For more details, refer to the InstaSPIN-MOTION LaunchPad documentation.



```
+-----+
| TIDA-00176
| Interface to Sin/Cos Position Encoders with High-Resolution Position Interpolation |
| TIDA-00176_SinCosEncoder_Firmware_F28069M_rev1_0
+-----+
+-----+
| Sin/Cos Encoder Init
+-----+
-> Enter Sin/Cos Encoder LINECOUNT: |
```

**Figure 32. TIDA-00176 User Interface at Startup**

### 6.3.4 User Interface

After startup, the user interface requires the user to enter the Sin/Cos encoder line count in decimal. After the line count is entered, the main menu is available, as shown in [Figure 33](#).

```

Interface to Sin/Cos Position Encoders with High-Resolution Position Interpolation |
| TIDA-00176_SinCosEncoder_Firmware_F28069M_rev1_0
+-----+
| Sin/Cos Encoder Init
+-----+
-> Enter Sin/Cos Encoder LINECOUNT: 2000
LINECOUNT entered: 2000
+-----+
| Main Menu
+-----+
key mode format
--- -----
b basic display mode [angle]
e expert display mode [angle index incr phase16 phase12 tick]
r raw data dump at 200Hz [QEP QEPL sin16 cos16 sin12 cos12 tick]
a angle dump at 200Hz [angle incr phase16 phase12 tick]
x reserved
--- -----
any any other key returns to this main menu
-> press key

```

**Figure 33.** TIDA-00176 User Interface Main Menu

Four menus are available. Each can be selected by pressing the characters b, e, r, or a. The menu item x is reserved for internal test modes during software development.

Press "b" or "e" to select the basic or expert display mode, which will print the interpolated angle in degrees or additional information. Note that initially the total angle is not absolute since the index has not occurred. This can be recognized by the Increments Marker set to "No" in the expert display mode. Slowly turn the encoder in clockwise direction until the Increments marker changes to "Yes". Now the interpolated angle is absolute with respect to the index marker position. To return to the main menu, press any key.

```

=====+
| High-resolution angle [degree]      |
+-----+
359.9804

+-----+
| Main Menu
+-----+
key mode format
--- -----
b basic display mode [angle]
e expert display mode [angle index incr phase16 phase12 tick]
r raw data dump at 200Hz [QEP QEPL sin16 cos16 sin12 cos12 tick]
a angle dump at 200Hz [angle incr phase16 phase12 tick]
x reserved
--- -----
any any other key returns to this main menu
-> press key

=====+
| Expert display mode [10Hz update rate] |
+-----+
| High-resolution angle | Increments | Phase/atan [PUI] |
| [degree]           | Marker   Count | ADS8354 F28069 |
+-----+           +-----+-----+
359.9804          No     0       0.8914  0.8926

```

**Figure 34.** Basic Angle Display and Expert Display Mode

Press "a" to start an angle data dump at a 200-Hz update rate. The data format is as outlined in [Section 5](#). A screenshot is shown in [Figure 35](#). Press any key to stop and return to the main menu.

Angle16PU	Angle12PU	Incr	Phase16PU	Phase12PU	Tick[32kHz]
0.85510715	0.85510683	7005	0.25946	0.25879	9190
0.85510674	0.85510638	7005	0.25862	0.25788	9270
0.85510715	0.85510668	7005	0.25945	0.25851	9350
0.85510679	0.85510661	7005	0.25871	0.25835	9430
0.85510692	0.85510671	7005	0.25898	0.25854	9510
0.85510753	0.85510694	7005	0.26022	0.25902	9590
0.85510702	0.85510659	7005	0.25919	0.25830	9670
0.85510717	0.85510682	7005	0.25949	0.25878	9750
0.85510726	0.85510671	7005	0.25967	0.25857	9830
0.85510681	0.85510660	7005	0.25876	0.25833	9910
0.85510682	0.85510658	7005	0.25877	0.25829	9990
0.85510727	0.85510681	7005	0.25970	0.25877	10070
0.85510728	0.85510672	7005	0.25972	0.25858	10150
0.85510755	0.85510694	7005	0.26027	0.25902	10230

**Figure 35. Angle Dump Mode at 200-Hz Update Rate**

Press "r" to start a raw data dump at a 200-Hz update rate. The data format is as outlined in [Section 5](#). A screenshot is shown in [Figure 36](#). Press any key to stop and return to the main menu.

OEP	QEPL	Vsin16	Vcos16	Vsin12	Vcos12	Tick[32kHz]
7005	7005	1.0044	0.0631	1.0280	0.0583	1542
7005	7005	1.0108	0.0631	1.0280	0.0583	1622
7005	7005	1.0069	0.0616	1.0280	0.0583	1622
7005	7005	1.0150	0.0662	1.0309	0.0597	1702
7005	7005	1.0089	0.0627	1.0324	0.0612	1782
7005	7005	1.0083	0.0643	1.0280	0.0597	1862
7005	7005	1.0101	0.0680	1.0295	0.0612	1942
7005	7005	1.0066	0.0636	1.0265	0.0597	2022
7005	7005	1.0072	0.0666	1.0265	0.0597	2102
7005	7005	1.0083	0.0595	1.0295	0.0568	2182
7005	7005	1.0047	0.0605	1.0251	0.0554	2262
7005	7005	1.0032	0.0610	1.0251	0.0583	2342
7005	7005	1.0040	0.0671	1.0280	0.0612	2422
7005	7005	1.0110	0.0643	1.0324	0.0597	2502

**Figure 36. Raw Data Dump Mode at 200-Hz Update Rate**

## 7 Test Results

Tests were done to characterize each individual functional block as well as the entire board. In particular, the following tests were conducted.

- Analog signal chain
- Power management
- Full system with Sin/Cos encoder signal emulation and Sin/Cos encoder
- EMC immunity (ED, EFT, and Surge)

Tests were done at room temperature around 22 to 23 degrees, or at 75 or 85 degrees. If not mentioned specifically, room temperature does apply.

The following equipment has been used for the TIDA-00176 testing session:

**Table 30. Test Equipment for TIDA-00176 Performance Tests**

TEST EQUIPMENT	PART NUMBER
Programmable 16-bit waveform generator	Keysight (Agilent) 33600A
Low speed oscilloscope (suitable for power supply tests)	Tektronix TDS2024B
High speed oscilloscope (suitable for analog signal tests)	Tektronix TDS784C
Adjustable SMPS	Knuerr-Heinzinger Polaris 125-5
24 V @ 2.5-A SMPS (power brick)	V-infinity 3A-621DN24
True RMS multimeter	Fluke 179
Differential probes	Tektronix P6630
Single ended probes	Tektronix P6139A
Programmable thermal chamber	Voetsch VT 4002
Programmable electronic load module	Chroma 63103
Control module for electronic load module	Chroma 6314
Thermal camera	Fluke TI40
Control system loop analyzer	Venable 3120
HEIDENHAIN shielded cables, PUR M23 male/female (4 × 2 × 0.14 mm; 4 × 0.5 mm), 10 m, 20 m, 50 m	298399-10,-20,-50
HEIDENHAIN M23/Sub-D15 Male Adapter Cable, 1m	310196-01
HEIDENHAIN Sin/Cos Encoders	ROD480-2000, ROD480-1024, ROD486-2048

## 7.1 Analog Performance Tests

Figure 37 shows a picture of the TIDA-00176 analog signal chain tests.

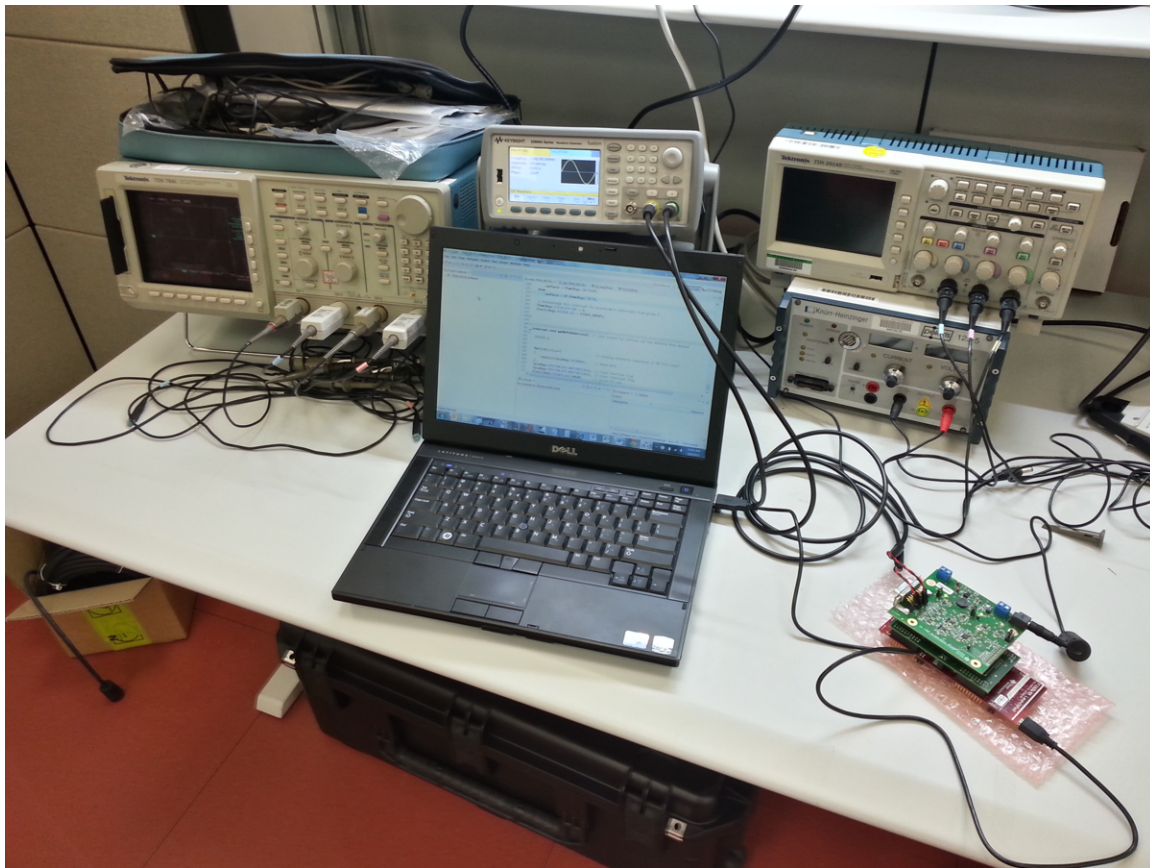


**Figure 37. Test Setup for TIDA-00176 Analog Signal Chain Performance Tests**

The high-resolution 16-bit signal path featuring fully differential amplifiers THS4531A and the dual 16-bit ADC ADS8353, as well as the differential to single-ended analog signal path have been tested. For the purpose, a dual output programmable function generator has been used. The inputs signals are applied at the connector J8 (differential inputs A, B, and R). The output waveforms have been collected at different probe points, depending on the signal path that was analyzed.

### 7.1.1 High-Resolution Signal Path

The measurements have been taken on the high-precision, high-resolution signal path. A sinusoidal signal with  $1 \text{ V}_{\text{PP}}$  was injected at the encoder connector J8 inputs A+, A- and B+, B- and the differential analog signals were measured at the ADS8354 differential inputs. Figure 38 outlines the input and output signals measured for the test.

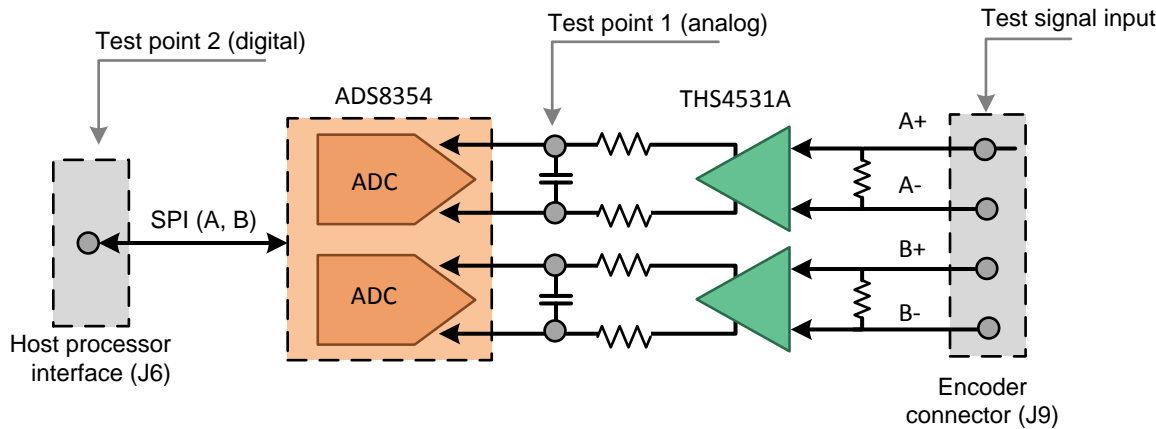


**Figure 38. High-Resolution Signal Chain Measurement Points**

#### 7.1.1.1 Bode Plot of Analog Path from Encoder Connector to ADS8354 Input

Figure 39 shows the magnitude and phase response, which is mainly defined by the THS4531A gain setting of 2 and the passive first order low-pass filter comprised of two  $10\text{-}\Omega$  series resistors and the  $2.2\text{-nF}$  parallel capacitor.

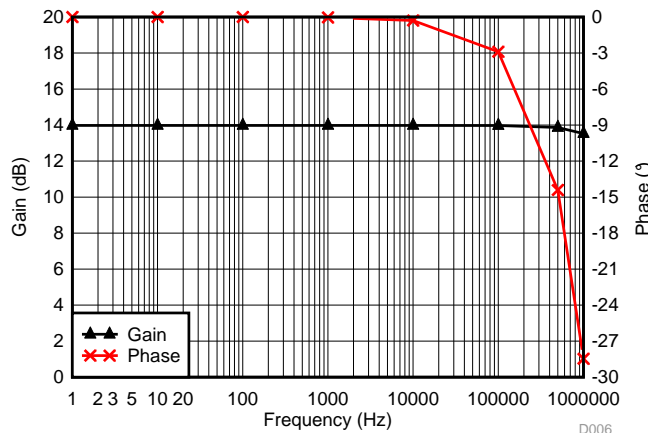


**Figure 39. Bode Plot for High-Resolution Analog from the Encoder Differential Input to ADS8354 Differential Input**

### 7.1.1.2 Performance Plots (DFT) for Entire High-Resolution Signal Path

For the following tests, the entire high-resolution signal chain, featuring the differential amplifier THS4531A connected through an RC filter to the dual 16-bit ADC ADS8354 has been tested. A sinusoidal test signal has been injected at the encoder differential input pins and the 16-bit digital data has been analyzed.

The analysis has been done in the frequency domain to evaluate the performance on signal-to-noise ratio (SNR), total harmonic distortions (THD), signal-to-noise and distortion (SINAD), and effective number of bits (ENOB). Essentially, all these parameters are different ways of quantifying the noise and distortion performance of an ADC based on a fast-fourier transform (FFT) analysis. A brief introduction on the theory of signal-to-noise measurement with ADCs is provided at the end of this section.

For the test, two types of input signals were used:

- A ultra-low noise DC source at 1.8 V
- A 1-kHz sine wave, at an amplitude of 0.6 V<sub>PP</sub>, which represents low output of Sin/Cos encoders

The input signal is applied to one of the input channels A+, A– or B+, B– at a time, while the other channel while the other channel is unconnected. The purpose is to measure and highlight the ultra-low cross-talk level among the two channels A and B (or sine and cosine, respectively).

The DC input is used to ensure the best noise performance (since no noise comes from the input/source). The 1-kHz sine wave is used to measure the effective number of bits on the two parallel channels.

Both channels A and B were sampled at 32 kHz and 8192 consecutive 16-bit samples were acquired for each channel A and B. The DFT has been calculated for the collected data to measure the SNR and THD.

The results are presented in the following figures.

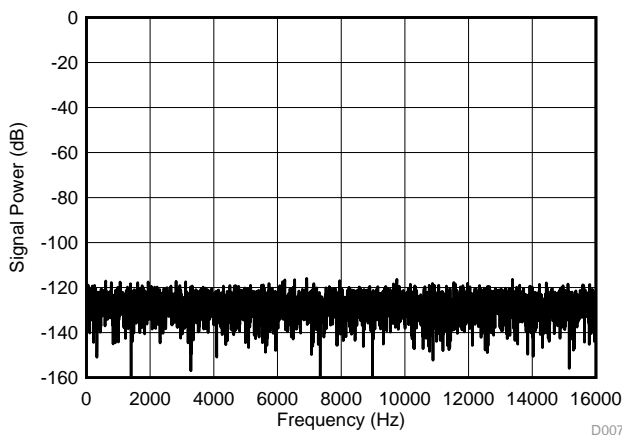


**Figure 40. DFT of 16-Bit Channel A Output  
With 1.8-V DC at Input A**

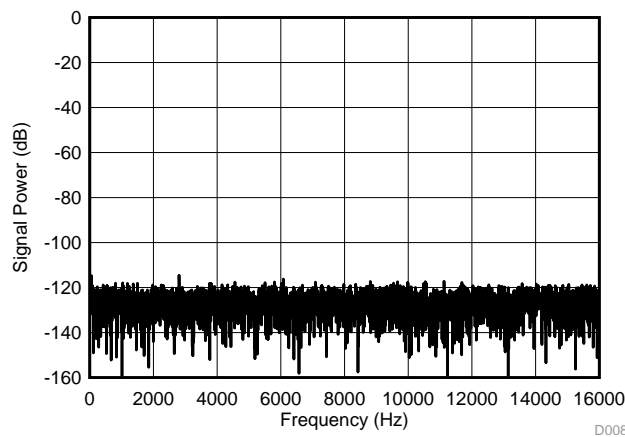


**Figure 41. DFT of 16-Bit Channel B Output  
With 1.8-V DC at Input B**

In the previous figures, the measured noise floor is below 120 dB, meaning this is the best performance that could be achieved. Also note that the plots are referred to the full scale input range, that is the maximum amplitude. 0 dB correspond to the maximum input possible for the ADS8354, which in this configuration would be  $2 \text{ V}_{\text{PP}}$ .

The following figures show the DFT of the entire high-resolution channel with a sinusoidal input voltage of  $0.6\text{-}\text{V}_{\text{PP}}$  amplitude and 1 KHz. This equals around  $-6\text{-dB}$  input level versus the theoretical full scale range input.

The input signal was applied either to the channel A or channel B. The other channel was left open in order to measured cross-talk as well.

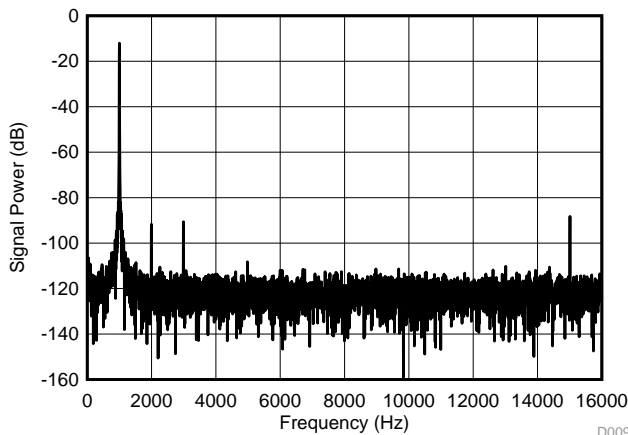


**Figure 42.** DFT of 16-Bit Channel A Output With  $600\text{-mV}_{\text{PP}}$ , 1-KHz Sine Wave Input Applied on Input A

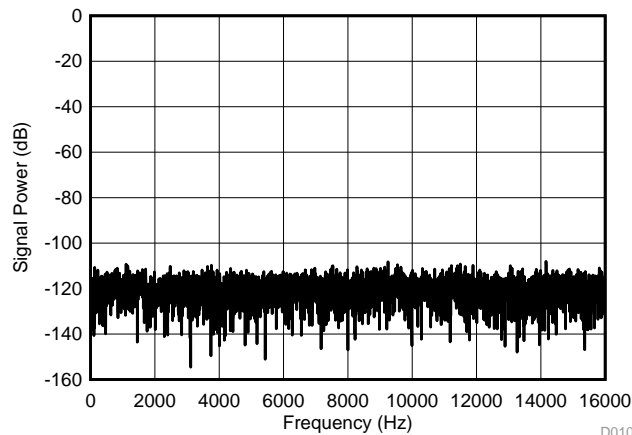


**Figure 43.** DFT of 16-Bit Channel B Output With  $600\text{-mV}_{\text{PP}}$ , 1-KHz Sine Wave Input Applied on Input A

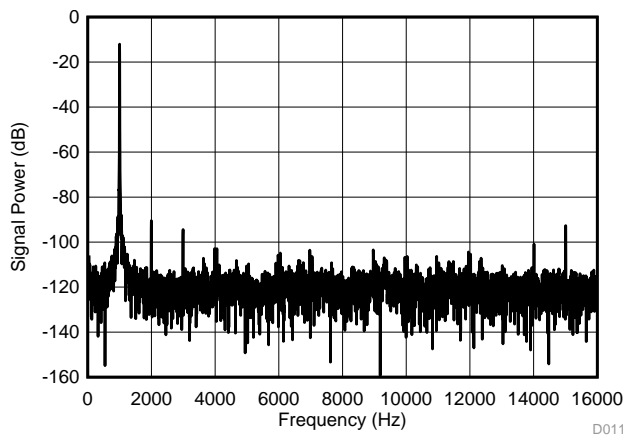


**Figure 44.** DFT of 16-Bit Channel B Output With  $600\text{-mV}_{\text{PP}}$ , 1-KHz Sine Wave Input Applied on Input B

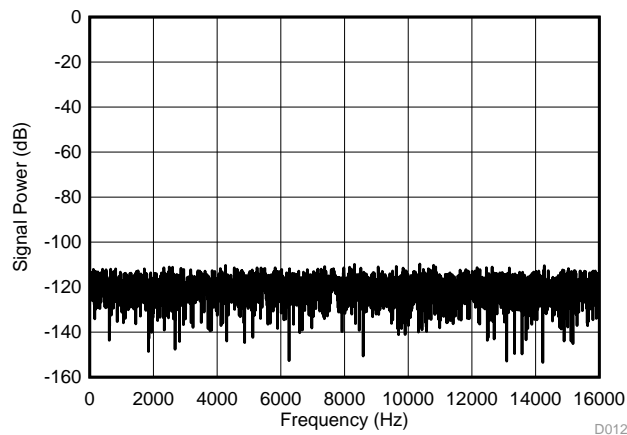


**Figure 45.** DFT of 16-bit Channel A Output With  $600\text{-mV}_{\text{PP}}$ , 1-KHz Sine Wave Input Applied on Input B

These figures are referred to the theoretical full scale input range. Note that the first and second harmonics of the 1-kHz sinusoidal signal are due to the signal source itself, (normally a very aggressive notch filter is used to isolate the frequency of the test signal; refer also to [SLAU515](#) for example).

Also note that the 1-kHz signal has a slight spread in frequency. This is not due to the TIDA-00176 hardware but due to a jitter in the F28069 software implementation, which triggered the SPI transfer to start the ADS8354 conversion (hold-mode) with a jitter of one CPU clock cycle equivalent to 12.5 ns.

The previous pictures also highlighted that there is basically no cross-talk between the two analog channels for sine (signal A+, A-) and cosine (B+, B-). The spectrum (DFT) is half the sampling frequency (the second half of the spectrum is a specular copy of the first half, so it is not shown in the plots). The Hann function ([http://en.wikipedia.org/wiki/Hann\\_function](http://en.wikipedia.org/wiki/Hann_function)) is used for windowing the data to obtain cleaner plots in the frequency domain.

THD, SNR and ENOB versus the full-scale signal can then be calculated for this design and are listed in [Table 31](#).

**Table 31. High-Resolution Signal Path (THS4531A and ADS8354) Typical Performance**

PARAMETER	VALUE (MEASURED)
SNR	89.1 dB
SINAD	88.5 dB
ENOB	14.4 bit
Cross-Talk	-107 to -109 dB

### 7.1.1.3 Background on AC Performance Definitions With ADCs

A typical FFT plot for an ADC is shown in [Figure 46](#).

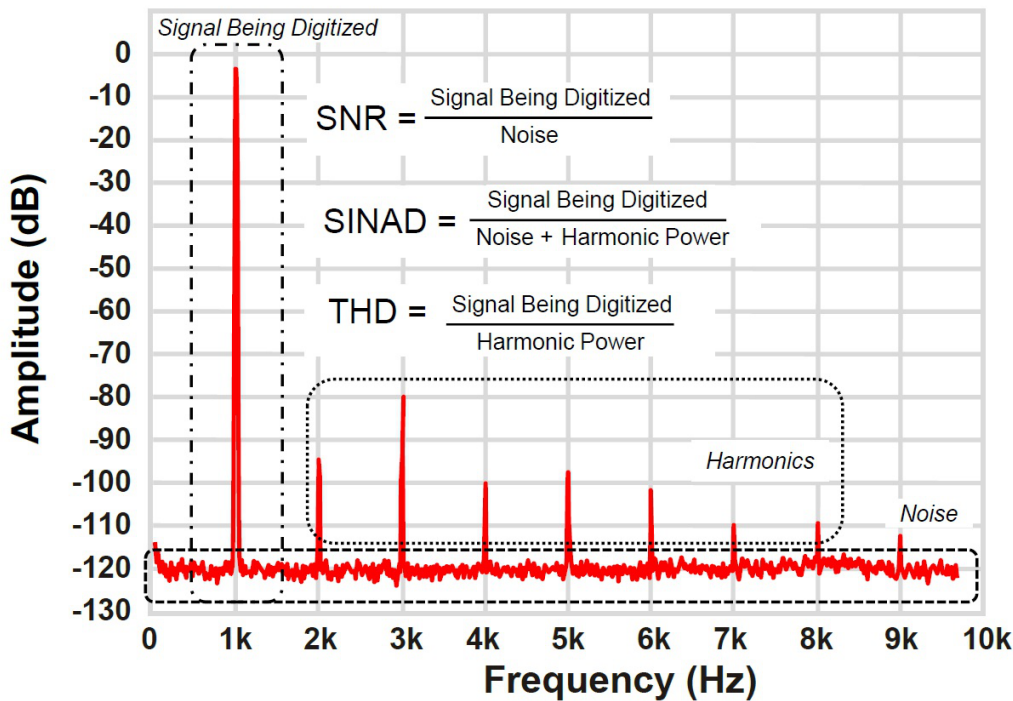


**Figure 46. Performance Definitions**

The SNR provides insight into the total noise of the system. The total noise of the data acquisition system is the root-sum-square (rss) of the front-end amplifier noise and the ADC noise. The ADC noise includes the quantization noise as well as the noise contributed by ADC internal circuitry. The total noise contributions from all these sources, denoted as  $V_{n\_TOT\_RMS}$ , are referred to the input of the ADC for calculating total SNR of the system:

$$\text{SNR} = \frac{V_{\text{SIGNAL\_RMS}}}{V_{\text{NOISE\_RMS}}} \quad (16)$$

THD is defined as the ratio of the rss of all harmonic components (generally, nine harmonics are used) to the power of the fundamental signal frequency. It is generally specified with an input signal near full-scale (FS), but in this design the input is kept 0.5 dB below FS to prevent clipping.

If the root-mean-square (rms) value of input signal is denoted as  $V_{\text{SIGNAL\_RMS}}$  and the power of the total first nine harmonics (except the fundamental) is denoted as  $V_{\text{HARMONICS\_RMS}}$ , the THD can be calculated as:

$$\text{THD} = \frac{V_{\text{SIGNAL\_RMS}}}{V_{\text{HARMONICS\_RMS}}} \quad (17)$$

SINAD combines the effect of distortion and noise to provide a cumulative measure of the overall dynamic performance of the system.

$$\text{SINAD} = \frac{V_{\text{SIGNAL\_RMS}}}{\sqrt{V_{\text{NOISE\_RMS}}^2 + V_{\text{HARMONICS\_RMS}}^2}} \quad (18)$$

Last but not least, the ENOB is an effective measurement of the quality of a digitized signal from an ADC, since it specifies the number of bits above the noise floor. It is calculated (starting from the SINAD expressed in dB) as:

$$\text{ENOB} = \frac{\text{SINAD}_{\text{dB}} - 1.76 \text{ dB}}{6.02 \text{ dB}} \quad (19)$$

Refer to [SLAU515](#) for more details about how the parameters have been calculated.

### 7.1.2 Differential to Single-Ended Analog Signal Path

Using the dual channel signal generator two coupled sine waves (same amplitude, same frequency, with a 90-degree phase shift among them) are generated and applied to the analog differential signals A+ and A- and B+ and B- using the J9 connector. Two differential probes are used to acquire the differential signals applied in input, while two single-ended probes are connected to the single-ended analog outputs A and B of the analog path, on connector J6, pin 18 and pin 20, respectively.

The amplitude of the outputs versus the inputs are measured in this way; at the same time, the phase shift between the differential inputs and the respective single ended output are measured. In this way, a Bode plot of the analog signal conditioning path could be calculated.

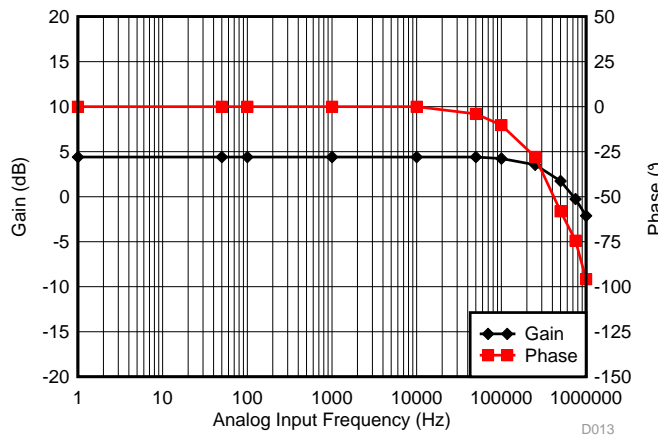


**Figure 47. Transfer Function of Differential to Single-Ended Analog Signal Path — Channel A and B**

The same measurements have been performed on the marker signal ( $R_+/R_-$ ). Note that the phase of the R signal is less than the equivalent for A and B since the output has been measured at the input to the comparator. The decoupling filter here has a five times higher cut-off frequency ( $R = 20 \Omega$ ,  $C = 2.2 \text{ nF}$ ) versus the output filter for A and B ( $R = 100 \Omega$ ,  $C = 2.2 \text{ nF}$ ).

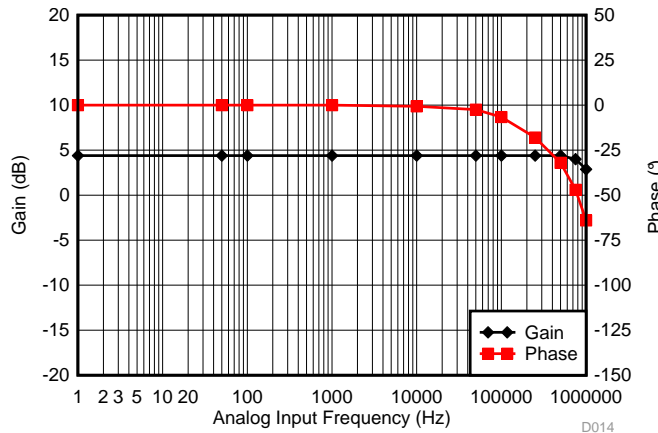


**Figure 48. Transfer Function of Differential to Single-Ended Index Marker R**

### 7.1.3 Comparator Subsystem With Digital Output Signals $A_{TTL}$ , $B_{TTL}$ , and $R_{TTL}$

In this section, the performance of the comparator with hysteresis that converts the single-ended analog signals A, B, and R into digital signals was tested.

The focus was on the propagation delay of the comparator output signals  $A_{TTL}$ ,  $B_{TTL}$ , and  $R_{TTL}$  at the host connector J6 versus the analog input at the ADS8354 for the high-resolution path as well as the single-ended analog signals for the analog path.

The aim of the test was to measure the overall signal delay of the comparator path versus the analog path, considering the delays introduced by hysteresis, phase shift due to low-pass filtering and the propagation delay of the comparator itself.

Since all three channels A, B, and R were done absolutely symmetrical with regards to the comparator output, measurements have only been conducted with channel A.

The analog signals were both measured with a single-ended probe, hence on the differential input of the ADS8354 only the positive differential signal was measured versus GND.

For the test sinusoidal input signals were injected at the encoder connector J9, A\_P, A\_M (sine) and B\_P, B\_M (cosine) as well as P\_M and R\_P.

For the high-resolution path, the amplitude was set to 1.0 V<sub>PP</sub> (typical) and 0.3 V<sub>PP</sub> (minimum) with 100 Hz and 500 kHz (maximum) to test the worst case scenario for the propagation delay. For analog path, the measurement was conducted at 0.3 V<sub>PP</sub> with 100 Hz and 500 kHz, as corner cases.

Test results are shown in the following figures. Note that both, the high-resolution path (at the differential input of the ADS8354) and the single-ended analog path (at connector J6.Pin 12) are compared versus the comparator output (at connector J6.Pin 18).

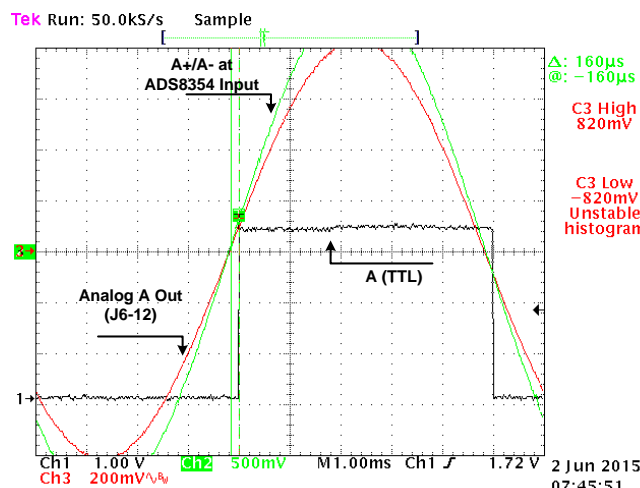


**Figure 49. Comparator Output  $A_{TTL}$  versus Differential Input to ADS8354 and Analog Output A (J6-12) With Input 1.0 V<sub>PP</sub>, 100 Hz at Encoder Connector J9-1, J9-2**

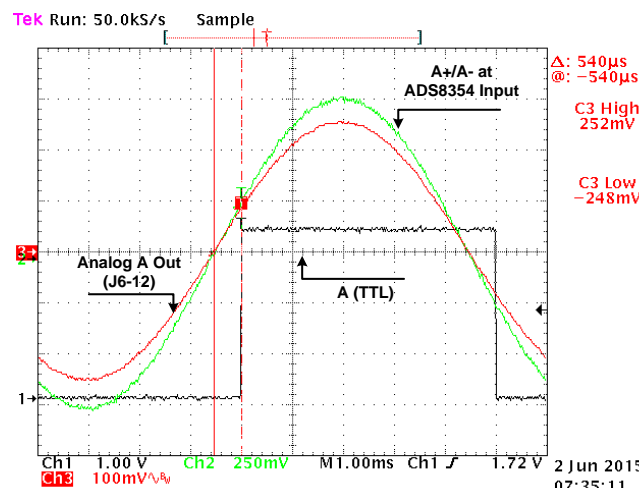


**Figure 50. Comparator Output  $A_{TTL}$  versus Differential Input to ADS8354 and Analog Output A (J6-12) With Input 0.3 V<sub>PP</sub>, 100 Hz at Encoder Connector J9-1, J9-2**

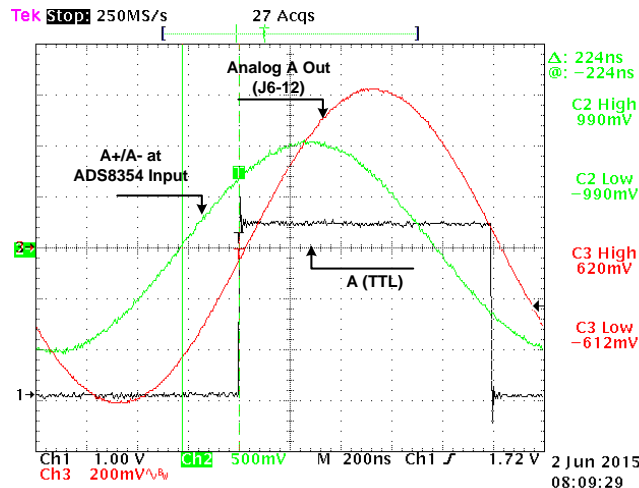


**Figure 51. Comparator Output  $A_{TTL}$  versus Differential Input to ADS8354 and Analog Output A (J6-12) With Input 1.0  $V_{pp}$ , 500-kHz Encoder Connector J9-1, J9-2**

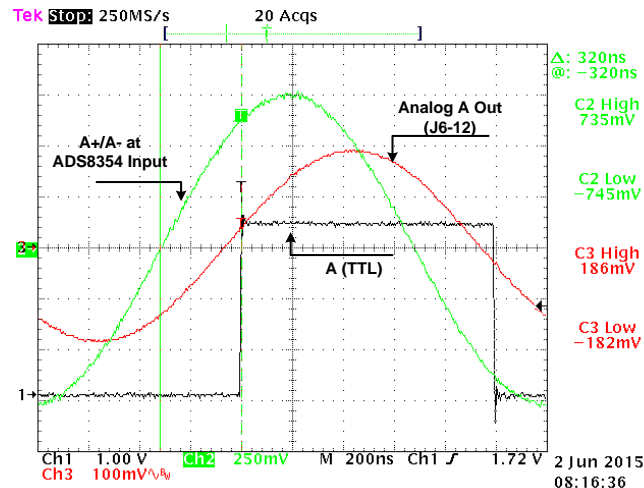


**Figure 52. Comparator Output  $A_{TTL}$  versus Differential Input to ADS8354 and Analog Output A (J6-12) With Input 0.3  $V_{pp}$ , 500 kHz at Encoder Connector J9-1, J9-2**

As expected, the maximum overall phase shift including RC filter decoupling networks occurs at 500 kHz with the lowest input amplitude and is total around 320 ns, equal to 57 degrees, which is well below 90 degree and within the 60 degree the specification per [Section 2](#). The very low propagation delay of the TLV3201 with typically 40 ns has a major impact on this low number. This also gives a major margin to compensate all the possible spreads in the parameters influencing the amount of phase delay like due to low-pass filters, and so on.

The propagation delay at 100 Hz is almost the same than for the high-resolution channel because the delay at lower frequencies is dominated by the amplitude-dependent hysteresis.

On the single-ended analog path, there's almost no delay at 500 kHz despite a 250-ns propagation delay of the comparator with hysteresis itself. This is due to the strong low-pass filter at the single-ended analog output ( $R = 100 \Omega$ ,  $C = 4.7 \text{ nF}$ ) to drive an embedded switched capacitor ADC like in the Piccolo MCU. This frequency depended phase delay slightly compensates the delay from the comparator at higher frequencies.

In a second step, only the delay related to the comparator with hysteresis was measured. The delay was specified as the input to the comparator (analog signal at  $R_{50}$ ) and the output of the comparator. Note that 0.3  $V_{pp}$  at the encoder input equals around 0.5  $V_{pp}$  at the comparator input due to the previous amplifier stage with gain of 1.66.

The delay introduced by the comparator block only (hysteresis and comparator propagation delay) has been measured and is listed in [Table 32](#).

**Table 32. Hysteresis Comparator Subsystem Delay**

INPUT AT ENCODER CONNECTOR	VOLTAGE AT COMPARATOR INPUT (FOR EXAMPLE, $R_{50}$ )	PROPAGATION DELAY	PHASE DELAY
1.0 $V_{pp}$ , 100 Hz	1.66 V	170 $\mu s$	6.1 degrees
0.3 $V_{pp}$ , 100 Hz	0.5 V	560 $\mu s$	20.1 degrees
1.0 $V_{pp}$ , 500 kHz	1.52 V	120 ns	21 degrees
0.3 $V_{pp}$ , 500 kHz	0.46 V	200 ns	36 degrees

The difference to the overall delay in [Figure 49](#) to [Figure 52](#) is to the low-pass noise filter in the analog path, which contributes to around further 22 degrees at 500 kHz for the high-resolution signal path. However, the delay is still well below 90 degrees.

If an ideal phase matching is desired, a corresponding low-pass filter can be implemented with the THS4531A as outlined in [Section 4.5](#).

## 7.2 Power Supply Tests

### 7.2.1 24-V DC/DC Input Supply

The following tests were performed to characterize the DC/DC buck converter, which converts the 24-V to a 6-V intermediate rail.

#### 7.2.1.1 Load-Line Regulation

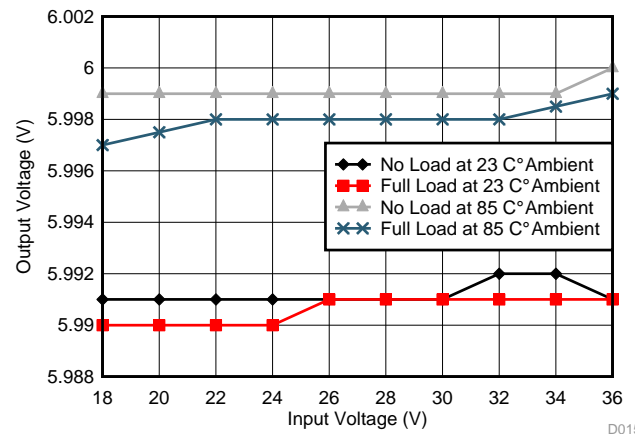


**Figure 53. Load-Line Regulation**

Comments: line-load regulation is within the  $\pm 10\text{-mV}$  range over the full working conditions.  $V_{\text{OUT}}$  is the expected 6 V  $\pm 2\%$  (regulator's accuracy) plus the accuracy of the resistor divider R7/R10.

#### 7.2.1.2 Output Voltage Ripple

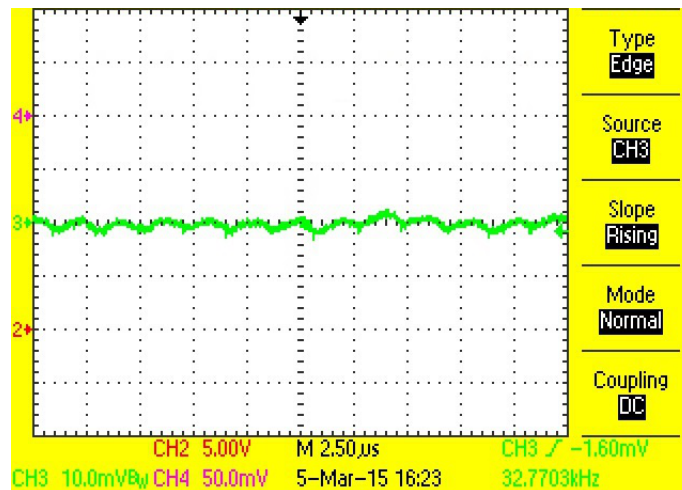


**Figure 54. Output Voltage Ripple at 24-V Input, No Load, @ 22°C Ambient Temperature**

Comments:  $V_{\text{OUT}}$  ripple is much lower than required 20 mV<sub>PP</sub>.

### 7.2.1.3 Switching Node and Switching Frequency

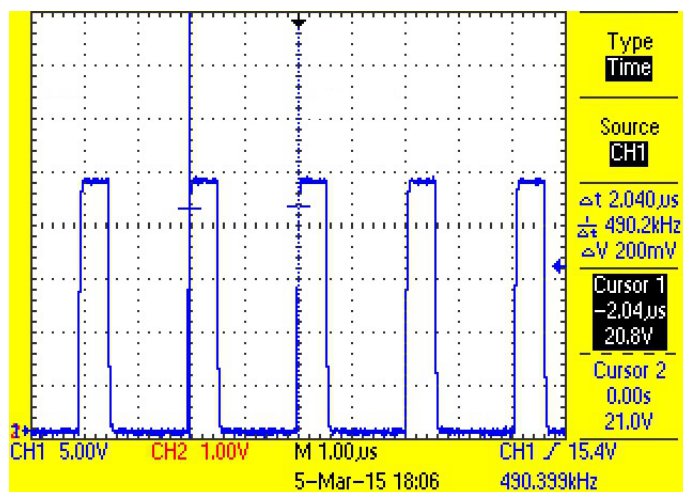


**Figure 55. Switching Frequency Measurement, Full Load, 24-V Input, Troom**

Comments: The switching frequency is in the expected range (500 KHz  $\pm 23\%$ ). The SMPS is stable, no jitter, no irregular switching, no voltage spike.

### 7.2.1.4 Efficiency

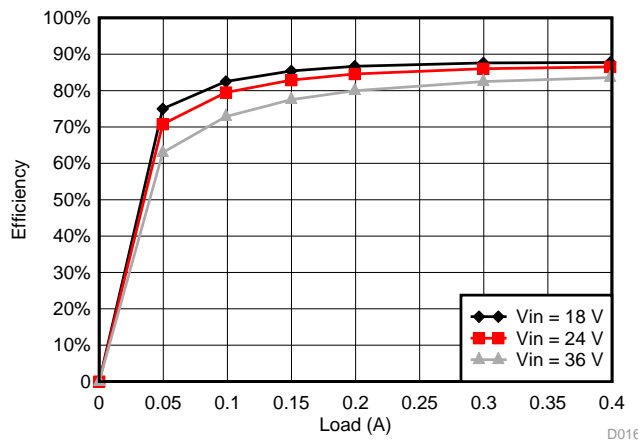


**Figure 56. Efficiency at 22°C With Reverse Polarity Protection Diode**

Comments: The effect of the diode for reverse polarity protection on the DC-DC converter efficiency is negligible. The 80% efficiency target at full load has fully met at any specified input voltage.

### 7.2.1.5 Bode Plot

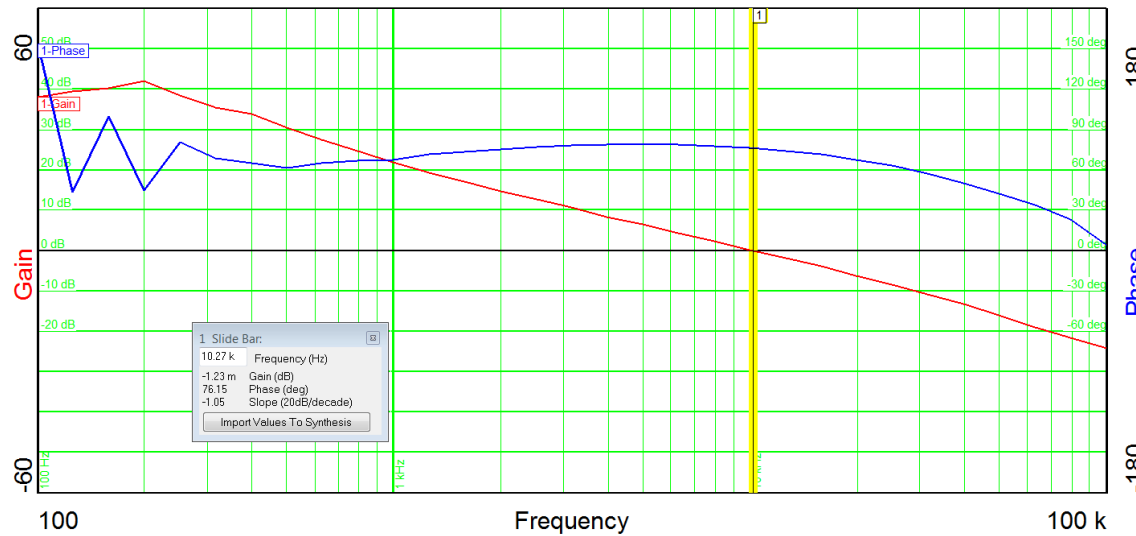


**Figure 57. Bode Plot at 24-V Input, Full Load**

**Table 33. Phase and Gain Margin**

INPUT VOLTAGE	PHASE MARGIN	FREQUENCY CROSS-OVER
36 V	78 degrees	10.3 KHz
24 V	76 degrees	10.3 KHz
17 V	74 degrees	10.2 KHz

Comments: Gain-loop analysis shows a 10-kHz system bandwidth with very good phase margin (> 60 degrees) at any working conditions.

### 7.2.1.6 Thermal Plot

A thermal picture has been grabbed to determine the hot-spot on the board at the maximum load conditions.

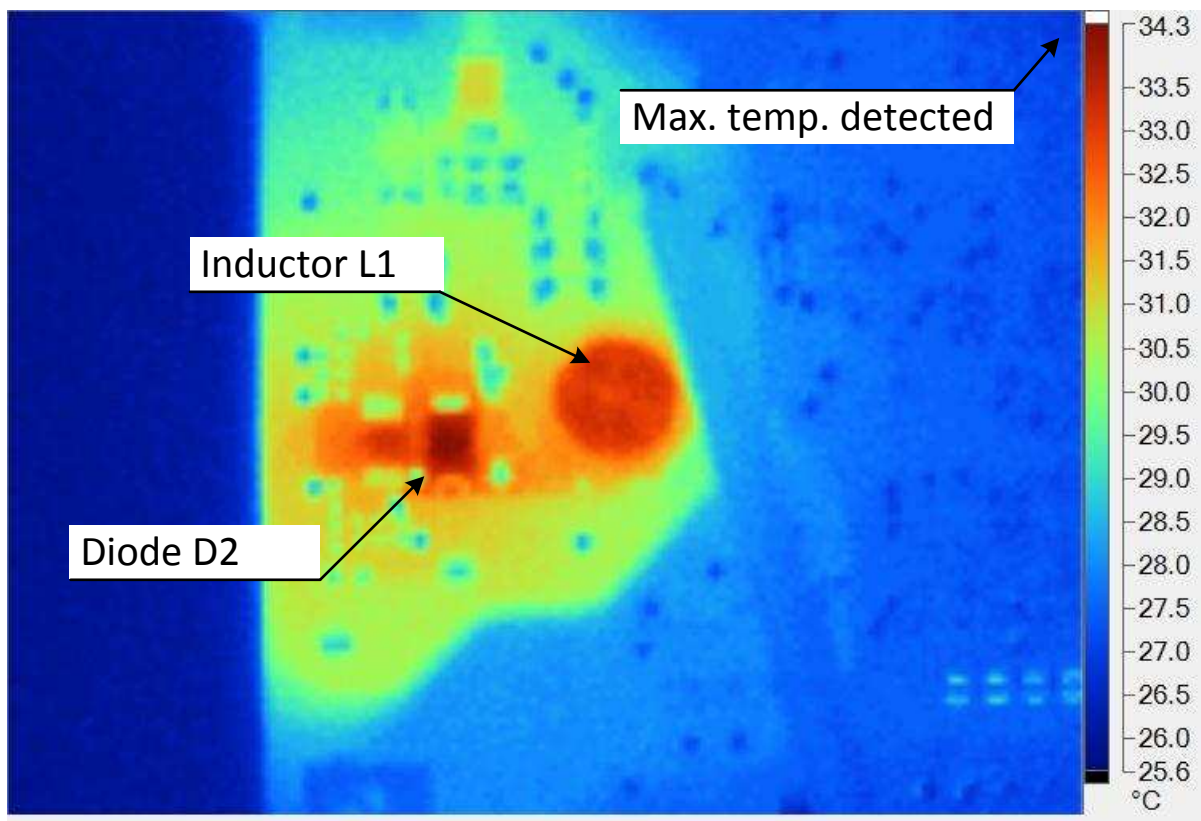


**Figure 58. Thermal Images, 24-V Input, Full Load, 22°C Ambient Temperature**

Comments: The detected hot-spot on the board corresponds to the non-synchronous rectifier or diode of the TPS54040A circuit. It shows a temperature increase of 11°C at room tests, depending on input voltage and output current. The maximum detected temperature on this part is 34°C.

Tests at 85°C did not show significant drifts in performances (refer to [Figure 53](#), load-line regulation @ 85°C).

### 7.2.2 Encoder Power Supply Output Voltage

The output voltage of the LDO providing the supply for the encoder is well regulated and meets the spec requirements, as for the following measurements.

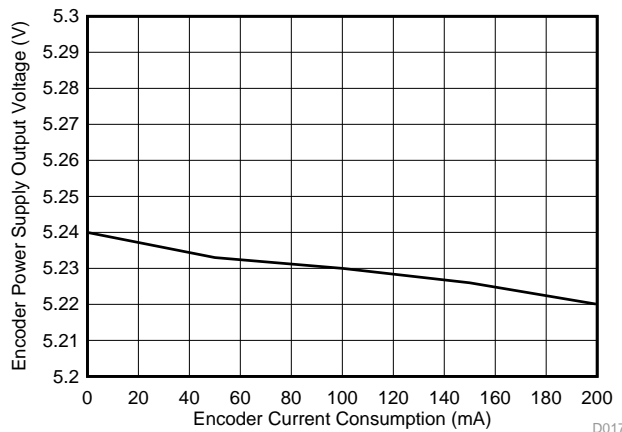


**Figure 59. Encoder Power Supply Output Voltage versus Load Current (0 to 200 mA)**

### 7.2.3 5-V and 3.3-V Point-of-Load

The output voltages of the two LDO to generate the point-of-load providing the supply for the signal chain block are well regulated and meet the spec requirements. Measurements are shown in [Table 34](#). The nominal current consumption on the 3.3-V and the 5-V rails was measured with a Sin/Cos encoder connected and the F28069M LaunchPad triggering a new measurement at 16 kHz.

**Table 34. Measured Output Voltage**

SPECIFIED OUTPUT VOLTAGE	MEASURED VOLTAGE AT NOMINAL LOAD	NOMINAL CURRENT
5 V	5.02 V	49.9 mA
3.3 V	3.34 V	0.2 mA

## 7.3 System Performance

### 7.3.1 Sin/Cos Encoder Output Signal Emulation

For this purpose the encoder output signals have been emulated using a 16-bit programmable dual-output signal generator Keysight (Agilent) 33600A. Sinusoidal test signals from DC up to 500 kHz were injected into the differential inputs A+/A- and B+/B-.

In this section, the system level performance have been measured. In particular:

- Accuracy over one electrical period (phase)
- Accuracy over one revolution at maximum input frequency 500 kHz. Here, the encoder emulation was based on a 2000-signal period equal to one emulated revolution

The tests were done at room temperature and have been repeated at 70 degrees to check the error drift versus temperature.

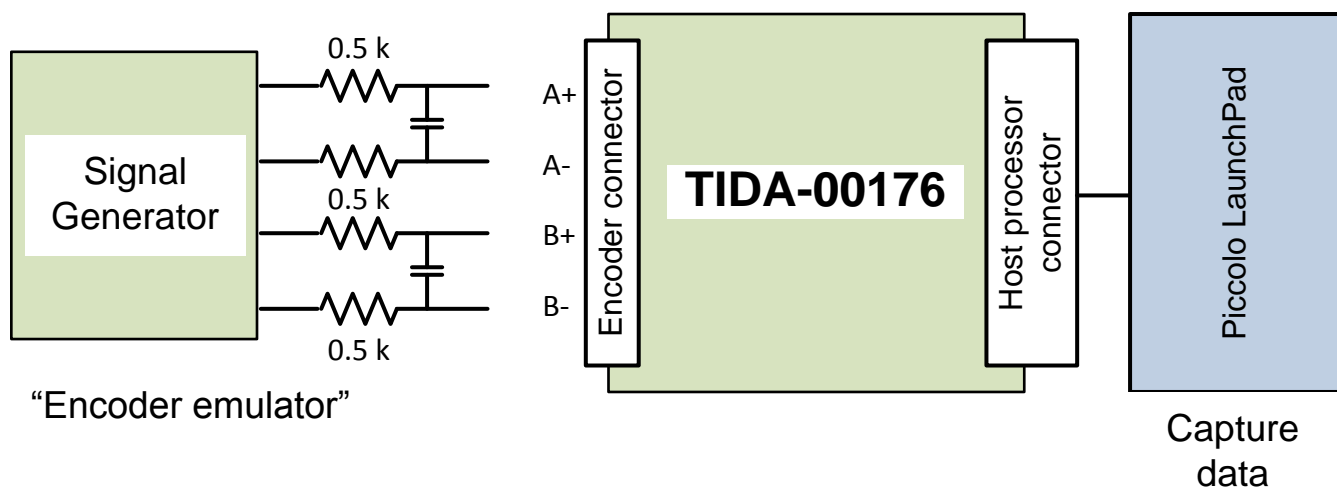


**Figure 60. Test Setup for Encoder Signal Emulation**

#### 7.3.1.1 One Period (Incremental Phase) Test

The first tests showed that the error injected by the dual output signal generator was much worse than the TIDA-00176 accuracy, spoiling completely the purpose of the tests. Noise and error sources for could be "briefly" summarized as:

- Gain error (amplitude of A not equal to the amplitude of B)
- Phase shift error (not exactly 90 degrees constant as expected)
- Offset error (average of A or B signal is not equal to 0)
- HF noise due to the quantization error of the function generator
- Frequency error (frequency of A not equal to the B one, even if the signal are "coupled")

**CAUTION**

To reduce the quantization error and noise introduced by the function generator a 1-K to 1- $\mu$ F LP filter is inserted between the signal generator and the TIDA-00176 inputs (the 1-K resistor is actually a series of two 500- $\Omega$  resistors to keep the network balanced) on the input.

To eliminate gain, offset, phase shift and frequency error between the two channels the following setup was applied: Only one output signal, filtered as described above was applied to both inputs A and B at the encoder connector J8 of the TIDA-00176, hence feeding with the same signal. This will eliminate the limitation of the function generator. Furthermore, any mismatch amongst the two channels of the ADS8354 (and their respective signal conditioning paths) can be better evaluated.

Indeed, the data acquired from the ADS8354 should show (in ideal world) two streams of raw identical data, while any mismatch at this level comes from the mismatch of the two channels, and not from the input itself. This can be also used to calibrate the system, since offset and gain error corrections could be performed to completely balance the A and B channels.

The data has been acquired at a 32-kHz sample rate using the F28069M LaunchPad connected to the TIDA-00176, as outlined in [Section 6](#).

After the ADS8354 channel A and B data has been acquired by the F28069M, the 16-bit raw data has been dumped into an Excel file. Then the raw data for channel B has been exactly phase shifted by 90 degrees. After that the phase has been calculated using the inverse tangent of the raw data A and 90-degree phase shifted raw data B.

This test has been repeated for the 1.0-V<sub>PP</sub> amplitude and frequencies of 10 Hz up to 500 Hz. The result is shown in the following figures.

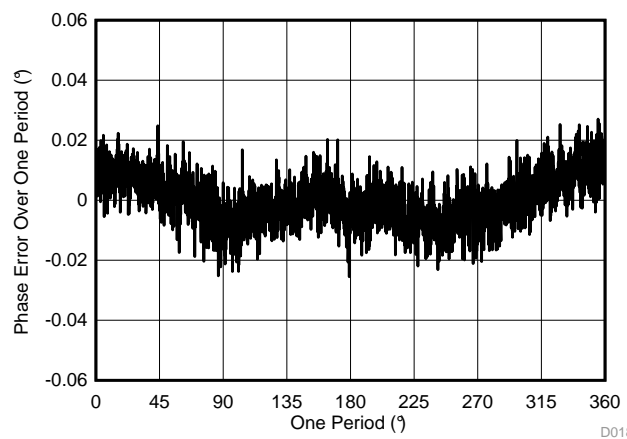


**Figure 61. Phase Error over One Signal Period when 1.0-V<sub>PP</sub> 10-Hz Input is Applied**

Within one incremental line (one signal period = 360 degrees), the phase error remains well within  $\pm 0.02$  degrees. This corresponds to an error  $\pm 0.02/360 = 0.0055\%$ . With respect to 16-bit resolution, this equals around  $\pm 3$  LSB only.

The noise distribution is even within  $\pm 0.01$  ( $\pm 1.5$  LSB). The phase error with the double period is due to a non-ideal 90-degree phase shift between the two signals A and B, as outlined in [Section 1](#).

Note that an error of  $\pm 0.02$  degrees over one signal period will correspond to a total error of  $\pm 10$  micro-degrees (0.036 arc seconds) for an encoder with 2000 line counts.

The same tests have been performed in the thermal chamber at nominal 70°C to evaluate the system performance drift and, in particular, the absolute error on the angular position.

Again the double frequency modulation comes from the non-perfect matching (90-degree phase shift, and so on) of the two-input signal.

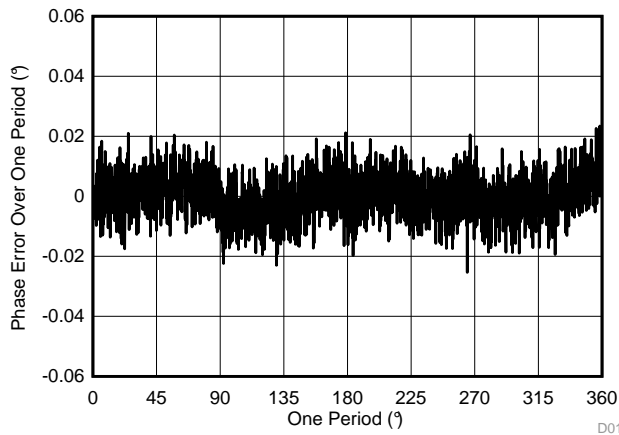


**Figure 62. Phase Error at 70°C Over One Signal Period When 1.0-V<sub>pp</sub> 10-Hz Input is Applied**

The same test was applied with a 0.6-V<sub>pp</sub> input in which the higher noise / lower SNR conditions are visible:

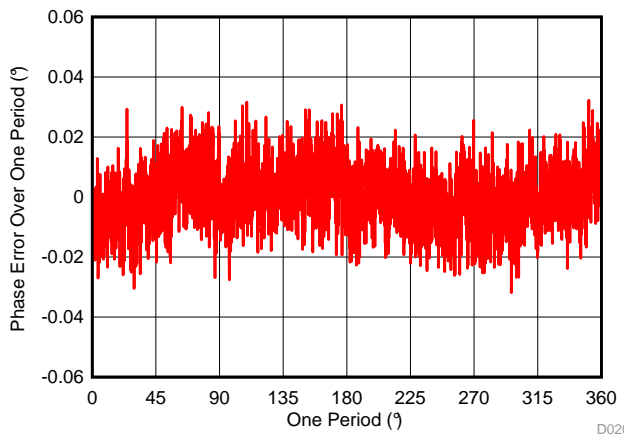


**Figure 63. Phase Error at 23°C Ambient Over One Signal Period When 0.6-V<sub>pp</sub> 10-Hz Input is Applied**

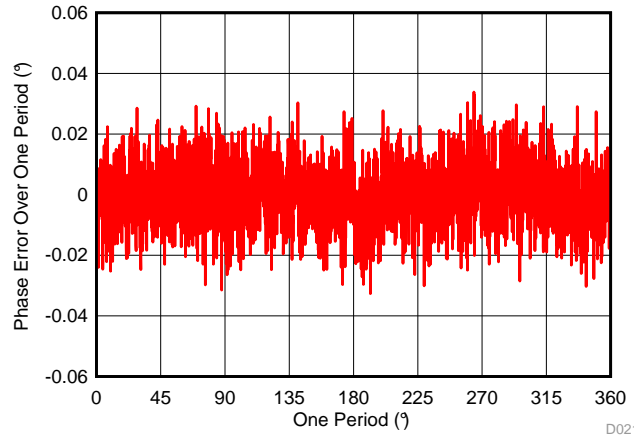


**Figure 64. Phase Error at 70°C Ambient Over One Signal Period (One Revolution/2000) When 0.6-V<sub>pp</sub> 10-Hz Input is Applied**

The ultra-low drift versus temperature is aligned to the expectation, also because of the characteristics of the selected op-amps and matched resistors used for the analog signal conditioning.

#### 7.3.1.2 One Mechanical Revolution Test at Maximum Speed

For this test, the high-resolution interpolated angle over one mechanical revolution was calculated within TIDA-00176 connected to the Piccolo F28069M LaunchPad. The sample rate was set to 32 kHz at 80-MHz CPU clock.

The aim of the test is to verify the interpolation algorithm works at maximum input signal frequency of 500 kHz, without missing any incremental count or mismatching the interpolated phase (arc tangent) and the corresponding line count (QEP) for example, due to mismatch of latching the analog samples and the QEP counter. This would translate into a larger error than the quantization noise measured in [Section 7.3.1.1](#).

For that purpose, a 360-degree spin of the encoder has been emulated using the dual signal generator. The test is performed with the dual output signal generator in the following way: The two output signals are coupled in amplitude and frequency, with a 90-degrees phase shift. The two signals are then applied as input at the TIDA-00176 encoder connector J9 A+/A- and B+/B- pins.

The total interpolated angle was stored in the F28069M RAM and read through CCS memory dump.

The calculated high-resolution angle is compared with an ideal phase assuming an encoder with 2000 line counts. Therefore, 2000 signal periods at 500K kHz equal one emulated revolution. The total angular phase ramps at a rate of  $360 \text{ degrees} \times 500 \text{ kHz}/2000 = 90,000 \text{ deg/s}$ . [Table 35](#) provides the timings for 1  $\mu\text{s}$  and for 100 ns, which equals one F28069M CPU clock at 80 MHz.

**Table 35. Angular Speed for Sin/Cos Encoder With Line Count 2000 Running at 15000 rpm**

IDEAL ANGULAR SPEED	ANGLE CHANGE IN 1 $\mu\text{s}$	ANGLE CHANGE IN 12.5 (CPU CLOCK)
90,000 deg/s	0.09	0.0011

A jitter on the signal generator as well as on the processor clock or even a CPU clock jitter of the host processor sampling the analog signal through SPI /CS cannot be avoided. Assuming an ideal ramp (due to a lack of reference) the measured angle will have a corresponding phase lag or lead, which translates into a velocity-dependent angle error.

[Figure 65](#) shows the interpolated angle error assuming an ideal ramp (500 kHz, 2000 signal periods per revolution) measured at 32 khz, which yields 128 consecutive samples per revolution.

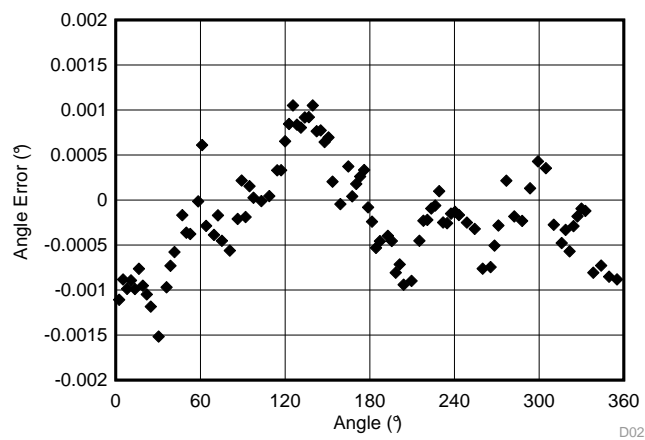


**Figure 65. Error of Interpolated Angle Over One Revolution With Encoder Emulation  
(1 V<sub>pp</sub>, 500-kHz Input @ 32-kHz Sampling)**

As previously mentioned, the aim was not to test for accuracy, but to verify that no increment was lost. With a 2000-line count emulation, one incremental line count would correspond  $360/2000 = 0.18$  degrees. The angle error (difference) to an ideal straight line remains within  $\pm 0.001$  degree; therefore, interpolation still works well at 500 kHz and no increment is lost.

As can be seen in figure the error is within  $\pm 0.0015$  degrees. This is due to the CPU clock jitter as well as other jitter like from the signal generator source with the CPU clock jitter determining the minimum accuracy.

The reason for this distribution is due to jitter with the F28069 software to trigger the SPI transfer /CS of one or two CPU clock cycles. Falling edge of /CS latches the analog input. Just a jitter of 12.5 ns translates into a phase difference of around  $12.5 \text{ ns}/2000 \text{ ns} \times 360/2000 \text{ degrees} \sim 0.0011$  degrees. Therefore, the angle difference is actually a speed depended angle error (velocity) lag.

## 7.4 Sin/Cos Encoder System Tests

Systems tests are done with Sin/Cos encoders ROD480-2000 and ROD480-1024 with a cable length of 1 m and 71 m, respectively.

### 7.4.1 Zero Index Marker R

The first test is to verify the synchronization or skew between the digital output signals A, B, and R available at the TIDA-00176 host processor interface connector J6, pin 12 (A<sub>TTL</sub>), pin 14 (B<sub>TTL</sub>), and pin 16 (R<sub>TTL</sub>). This test is to verify the proper configuration of the TIDA-00176 comparator subsystem.

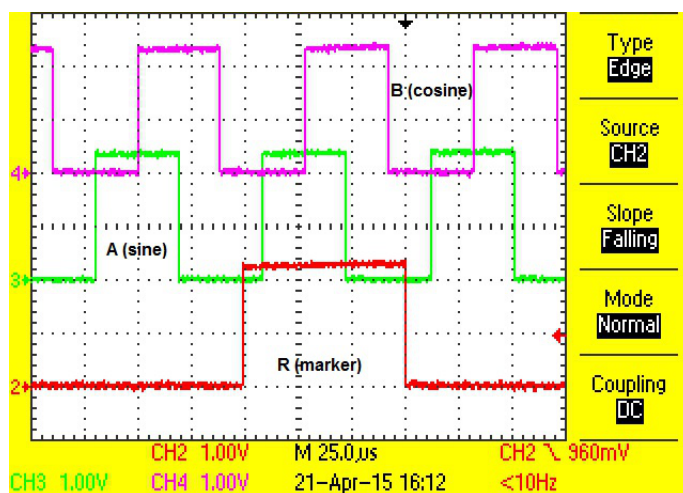


**Figure 66. Measured TTL Signals A, B, and R at TIDA-00176 Comparators Output J6-12, 14, and 18**

The transitions on the comparator output signal R occur only when both A and B are low, as expected. This result means the sequence between A, B, and R signals depends on the rotation direction of the Sin/Cos encoder shaft. In Figure 66, the encoder is turned clockwise as the rising edge of B occurs after the rising edge of A.

A closer look to the skew between A, B, and R has been done at a higher speed of around 400 rpm and for the rising and falling edge of R.. The rising and falling edge of R still occurs when both signals A and B are low.

Note that the rotation direction of Figure 67 and Figure 68 is counter clockwise (CCW).

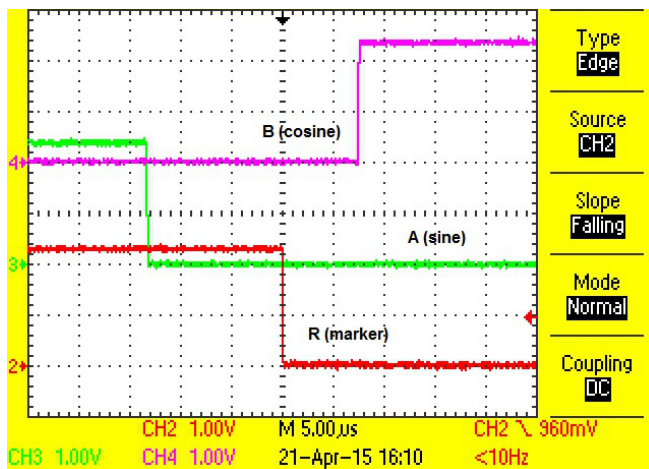


**Figure 67. Falling Index Signal R versus A and B in CCW Direction**

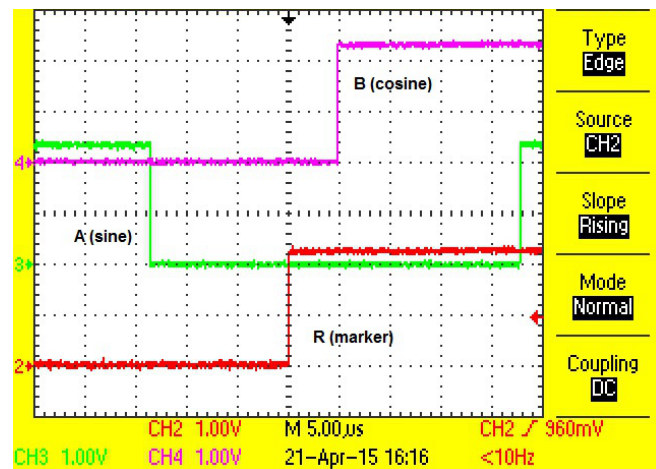


**Figure 68. Rising Index Signal R versus A and B in CCW Direction**

#### 7.4.2 Functional System Tests

The following static angle tests have been done with a ROD480-1024 Sin/Cos Encoder at 1-m and 71-m cable length. Total accuracy measurements with a precision better than 0.003 degrees (10 arc seconds) were not possible due to a lack of a mechanical precise enough encoder test bench. A picture of the test setup is shown in [Figure 69](#).

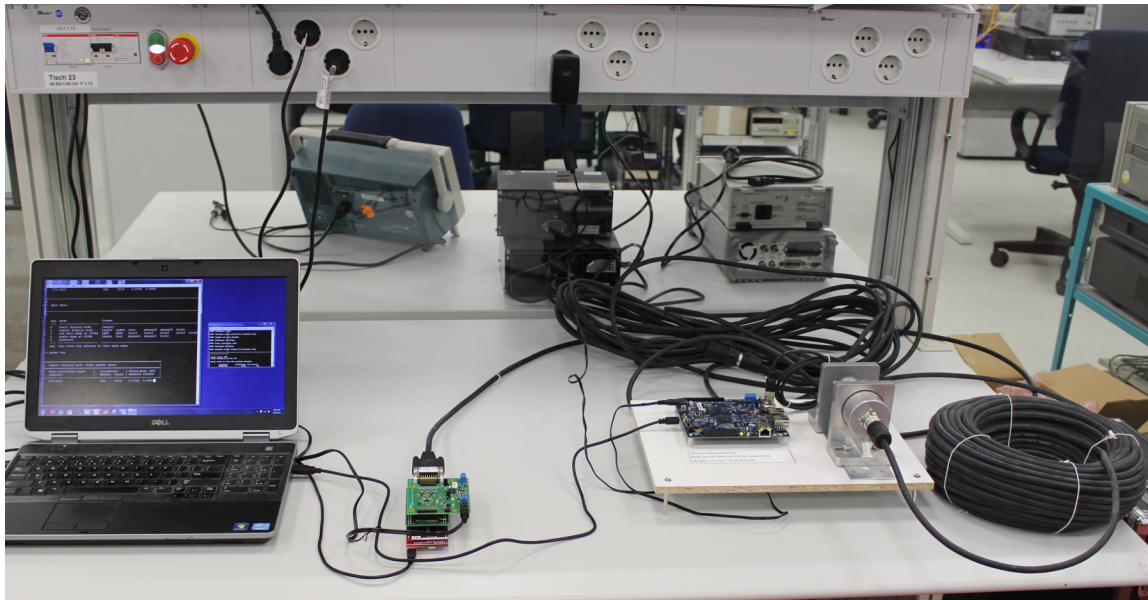


**Figure 69. TIDA-00176 Test Setup with 70-m Cable (20 m + 50 m) and ROD4800-1024 Sin/Cos Encoder**

[Figure 70](#) and [Figure 71](#) show the measured angle with the ROD480-1024 (1024 line count) over time for a static angle at the 1-m and 70-m cable lengths accordingly. The shaft was not fixed.

Note that the absolute angle for the 1-m and 71-m measurement slightly changed due mechanical vibrations when unscrewing the 1-m cable from the encoder and mounting the 70-m cable instead.

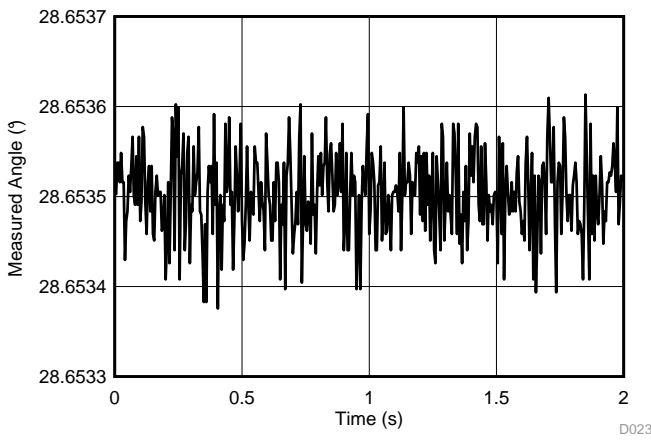


**Figure 70. System Test, Measured Angle Distribution With ROD480-1024 at 1-m Cable Length**

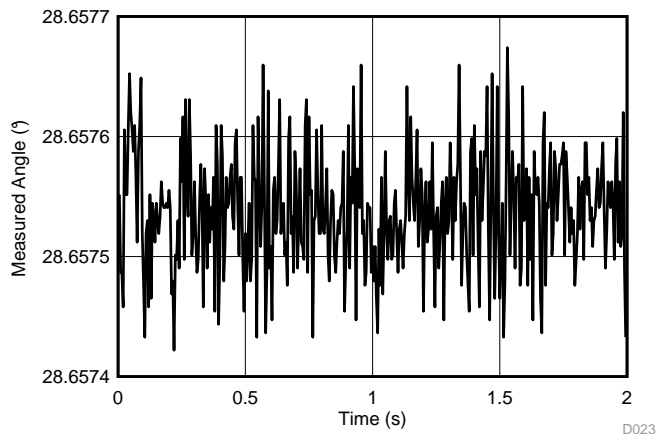


**Figure 71. System Test, Measured Angle Distribution With ROD480-1024 at 71-m Cable Length**

The measured angle with the ROD480-1024 has a noise distribution of  $\pm 0.0001$  degree (0.36 arc seconds). There is no significant difference between the 1-m and 70-m measurements because the attenuation of the cable was around  $-1.5$  dB at 0 Hz.

To verify the basic accuracy and repeatability of the TIDA-00176 design with a Sin/Cos encoder, the ROD480-1024 Sin/Cos encoder is mechanically coupled with an EnDat 2.2 encoder ROQ437. The ROD480-1024 is connected through a 70-m cable. A picture of the test setup is shown in [Figure 73](#).

**Figure 72** shows the angle difference between the TIDA-00176 connected to a ROD480-1024 Sin/Cos encoder and a ROQ437 EnDat 2.2 absolute encoder, where the absolute angle is read through a Sitara AM437x EnDat 2.2 Master. The absolute angle exhibits a cosine-shape error, which is due to a non-ideal, non-centric coupling of the two shafts with a small run-out.

The encoder was turned multiple times and the angle was captured accordingly to check repeatability too.

As expected, however, the mechanical setup was not accurate and precise enough to draw conclusions on the overall absolute system accuracy. Therefore, the tests conducted in [Section 7.3](#) based on Encoder emulation are more representative to the performance to be expected from the TIDA-00176 reference design.

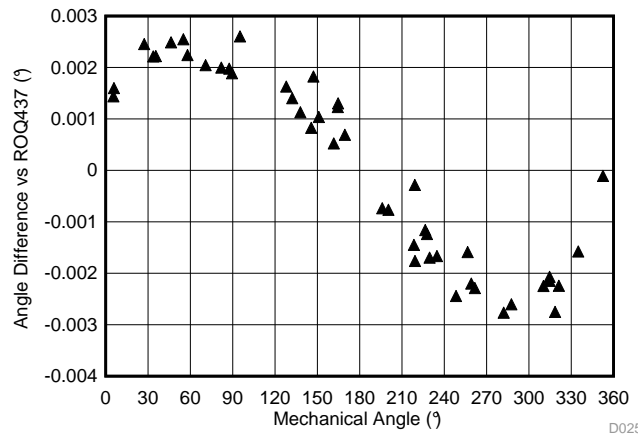


**Figure 72. Basic System Accuracy Test With Sin/Cos Encoder at 70-m Cable Length**

## 7.5 EMC Test Result

The TIDA-00176 TI design has been tested for IEC61000-4-2, 4-4, and 4-5 (ESD, EFT, and Surge) with test levels and performance criterion specified in the standard IEC 61800-3 "EMC immunity requirements and specific test methods applicable in adjustable speed, electrical-power drive systems".

The design is compliant to these standards and exceeds the voltage requirements according to IEC61800-3 EMC immunity requirements. A summary is shown in the below tables and more details in the following chapters.

The performance criterion A is often customer specific and the expected accuracy is depending system requirements. Refer to [Section 7.5.1](#) for details on test specification details.

**Table 36. IEC61800-3 EMC Immunity Requirements for Second Environment and Measured Voltage Levels and Class**

REQUIREMENTS					TIDA-00176 MEASUREMENTS		
PORT	PHENOMENON	BASIC STANDARD	LEVEL	PERFORMANCE (ACCEPTANCE) CRITERION	LEVEL	PERFORMANCE (ACHIEVED) CRITERION <sup>(1)</sup>	TEST
Enclosure ports	ESD	IEC61000-4-2	$\pm 4\text{-kV}$ CD or $8\text{-kV}$ AD, if CD not possible	B	$\pm 8\text{-kV}$ CD	B	PASS (EXCEED)
Ports for control lines and DC auxiliary supplies <60 V	Fast transient Burst (EFT)	IEC61000-4-4	$\pm 2\text{-kV}/5\text{-kHz}$ capacitive clamp	B	$\pm 4\text{ kV}$	B	PASS (EXCEED)
	Surge 1.2/50 $\mu\text{s}$ , 8/20 $\mu\text{s}$	IEC61000-4-5	$\pm 1\text{ kV}$ . Since shielded cable >20 m, direct coupling to shield ( $2\ \Omega/500\text{ A}$ )	B	$\pm 1\text{ kV}$	B	PASS

<sup>(1)</sup> Class A is considered when the difference between the measured angle and the initial mechanical reference position during the EMC event was always less than the incremental angle accuracy. The incremental line accuracy is 360/N degrees. For test a Sin/Cos encoder with 2000 line counts was used (HEIDENHAIN ROD480), where the incremental resolution equals 0.18 degrees.

The performance (acceptance) criterion is defined, as follows:

**Table 37. Performance Criterion**

PERFORMANCE (ACCEPTANCE) CRITERION	DESCRIPTION
A	The module shall continue to operate as intended. No loss of function or performance even during the test.
B	Temporary degradation of performance is accepted. After the test, the module shall continue to operate as intended without manual intervention.
C	During the test, loss of functions accepted, but no destruction of hardware or software. After the test, the module shall continue to operate as intended automatically, after manual restart, or power off, or power on.

### 7.5.1 Test Setup

The TIDA-00176 TI design has been tested at the testing laboratory of CSA Group Bayern in Strasskirchen, Germany. A picture of the basic setup for the TIDA-00176 design is shown in [Figure 73](#).

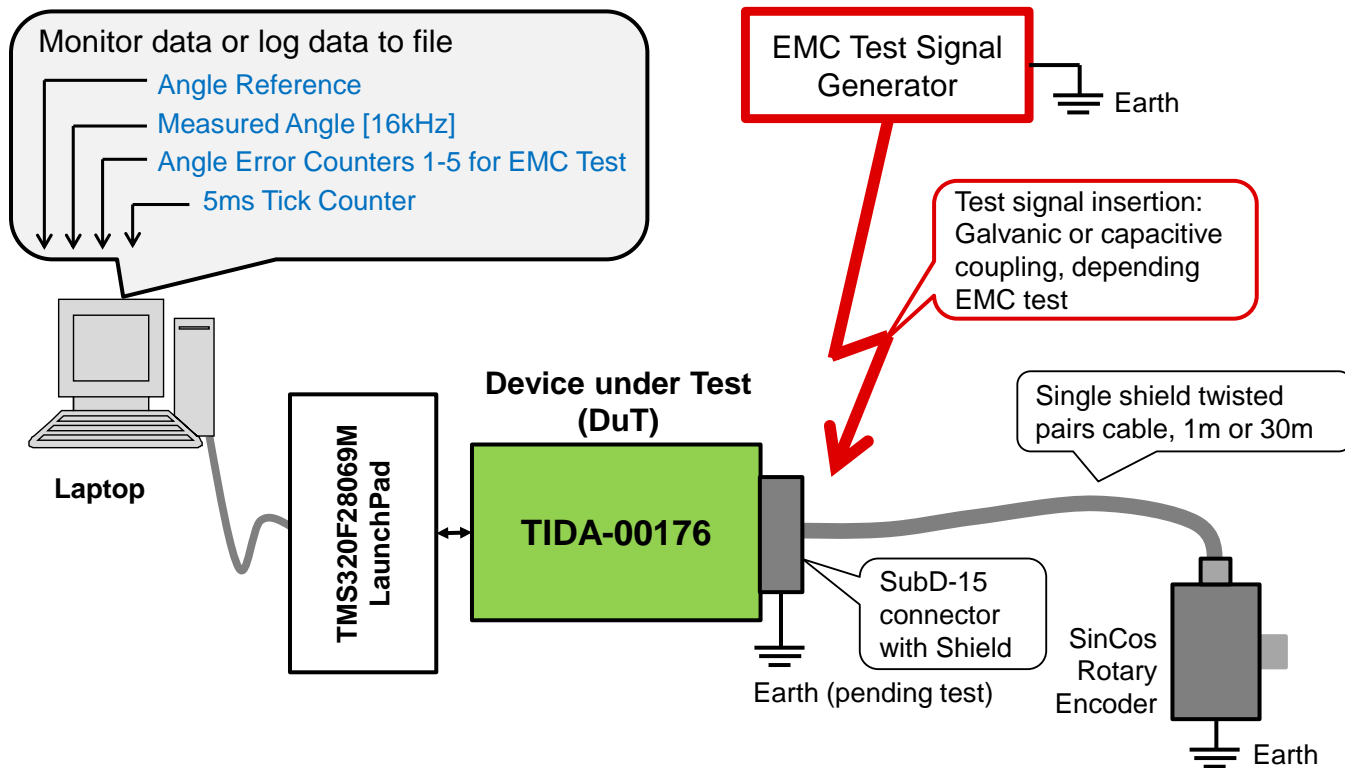


**Figure 73. Simplified System Block Diagram of TIDA-00176 With Piccolo F2069M LaunchPad**

To verify the interpolated angle signal integrity during and after the EMC test, the Sin/Cos encoder initial angle position (standstill) was used as a reference during the EMC tests and the encoder was not turned.

The interpolated angle was measured every 16 kHz and the result was compared to the initial reference angle position. Due to the very high resolution and analog input signals, the angular error was divided into six ranges listed in [Table 38](#). Every time an error occurred in a specific range, the corresponding error counter was increased by 1.

**Table 38. TIDA-00176 High-Resolution Angle Error Range Definitions**

ERROR COUNTER	ANGULAR ERROR RANGE (DEGREE)	ANGULAR ERROR RANGE (ARC SEC)	COMMENT
Error range 1	>1.0		
Error range 2	0.18 ≤ Error < 1.0		
Error range 3	0.1 ≤ Error < 0.18		Still no incremental line count errors
Error range 4	0.01 ≤ Error < 0.1		
Error range 5	0.001 ≤ Error < 0.01	3.6 ≤ Error < 36	
Error range 6	0.0001 ≤ Error < 0.001	< 3.6	Not considered

The error ranges were selected according to the line count of the encoder. For this test a Sin/Cos encoder with 2000 line counts was used (HEIDENHAIN ROD480-2000), where the line count resolution equals 0.18 degrees.

Note that the error range 6 counter is counting differences below 1/1000 of a degree (3.6 arc seconds), which was within the standard angle measurement distribution of the TI design and thus not considered during the EMC test.

The firmware used was the TIDA-00176\_SinCosEncoder\_Example\_Firmware\_rev1\_0.out, as provided with this design. The firmware runs on the TMS320F28069M Piccolo MCU.

A specific EMC test interface mode was entered by typing "9999" as line count to initialize the Sin/Cos encoder and reference angle position and start the data dump at 200 Hz. The EMC test menu initializes with a fixed line count of 2000, and will not leave this test mode again. This was done to ensure fixed program flow, as the USB port on the laptop (not part of the design) turned out to be quite sensitive to EMC.

A picture of the specific test setup for ESD, EFT, and Surge is shown in the corresponding following chapters.

### 7.5.2 IEC-61000-4-2 ESD Test Results

Figure 74 shows the ESD test setup. The ESD strike was applied to the SubD-15 female connector's shield. The shield was also connected to Earth and the Sin/Cos encoder was connected through a 1-m shielded twisted pairs cable.

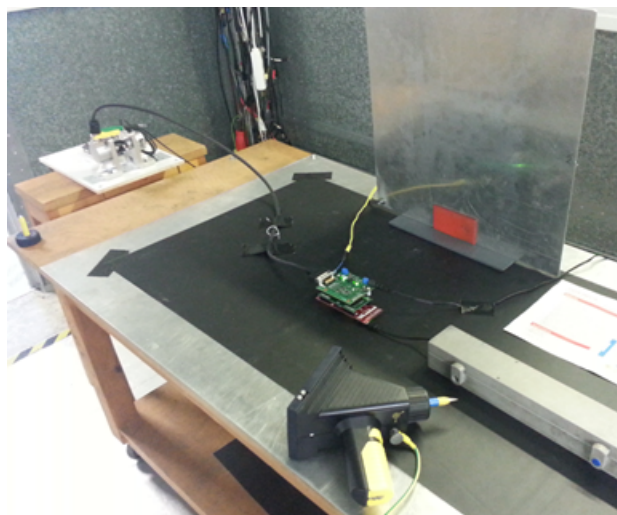


Figure 74. IEC61000-4-2 ESD Test Setup for TIDA-00176

**Table 39** shows the complete ESD test results for contact and air discharge at voltage levels, which also exceed the requirements per IEC618000-3. This is marked accordingly.

**Table 39. IEC-61000-4-2 ESD Test Results for TIDA-00176**

PHENOMENON	BASIC STANDARD	LEVEL	TIDA-00176 CONNECTOR	ACHIEVED PERFORMANCE CRITERION <sup>(1)</sup>	COMMENT
ESD	IEC61000-4-2	$\pm 4\text{-kV}$ contact discharge	SubD-15	B	
ESD	IEC61000-4-2	$\pm 6\text{-kV}$ contact discharge	SubD-15	B	Not required per IEC61800-3
ESD	IEC61000-4-2	$\pm 8\text{-kV}$ contact discharge	SubD-15	B	Not required per IEC61800-3
ESD	IEC61000-4-2	$\pm 8\text{-kV}$ air discharge	SubD-15	B	
ESD	IEC61000-4-2	$\pm 15\text{-kV}$ air discharge	SubD-15	B	Not required per IEC61800-3

<sup>(1)</sup> At least Class B was achieved because any angle measured during the ESD test did not deviate more than 0.1 degrees from the reference angle. This was smaller than the incremental line count resolution. The angle errors within each range are listed in **Table 38**. For class A, see **Table 36**, note 1.

**Table 40. IEC-61000-4-2 ESD Angle Error Distribution During Entire Test**

ERROR COUNTER	ANGULAR ERROR RANGE (DEGREE)	OCCURRENCE @ 4-kV CD	OCCURRENCE @ 6-kV CD	OCCURRENCE @ 8-kV CD
Error Range 1	>1.0	0	0	0
Error Range 2	$0.18 \leq \text{Error} < 1.0$	0	0	0
Error Range 3	$0.1 \leq \text{Error} < 0.18$	0	0	0
Error Range 4	$0.01 \leq \text{Error} < 0.1$	1	2	3
Error Range 5	$0.001 \leq \text{Error} < 0.01$	0	1	31878

The angle before and after the ESD tests did not differ more than 0.0005 degrees, which was within normal distribution at a fixed angle. For example, the angle was 80.0272 degree prior to the 6-kV CD ESD test and 80.0274 degrees after the ESD test, which was within standard distribution at fixed angle.

### 7.5.3 IEC-61000-4-4 EFT Test Results

A picture of the EFT test setup for TIDA-00176 is shown in [Figure 75](#). During the EFT test, the SubD-15 female connector was connected to a 30-m (10 m + 20 m) twisted pair shielded cable with a ROD480 Sin/Cos encoder at the far end.



**Figure 75. IEC61000-4-4 EFT Test Setup for TIDA-00176 (Right Side on Top, Left Side on Bottom)**

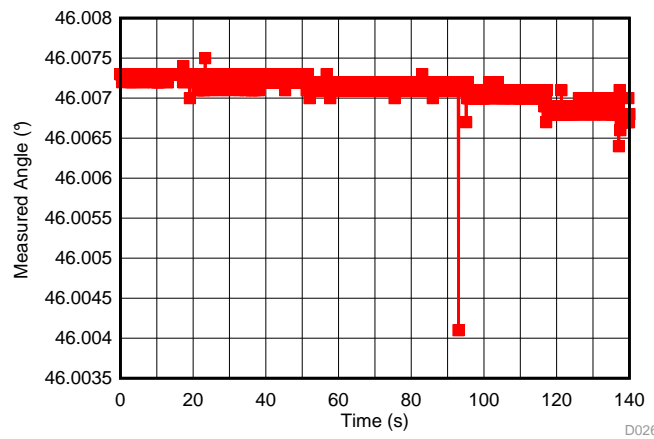
**Table 41. IEC-61000-4-4 EFT Test Results for TIDA-00176**

PHENOMENON	BASIC STANDARD	LEVEL	TIDA-00176 CONNECTOR	ACHIEVED PERFORMANCE CRITERION <sup>(1)</sup>	COMMENT
EFT	IEC61000-4-4	$\pm 2$ kV/5 kHz, capacitive clamp	SubD-15	B	
EFT	IEC61000-4-4	$\pm 2$ kV/5 kHz, capacitive clamp	SubD-15	B	
EFT	IEC61000-4-4	$\pm 4$ kV/5 kHz, capacitive clamp	SubD-15	B	Not required per IEC61800-3
EFT	IEC61000-4-4	$\pm 4$ kV/5 kHz, capacitive clamp	SubD-15	B	Not required per IEC61800-3

<sup>(1)</sup> At least Class B was achieved because any angle measured during the ESD test did not deviate more than 0.045 degrees from the reference angle. For class A, see [Table 36](#), note 1).

**Table 42. IEC-61000-4-4 EFT Angle Error Distribution During Entire Test**

ERROR COUNTER	ANGULAR ERROR RANGE (DEGREE)	OCCURRENCE @ 2-kV EFT	OCCURRENCE @ 4-kV EFT
Error Range 1	>1.0	0	0
Error Range 2	$0.18 \leq \text{Error} < 1.0$	0	0
Error Range 3	$0.1 \leq \text{Error} < 0.18$	0	0
Error Range 4	$0.01 \leq \text{Error} < 0.1$	254	1302
Error Range 5	$0.001 \leq \text{Error} < 0.01$	1658	3413

**Figure 76. Measured Angle During  $\pm 2$ -kV EFT Test Period at 10-Hz Update Rate**

The angle remains constant prior, during, and after the EFT test at 2 kV. The maximum error on the plot is 0.003 degrees. As the update rate is only 10 Hz (due to 115000-baud UART), the angle is higher than the 0.001-degree error that likely occurred in between and were not printed. Note that the error counters are updated at 16 kHz.

### 7.5.4 IEC-61000-4-5 Surge Test Results

Figure 77 shows a picture of the surge test setup for TIDA-00176. During the EFT test, the SubD-15 female connector was connected to a 30-m (10 m + 20 m) twisted pair shielded cable with a ROD480 Sin/Cos encoder at the far end.

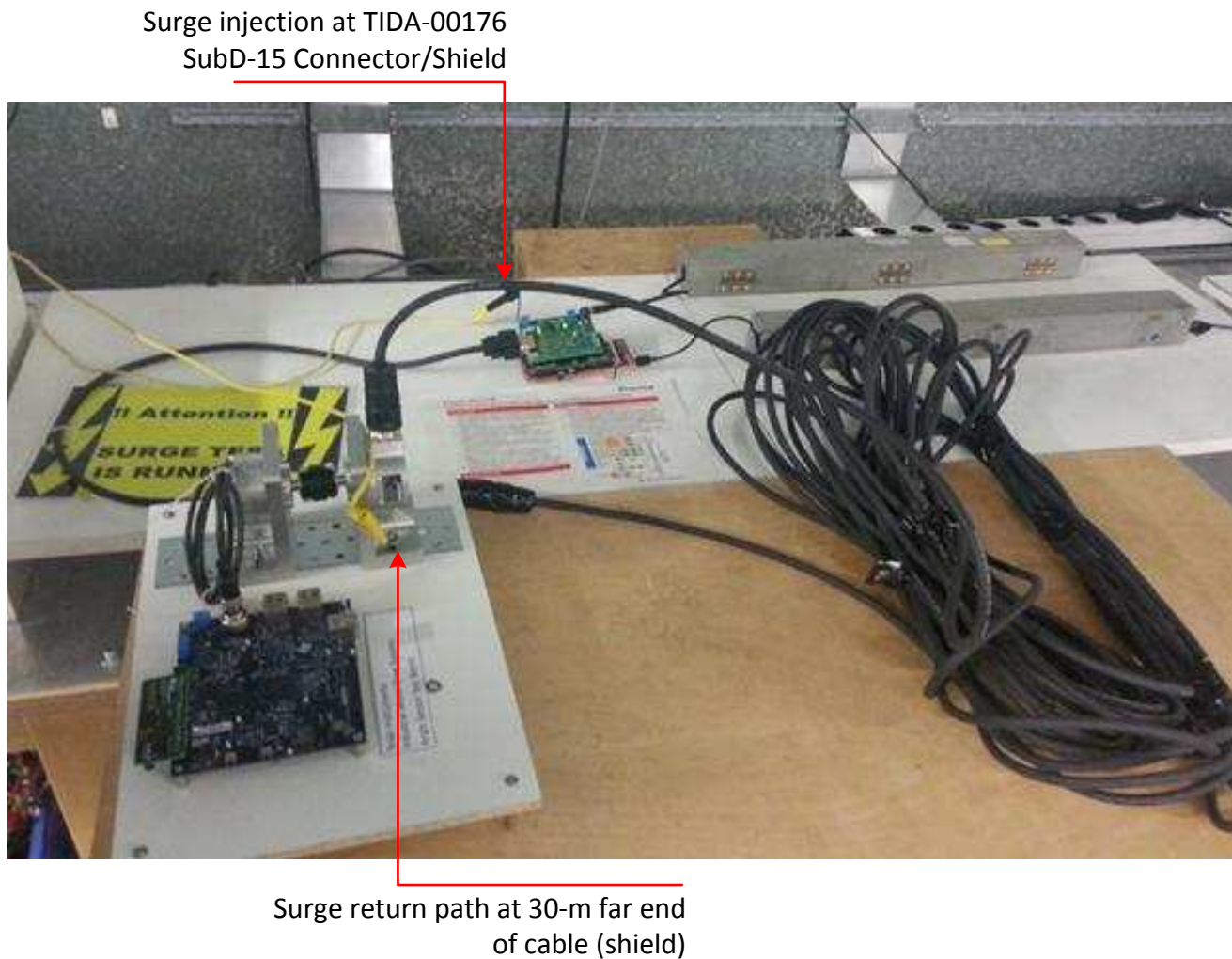


**Figure 77. IEC61000-4-5 Surge Test Setup for TIDA-00176**

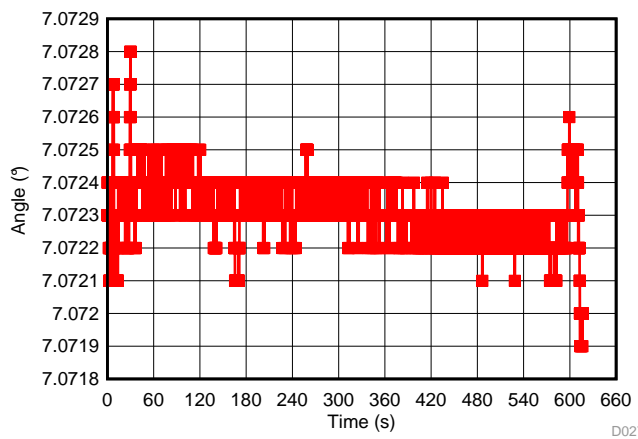
**Table 43. IEC-61000-4-5 Surge Test Results for TIDA-00176**

PHENOMENON	BASIC STANDARD	LEVEL	TIDA-00176 CONNECTOR	ACHIEVED PERFORMANCE CRITERION <sup>(1)</sup>	COMMENT
Surge	IEC61000-4-4	$\pm 0.5 \text{ kV}/2 \Omega$ (10-m + 20-m shielded cable)	SubD-15	B	
Surge	IEC61000-4-4	$\pm 1 \text{ kV}/2 \Omega$ (10-m + 20-m shielded cable)	SubD-15	B	

<sup>(1)</sup> At least Class B was achieved because any angle measured during the ESD test did not deviate more than 0.045 degrees from the reference angle. For class A, see Table 36, note 1).

**Table 44. IEC-61000-4-5 Surge Angle Error Distribution During Entire Test**

ERROR COUNTER	ANGULAR ERROR RANGE [DEGREE]	OCCURRENCE @ 0.5 kV	OCCURRENCE @ 1 kV
Error Range 1	>1.0	0	0
Error Range 2	0.18 ≤ Error < 1.0	0	0
Error Range 3	0.1 ≤ Error < 0.18	1	5
Error Range 4	0.01 ≤ Error < 0.1	1	4
Error Range 5	0.001 ≤ Error < 0.01	204	5669

**Figure 78. Measured Angle During ±1-kV Surge Test Period at 10-Hz Update Rate**

The angle remains constant prior and after the surge test at 1-kV. The maximum error on the plot was just 0.0009 degrees. As the update rate is only 10 Hz, the angle with the higher error as listed in [Figure 44](#) is not printed through the UART.

The mechanical M23 connectors between the three cables did not allow for a mechanical robust continuous connection of the shield due to a lack of screws. A proper electrical connection is made with copper and verified by the operator from CSA Group through a measured surge current. Once tests at ±2 kV have been conducted with a cable with appropriate mechanical connectors, the design guide will be updated accordingly.

## 8 Design Files

### 8.1 Schematics

To download the schematics, see the design files at [TIDA-00176](#).

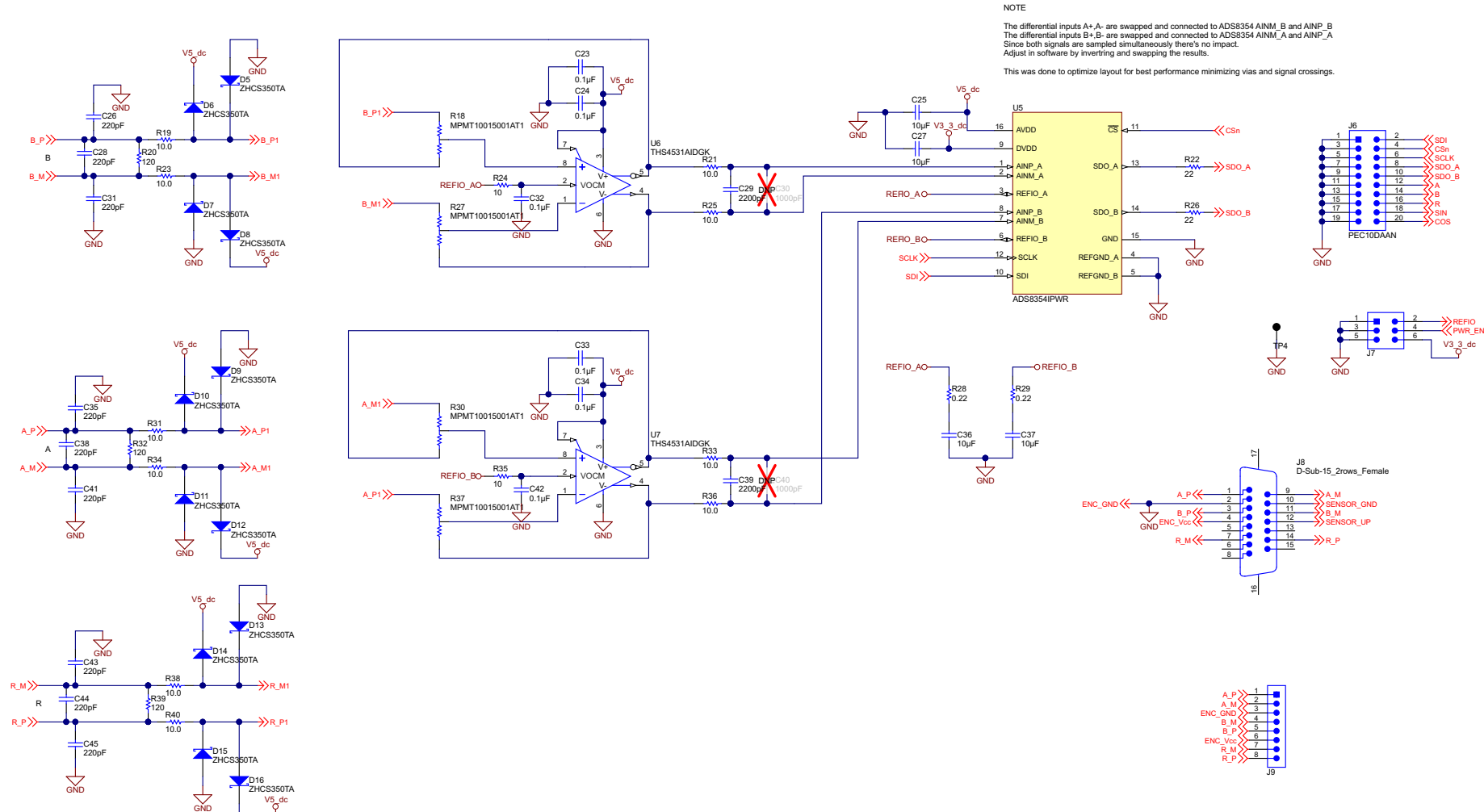


**Figure 79. Schematic of High-Resolution Analog Path with 16-bit ADC**

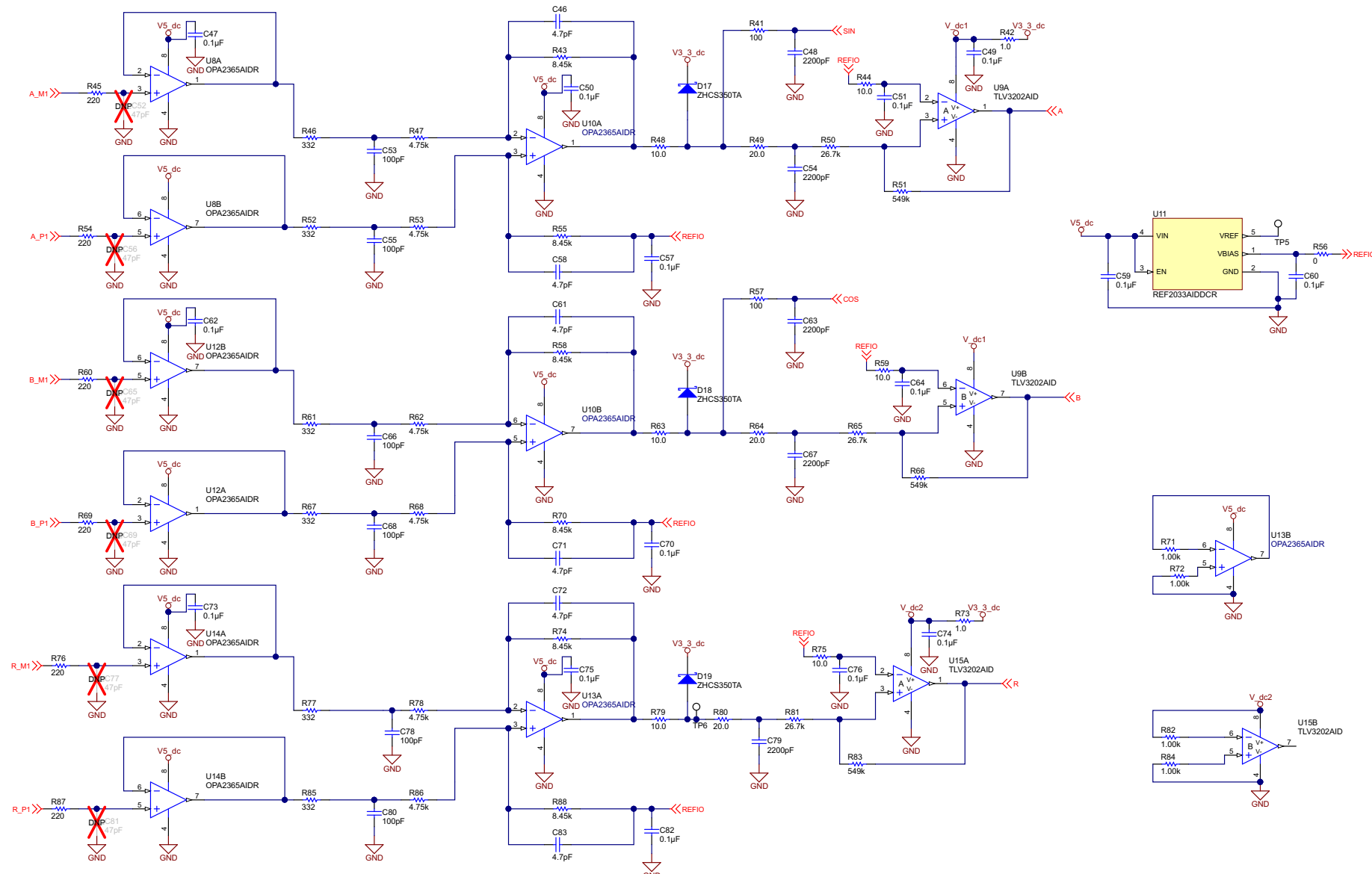


**Figure 80. Schematic of Differential to Single-Ended Analog Path and Comparators**

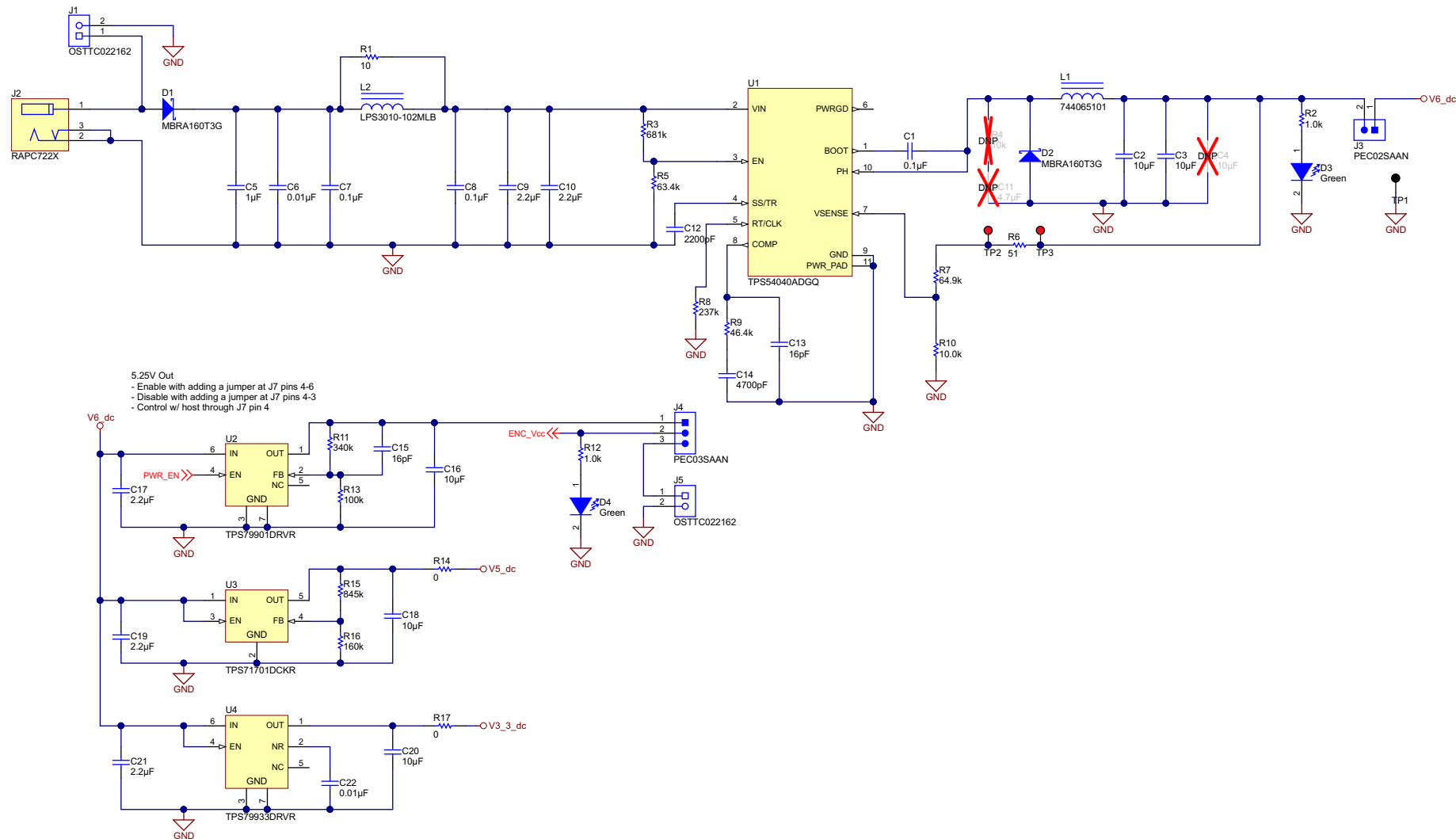


**Figure 81. Schematic of Power Management**

## 8.2 Bill of Materials

To download the bill of materials (BOM), see the design files at [TIDA-00176](#).

## 8.3 PCB Layout Guidelines

Device specific layout guidelines for each individual TI part used in this design can be found in the corresponding datasheet.

The following pictures provide layout guidelines specific to the TIDA-00176 design.

Because of the sensitivity of the analog signal conditioning parts, the design of a four-layers PCB with at least one complete ground plane is highly recommended; this will improve the noise immunity of the system.

Particular attention is also necessary when routing the two sine/cosine signals (to avoid cross-talk problems/interferences); also the power management section (the switcher TPS54040A, in particular) should be properly routed and well separated from the sensitive part of the board to avoid the latter catching noise from the switcher.

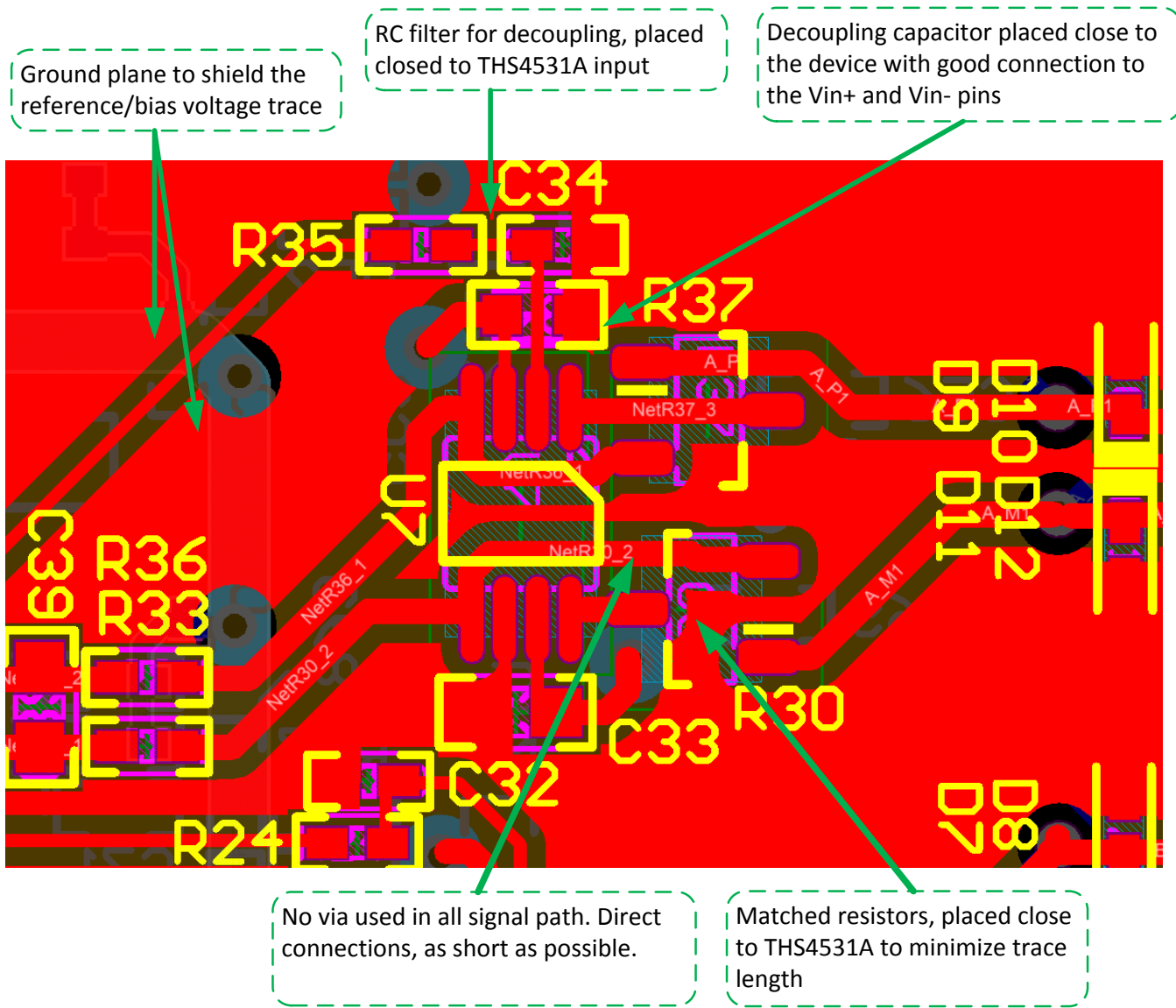


Figure 82. THS4531A Layout

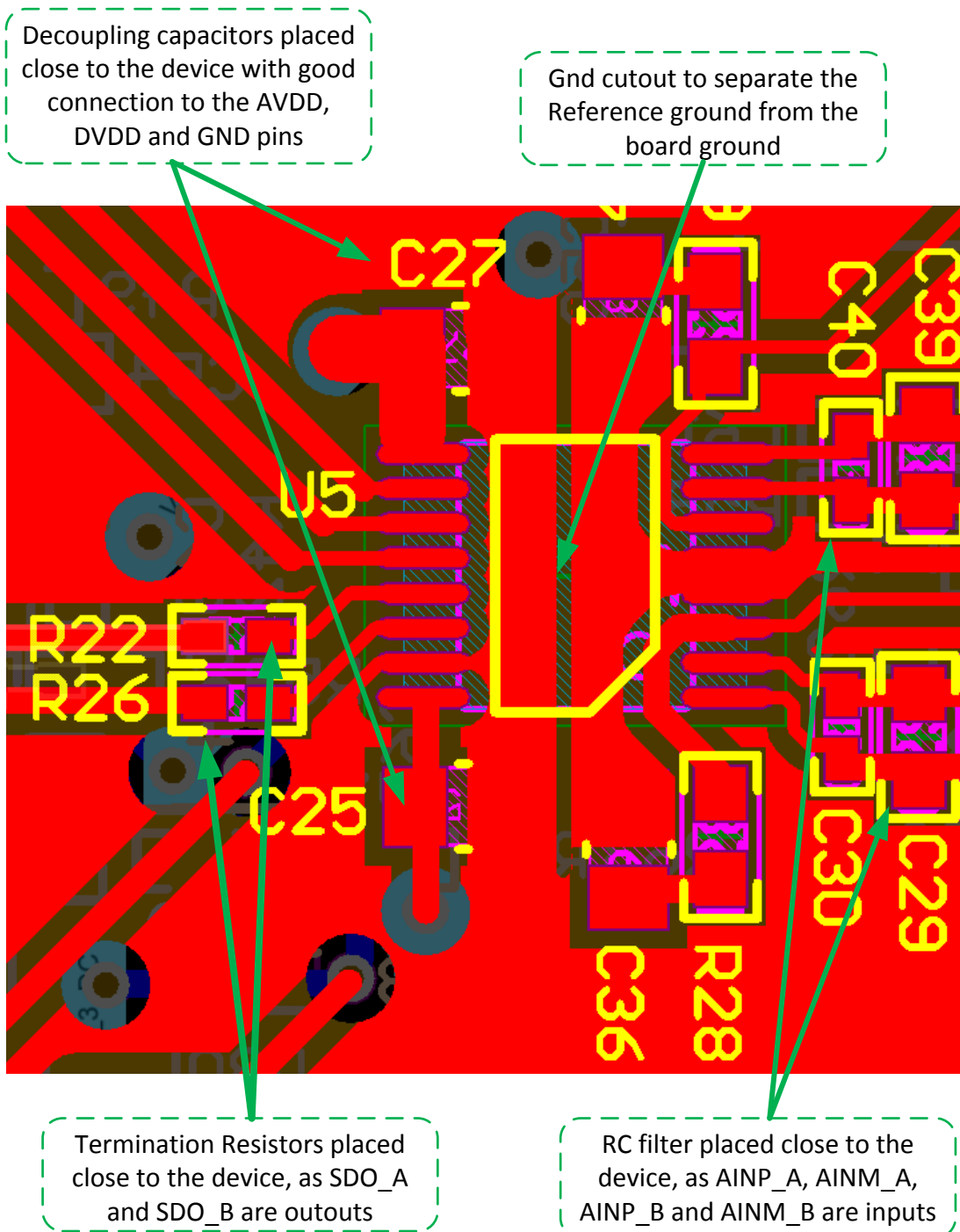
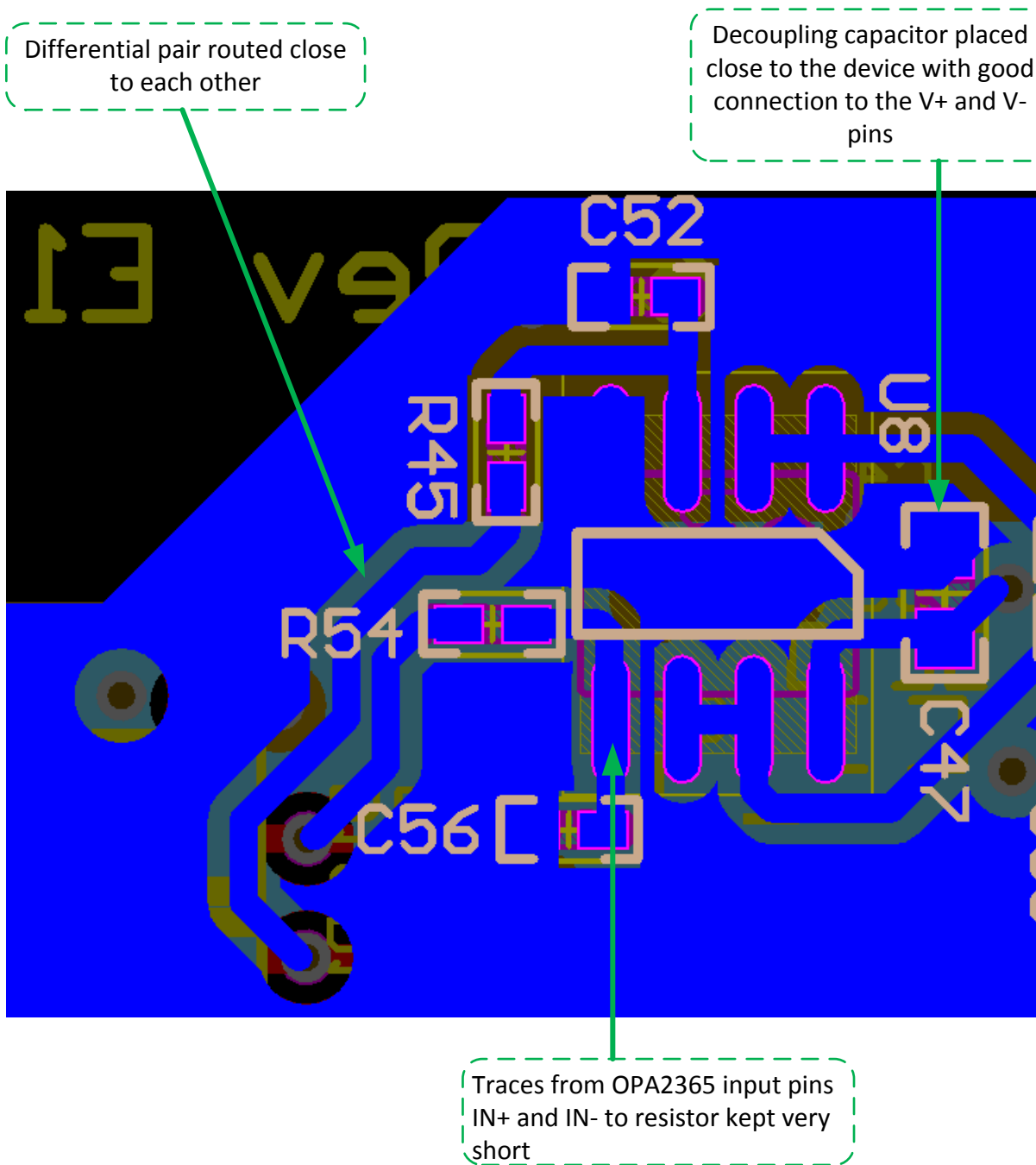
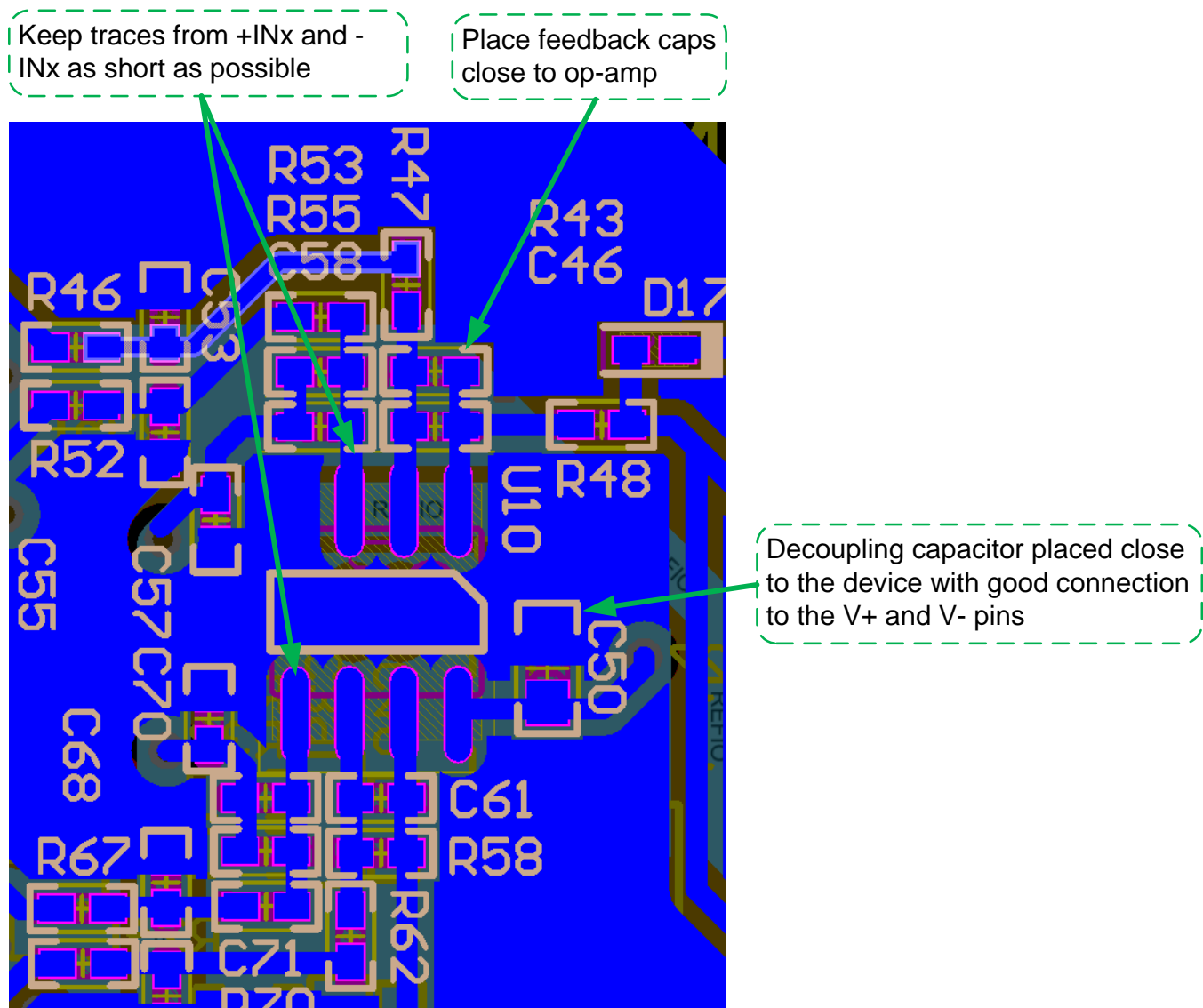


Figure 83. ADS8354, 16-Bit ADC Layout



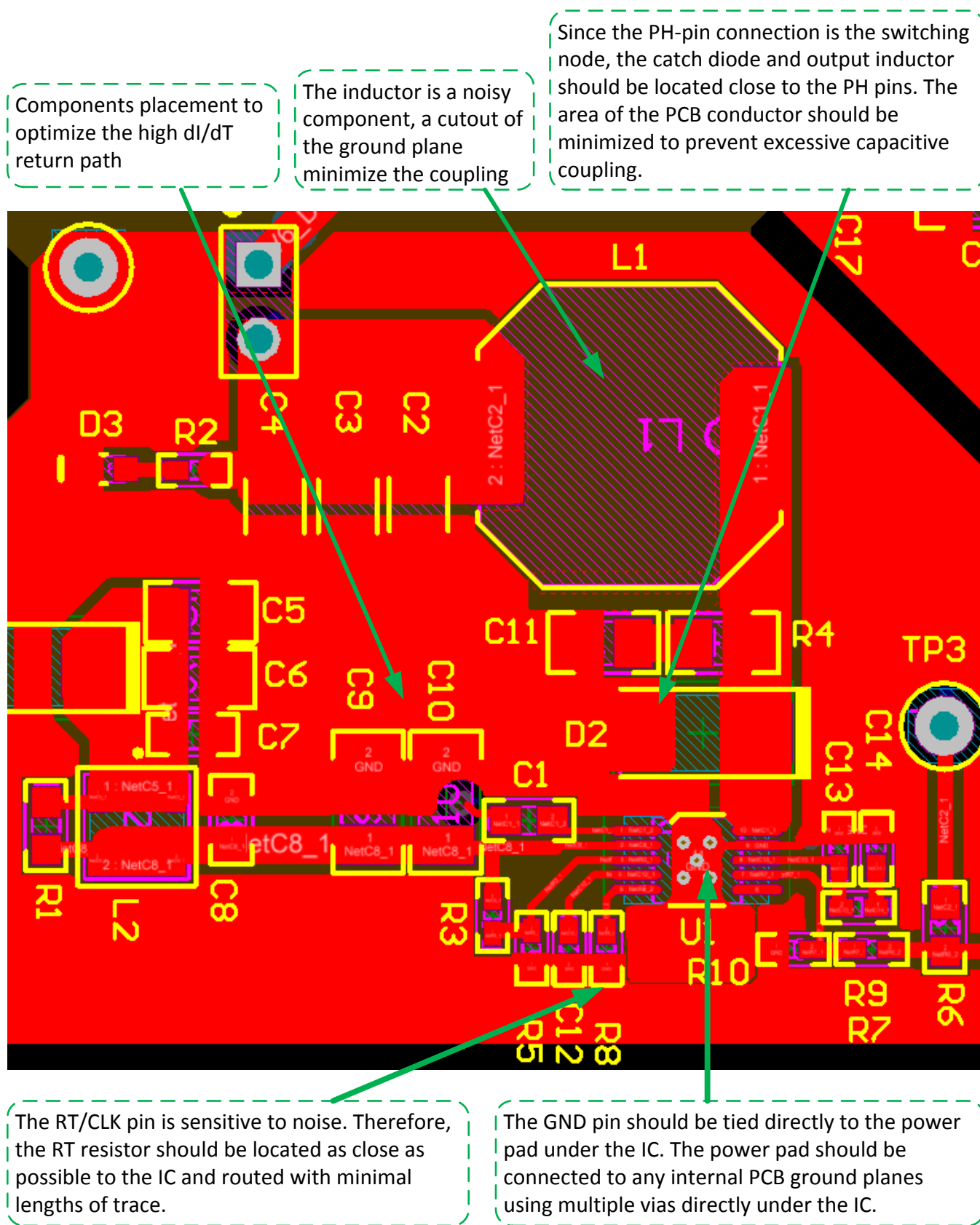
**Figure 84. OPA2365 Input Buffer Layout Hint**



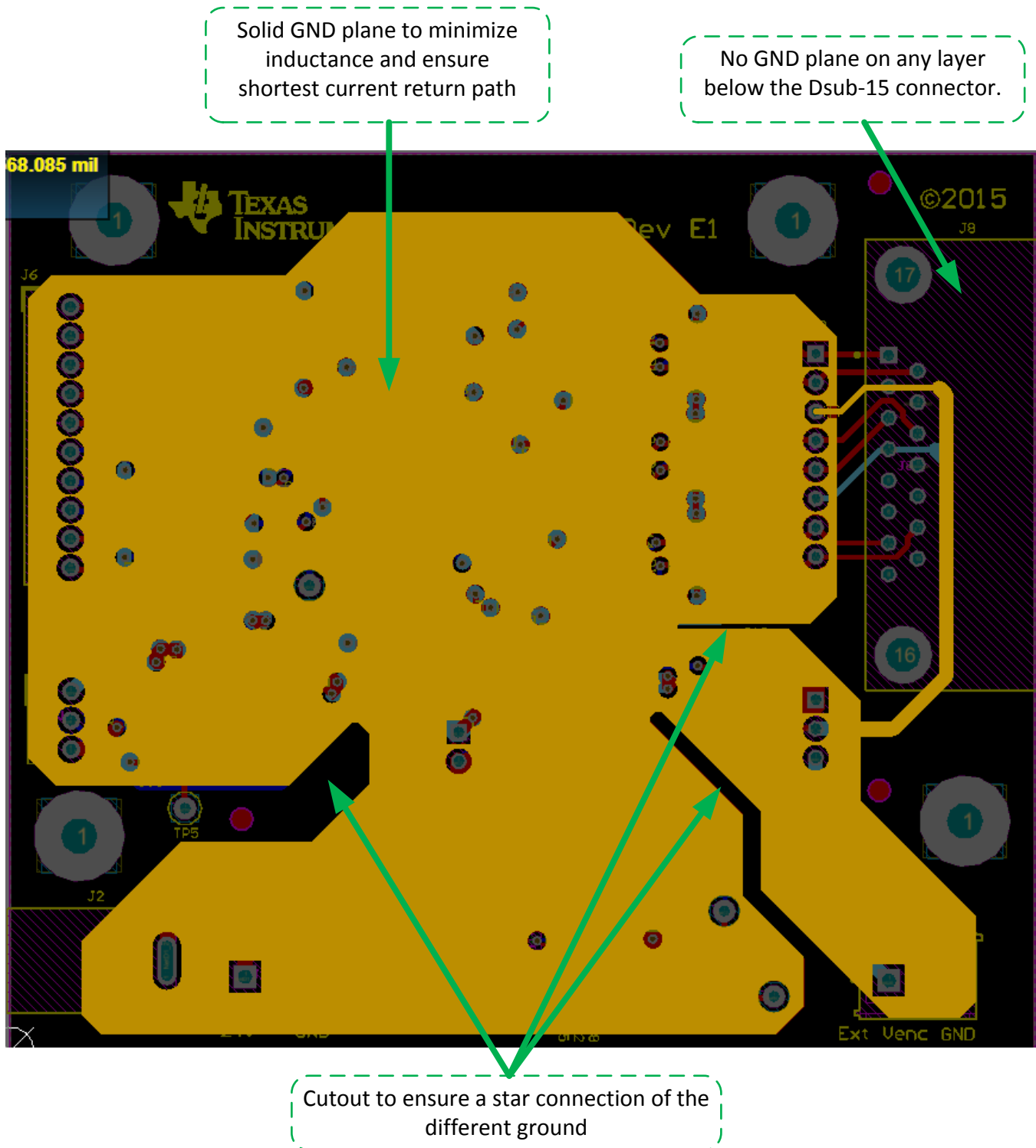
**Figure 85. OPA2365 Differential to Single-Ended Amplifier Layout Hint**



**Figure 86. TLV3202 Layout**



**Figure 87. TPS54040A Layout**


**Figure 88. GND Layer**

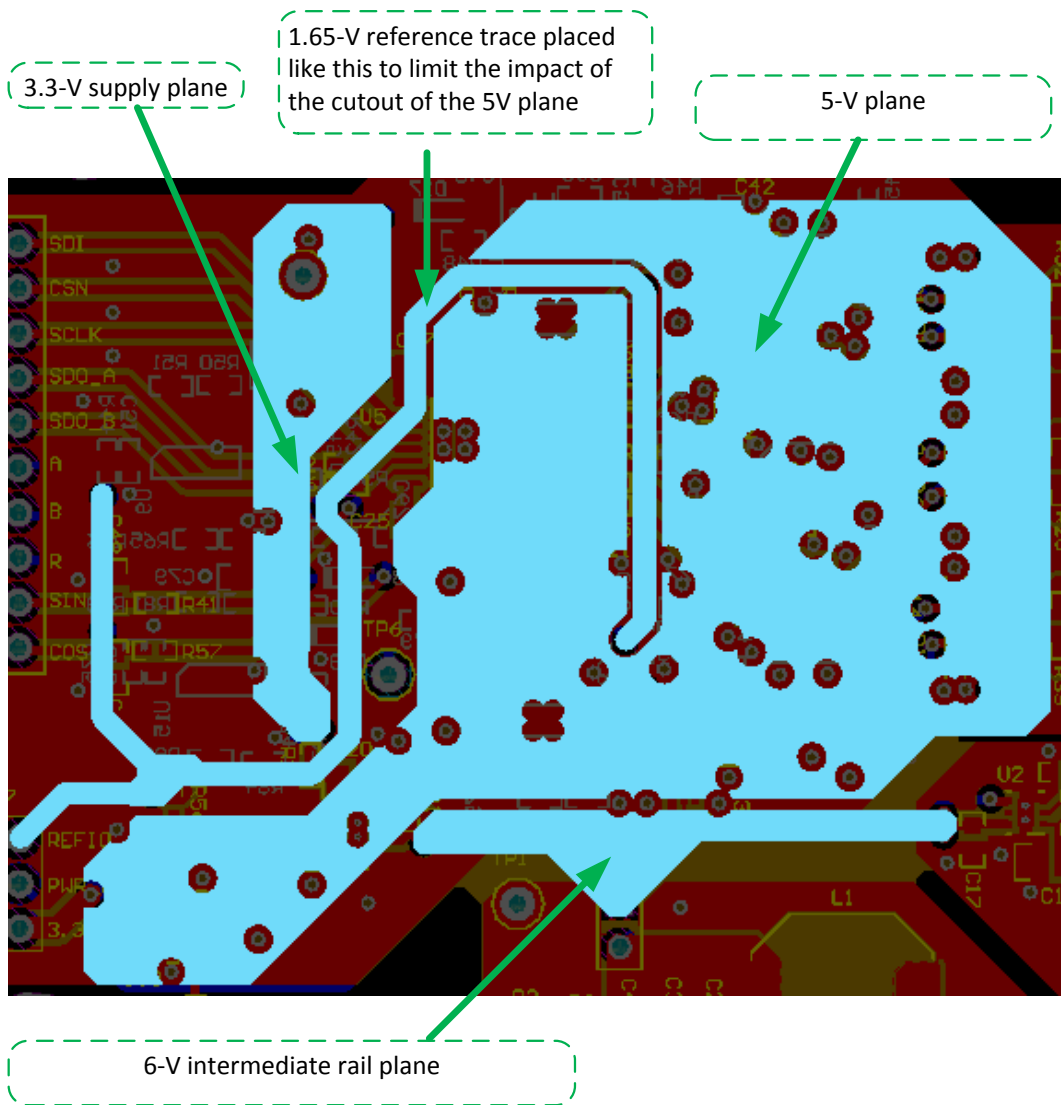


**Figure 89. Supply Layer**

### 8.3.1 PCB Layer Plots

To download the layer plots, see the design files at [TIDA-00176](#).

### 8.4 Altium Project

To download the Altium project files, see the design files at [TIDA-00176](#).

### 8.5 Gerber Files

To download the Gerber files, see the design files at [TIDA-00176](#).

### 8.6 Software Files

To download the software files, see the design files at [TIDA-00176](#).

## 9 References

**NOTE:** Also refer to the technical documents of the [Design Resources](#).

1. Texas Instruments, *Power Supply with Programmable Output Voltage and Protection for Position Encoder Interfaces*, TIDA-00180 Design Guide ([TIDU533](#))
2. Texas Instruments, *18-Bit, 1MSPS Data Acquisition Block (DAQ) Optimized for Lowest Distortion and Noise*, TI Precision Designs ([SLAU515](#))
3. Texas Instruments, *TPS799 200-mA, Low-Quiescent Current, Ultralow Noise, High-PSRR Low-Dropout Linear Regulator*, TPS799 Datasheet ([SBVS056](#))
4. Texas Instruments, *TPS717xx Low-Noise, High-Bandwidth PSRR, Low-Dropout, 150-mA Linear Regulator*, TPS717 Datasheet ([SBVS068](#))
5. Texas Instruments, *AN-2162 Simple Success With Conducted EMI From DC-DC Converters*, Application Report ([SNVA489](#))
6. Texas Instruments, *TMS320F240 DSP-Solution for High-Resolution Position with Sin/Cos-Encoders*, Application Report, ([SPRA496](#))
7. IEC 61800-3 ed2.0 (2004-08), *Adjustable speed electrical power drive systems - Part 3: EMC requirements and specific test methods*, [IEC 61800-3 ed2.0 (2004-08)].
8. IEC 61800-3-am1 ed2.0 (2011-11), *Amendment 1 - Adjustable speed electrical power drive systems - Part 3: EMC requirements and specific test methods*, [IEC 61800-3-am1 ed2.0 (2011-11)].
9. Interfaces of HEIDENHAIN Encoders, March 2015, Brochure #1078628-21, [www.heidenhain.com](#)
10. Rotary Encoders, November 2014, Brochure #349529-2E, [www.heidenhain.com](#)

## 10 About the Author

**VINCENZO PIZZOLANTE** is a System Engineer in the Industrial Systems-Motor Drive team at Texas Instruments, responsible for developing reference designs for industrial drives.

**MARTIN STAEBLER** is a System Engineer in the Industrial Systems-Motor Drive team at Texas Instruments, responsible for developing reference designs for industrial drives.

**KEVIN STAUDER** is a System Engineer in the Industrial Systems-Motor Drive team at Texas Instruments, responsible for developing reference designs for industrial drives.

## Recognition

The authors would like to give special recognition to the excellent contribution from **FERDINAND von MOLO**, who has conducted his Bachelor Thesis at Texas Instruments on an Interface to Sin/Cos Encoders with Piccolo MCU based on TIDA-00176.

## Revision History

<b>Changes from Original (June 2015) to A Revision</b>	<b>Page</b>
• Changed from preview page.....	1

NOTE: Page numbers for previous revisions may differ from page numbers in the current version.

## IMPORTANT NOTICE FOR TI REFERENCE DESIGNS

Texas Instruments Incorporated ("TI") reference designs are solely intended to assist designers ("Buyers") who are developing systems that incorporate TI semiconductor products (also referred to herein as "components"). Buyer understands and agrees that Buyer remains responsible for using its independent analysis, evaluation and judgment in designing Buyer's systems and products.

TI reference designs have been created using standard laboratory conditions and engineering practices. **TI has not conducted any testing other than that specifically described in the published documentation for a particular reference design.** TI may make corrections, enhancements, improvements and other changes to its reference designs.

Buyers are authorized to use TI reference designs with the TI component(s) identified in each particular reference design and to modify the reference design in the development of their end products. **HOWEVER, NO OTHER LICENSE, EXPRESS OR IMPLIED, BY ESTOPPEL OR OTHERWISE TO ANY OTHER TI INTELLECTUAL PROPERTY RIGHT, AND NO LICENSE TO ANY THIRD PARTY TECHNOLOGY OR INTELLECTUAL PROPERTY RIGHT, IS GRANTED HEREIN,** including but not limited to any patent right, copyright, mask work right, or other intellectual property right relating to any combination, machine, or process in which TI components or services are used. Information published by TI regarding third-party products or services does not constitute a license to use such products or services, or a warranty or endorsement thereof. Use of such information may require a license from a third party under the patents or other intellectual property of the third party, or a license from TI under the patents or other intellectual property of TI.

**TI REFERENCE DESIGNS ARE PROVIDED "AS IS". TI MAKES NO WARRANTIES OR REPRESENTATIONS WITH REGARD TO THE REFERENCE DESIGNS OR USE OF THE REFERENCE DESIGNS, EXPRESS, IMPLIED OR STATUTORY, INCLUDING ACCURACY OR COMPLETENESS. TI DISCLAIMS ANY WARRANTY OF TITLE AND ANY IMPLIED WARRANTIES OF MERCHANTABILITY, FITNESS FOR A PARTICULAR PURPOSE, QUIET ENJOYMENT, QUIET POSSESSION, AND NON-INFRINGEMENT OF ANY THIRD PARTY INTELLECTUAL PROPERTY RIGHTS WITH REGARD TO TI REFERENCE DESIGNS OR USE THEREOF.** TI SHALL NOT BE LIABLE FOR AND SHALL NOT DEFEND OR INDEMNIFY BUYERS AGAINST ANY THIRD PARTY INFRINGEMENT CLAIM THAT RELATES TO OR IS BASED ON A COMBINATION OF COMPONENTS PROVIDED IN A TI REFERENCE DESIGN. IN NO EVENT SHALL TI BE LIABLE FOR ANY ACTUAL, SPECIAL, INCIDENTAL, CONSEQUENTIAL OR INDIRECT DAMAGES, HOWEVER CAUSED, ON ANY THEORY OF LIABILITY AND WHETHER OR NOT TI HAS BEEN ADVISED OF THE POSSIBILITY OF SUCH DAMAGES, ARISING IN ANY WAY OUT OF TI REFERENCE DESIGNS OR BUYER'S USE OF TI REFERENCE DESIGNS.

TI reserves the right to make corrections, enhancements, improvements and other changes to its semiconductor products and services per JESD46, latest issue, and to discontinue any product or service per JESD48, latest issue. Buyers should obtain the latest relevant information before placing orders and should verify that such information is current and complete. All semiconductor products are sold subject to TI's terms and conditions of sale supplied at the time of order acknowledgment.

TI warrants performance of its components to the specifications applicable at the time of sale, in accordance with the warranty in TI's terms and conditions of sale of semiconductor products. Testing and other quality control techniques for TI components are used to the extent TI deems necessary to support this warranty. Except where mandated by applicable law, testing of all parameters of each component is not necessarily performed.

TI assumes no liability for applications assistance or the design of Buyers' products. Buyers are responsible for their products and applications using TI components. To minimize the risks associated with Buyers' products and applications, Buyers should provide adequate design and operating safeguards.

Reproduction of significant portions of TI information in TI data books, data sheets or reference designs is permissible only if reproduction is without alteration and is accompanied by all associated warranties, conditions, limitations, and notices. TI is not responsible or liable for such altered documentation. Information of third parties may be subject to additional restrictions.

Buyer acknowledges and agrees that it is solely responsible for compliance with all legal, regulatory and safety-related requirements concerning its products, and any use of TI components in its applications, notwithstanding any applications-related information or support that may be provided by TI. Buyer represents and agrees that it has all the necessary expertise to create and implement safeguards that anticipate dangerous failures, monitor failures and their consequences, lessen the likelihood of dangerous failures and take appropriate remedial actions. Buyer will fully indemnify TI and its representatives against any damages arising out of the use of any TI components in Buyer's safety-critical applications.

In some cases, TI components may be promoted specifically to facilitate safety-related applications. With such components, TI's goal is to help enable customers to design and create their own end-product solutions that meet applicable functional safety standards and requirements. Nonetheless, such components are subject to these terms.

No TI components are authorized for use in FDA Class III (or similar life-critical medical equipment) unless authorized officers of the parties have executed an agreement specifically governing such use.

Only those TI components that TI has specifically designated as military grade or "enhanced plastic" are designed and intended for use in military/aerospace applications or environments. Buyer acknowledges and agrees that any military or aerospace use of TI components that have **not** been so designated is solely at Buyer's risk, and Buyer is solely responsible for compliance with all legal and regulatory requirements in connection with such use.

TI has specifically designated certain components as meeting ISO/TS16949 requirements, mainly for automotive use. In any case of use of non-designated products, TI will not be responsible for any failure to meet ISO/TS16949.